2D and 3D Isophlorinoids: Synthesis, Structural Characterization, Redox and Electronic Properties

A Thesis

Submitted in Partial Fulfilment of the Requirements

for the Degree of

Doctor of Philosophy

By

Ashok Kumar B

ID: 20143324

Indian Institute of Science Education and Research (IISER), Pune

2022

DEDICATED

TO

MY PARENTS AND BROTHER

Certificate

Certified that the work described in this thesis entitled "***2D and 3D Isophlorinoids: Synthesis, Structural Characterization, Redox and Electronic Properties***" submitted by *Mr. Ashok Kumar B.* was carried out by the candidate, under my supervision. The work presented here or any part of it has not been included in any other thesis submitted previously for the award of any degree or diploma from any other university or institution.

Date: 8th February, 2022

Prof. V. G. Anand

Research Supervisor

Declaration

I declare that this written submission represents my ideas in my own words and wherever other's ideas have been included, I have adequately cited and referenced the original sources. I also declare that I have adhered to all principles of academic honesty and integrity and have not misrepresented or fabricated or falsified any idea/data/fact/source in this submission. I understand that violation of the above will result in disciplinary actions by the Institute and can also evoke penal action from the sources, which have thus not been properly cited or from whom appropriate permission has not been taken when needed.

Date: 8th February, 2022

(Ashok Kumar B)
ID: 20143324

Acknowledgement

This thesis would not have been possible without the support of many people. I would like to express my sincere gratitude to all of them.

Firstly I would like to express my sincere thanks to my thesis advisor Prof. V. G. Anand, for your patience, guidance, and support during this research work. I have benefited greatly from your wealth of knowledge. I am extremely grateful that you took me on as a student and continued faith in me over the years.

I am extremely thankful to Prof. K. N. Ganesh, Former Director, IISER Pune, for providing excellent research facilities and an outstanding research ambience.

I am also grateful to the Research Advisory Committee members Dr. Raghavendra Kikkeri (IISER, Pune) and Dr. Rajesh G. Gonnade (NCL, Pune), for their valuable suggestions and motivating guidance.

I would like to express my sincere thanks to Prof. Ramakrishna G. Bhat for his encouragement, suggestions and fruitful discussions during my stay at IISER Pune. In fact, I owe heartiest thank to every faculty in IISER-Pune.

My heartiest thanks to all my teachers who have taught me at various levels of academic life.

I am appreciative to all the members of the VGA group past and present who have made the lab a great place to be. I thank all my seniors Dr. Gopal, Kiran, Gadekar, Sujit and Rashmi, for their help and guidance. It's my pleasure to thank Neelam, Jyostna, Brijesh, Tarun, Sunita, Panchal, Rakesh, Madan, Udaya, Prachi, Vishnu, Pragati, Markose and Ramesh for always being helpful and cooperative. They all have played a major role in polishing my research skills. Their endless guidance is hard to forget throughout my life.

Many thanks to all of the staff members of IISER Pune and the chemistry department especially Thushar, Mayuresh, Mahesh, Nitin, Sandeep, Yatish, Ravindra and Sandeep (for NMR experiments) for their kind support during my PhD study.

Special thanks goes to the my IISER Pune friends, especially Chandan, Shatruhan, Kamal, Vinay, Sanjit, Ajay, Bappa, Bala, Ganesh, Manoj, Uday, Puneeth, Chethan, Sharath, Deepak, Madhu, Goudappa and Thripura (NCL Pune) for always being there in all situations. I will never forget the wonderful times we shared, especially trekking, late-night debates, and cooking Saturday nights.

Finally, my deep and sincere gratitude to my family for their continuous and unparalleled love, help and support. I am grateful to my brother for always being there for me. I am forever indebted to my parents for giving me the opportunities and experiences that have made me who I am. This thesis is dedicated to them.

Due acknowledgments to them, whose names are unintentionally missed out, despite their unconditional help during my stay at IISER Pune.

Ashok

CONTENTS

CHAPTER IV
Synthesis of 3D π-Conjugated Molecular Cages

Synopsis

The thesis entitled ***"2D and 3D Isophlorinoids: Synthesis, Structural Characterization, Redox and Electronic Properties"*** describes synthetic chemistry of two and three dimensional anti-aromatic expanded isophlorinoids intertwined with their structural, electronic and redox characteristics. The 20π tetrapyrrolic isophlorin was proposed as an intermediate during the synthesis of porphyrin. By virtue of unstable nature it undergoes two electron oxidation followed by deprotonation to yield the aromatic porphyrin. Despite much effort, very few strategies reported to sythesise stable isophlorin and its expanded versions using structurally similar heterocycles such as furan / thiophene / selenophene. In general anti-aromaticity has not gained significant attention mainly due to the lack of stable 4nπ systems. In this regard, a stable isophlorin and its expanded derivatives provide a hope to glance into the world of anti-aromatic systems and also studying these systems through annulene chemistry prospective is really interesting. This thesis demonstrates the results of successful attempts to synthesize and characterize expanded isophlorinoids. Along with the many analytical techniques, quantum chemical calculations were also employed to evaluate the anti-aromatic characteristics of novel expanded isophlorinoid systems. This thesis is described in four chapters. The first chapter provides an apt introduction to the concept of antiaromaticity in porphyrinoids and the emerging 3D aspects of conjugated systems. There have been limited but significant contributions towards the design and synthesis of anti-aromatic macrocycles. A remarkable property of 4nπ systems is their ability to undergo reversible two-electron oxidation to form aromatic dication. Apart from the interesting redox chemistry, serendipitous discoveries have led to the possibility of identifying and isolating neutral radical species which exhibits amphoteric properties. It can undergo reversible one-electron reduction or oxidation to yield the corresponding anionic and cationic species respectively. Along with the synthetic aspects, the structural, electronic, and redox properties of isophlorin and its expanded derivatives will be described in detail.

Core modified and expanded isophlorins have been characterized as stable 4nπ macrocycles with electronic and redox properties those are not observed in aromatic systems. The length of the π–conjugated network can be increased by inserting additional heterocyclic units or by increasing the number of *meso* carbon bridges to get expanded isophlorins with different optical and electronic property. One of the main strategies used is replacing the *meso* carbon bridges with ethylene or acetylene linkages to get higher homologues of isophlorins. Majority

the expanded isophlorins reported with acetylene links with varying number of thiophene units have disadvantages like laborious and multistep synthesis approach and lack of ring current effects. The second chapter of this thesis describes the attempts to synthesise acetylene bridged antiaromatic macrocycles from thiophene precursors. But, due to the unpredicted reactivity of acetylene precursors, an unexpected stable and neutral (4n+1)π radical macrocycle was isolated from this reaction. A detailed analysis was carried out to confirm the neutral radical nature of the macrocycle. From single crystal X-ray diffraction analysis, an unprecedented molecular structure with cyclo pentathiophene core was identified for the isolated radical molecule. Further, one-electron oxidation and reduction reactions were done to identify the respective cationic antiaromatic and anionic aromatic macrocycles. All these cation, anion and neutral macrocycles redox properties were studied in detail through cyclic voltammetry and spectroelectrochemically. These observed redox properties and electronic properties were further buttressed by computational studies. A plausible mechanism was proposed for the unexpected formation of the radical molecule based on the reactions carried out using β-methylated thiophene monomers.

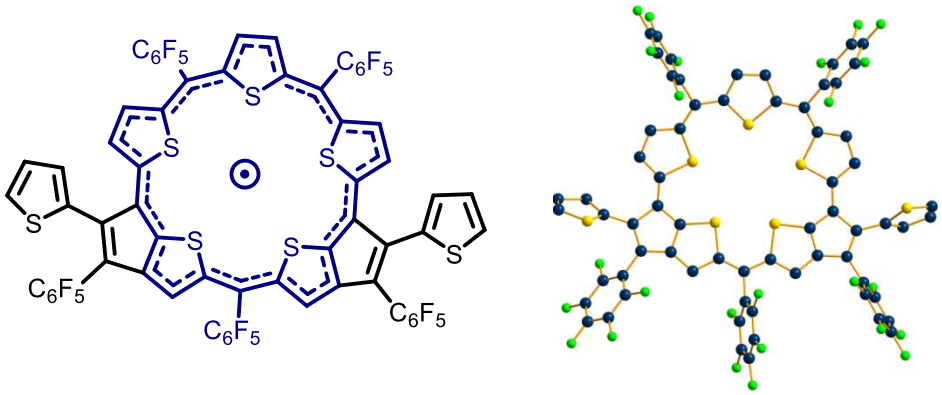

Invariably large π-conjugated macrocycles have a tendency to twist and adopt nonplanar figure of eight conformation due to their flexible nature. Relative to aromatic systems, the experimental evidence reported for large antiaromatic systems are far less than satisfactory. Despite much effort, there are few strategies reported to sythesise planar expanded isophlorins. These strategies, although very successful at synthesizing large macrocycles adds considerable synthetic steps and lack of effective conjugation in the π framework. One of the main strategies employed in the synthesis of expanded 4nπ and (4n+2)π systems is by using less number of *meso* carbons and a greater number of directly linked heterocyclic units. The synthesis, structural features and redox properties of isoelectronic macrocycles of 40π isophlorins having planar topology is explained in the third chapter. Ethylene bridged

precursors of thiophene and furan were used to incorporate ethylene bridges in the π conjugation pathway of macrocycles. A directly α-α connected rigid bithiophe was used to induce the planarity in to the macrocycle. Despite having a planar structure, the synthesised 40π macrocycle shows weak paratropic ring current effects confirmed by ^{1}H NMR and estimated NICS values. The non-covalent interaction between 40π isophlorin and fullerene is studied in the solid state. The formation of 1:2 supramolecular complex of macrocycle and fullerene was revealed by X-ray diffraction studies. These non-covalent interactions are much stronger than the C60 and porphyrin assembly. The Uv-Visible absorption and cyclic voltammetry studies show the irreversible formation of the oxidised species. Two-electron ring oxidation of these macrocycles yield 38π dicationic species which could be identified as diradical species by ESR spectroscopy and computational studies. These dicationic macrocycles displays open shell singlet diradical ground state with moderate diradical character because of a small singlet-triplet energy gaps.

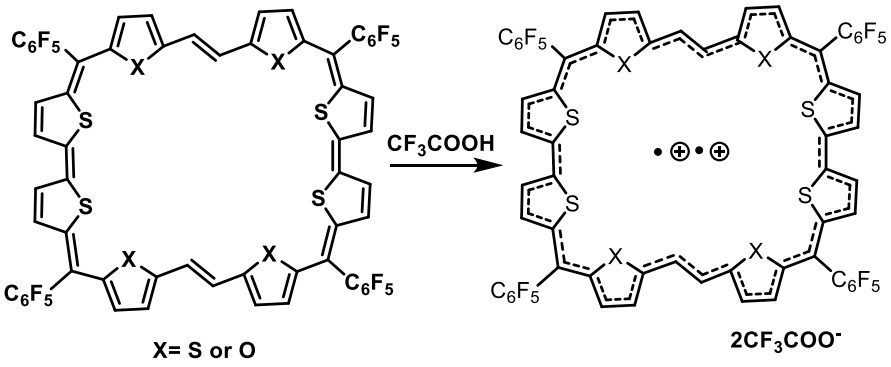

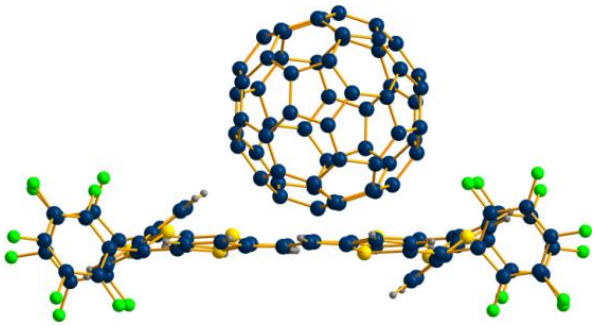

The fourth chapter describes the novel synthetic protocol serendipitous discovered for the synthesis of three dimensional π-conjugated cage and semi-cage like molecules. During the attempted synthesis of a possible isophlorinoid macrocyclic dimer due to the steric hindrance induced by thiophene unit forms cage-like π-conjugated systems at the expense of macrocycles. Further, by varying the stoichiometric ratio of precursors, significant control over the yield of these products is achieved.

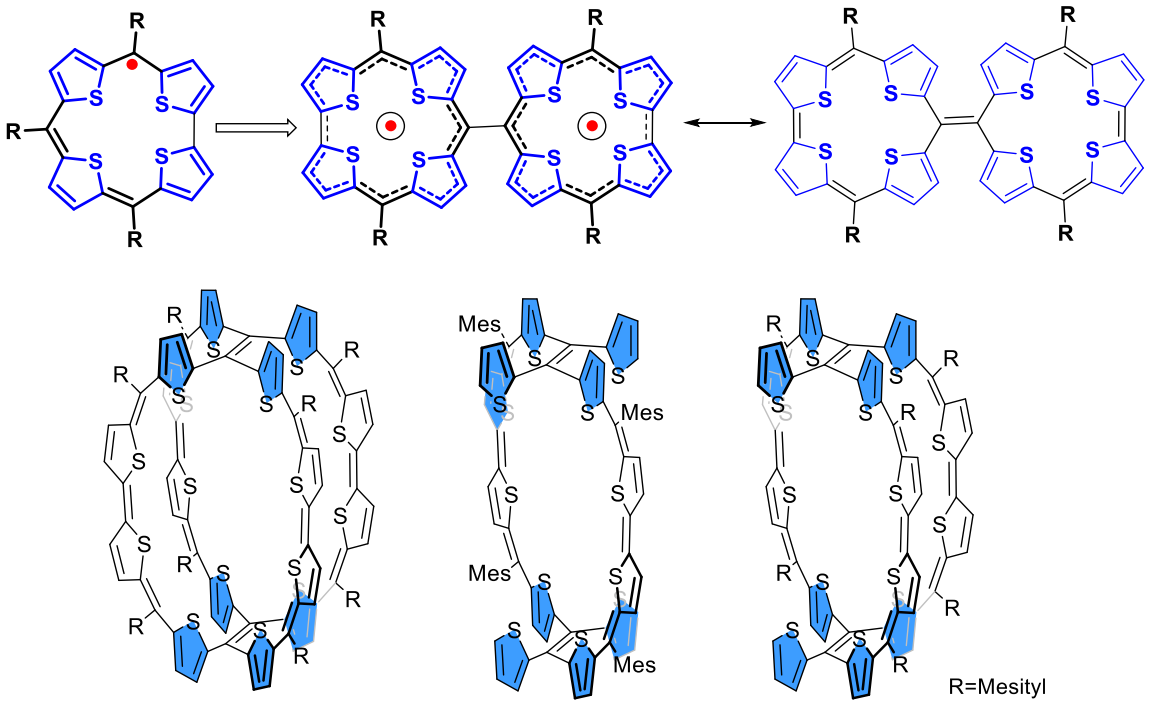

The structural elucidation of these π-conjugated molecular cage and quasi-cage like molecules is done through variable temperature ^{1}H NMR and single crystal X-ray diffraction analysis. The redox properties of the cage and semi cage molecules are investigated through UV-Vis, Cyclic voltammetry and spectroelectrochemistry. Generally, the synthesis of three dimensional π-conjugated molecular cages is a challenging task because of the multistep syntheses, preorganization of monomer units, non-availability of general methods and overall poor yields. Therefore, using this novel synthetic protocol, expanded and contracted 3D π-conjugated molecular cages were synthesised by varying the bridging unit length.

Publications

- Three dimensional isophlorinoid tetrapodal molecular cage. **Ashokkumar Basavarajappa**, Madan D Ambhore and V. G. Anand, *Chemical Communication*, **2021**, *57*, 4299–4302.
- Isophlorinoids: The antiaromatic congener of Porphyrinoids. B. Kiran Reddy, **Ashokkumar Basavarajappa**, Madan D Ambhore and V. G. Anand, *Chemical Reviews*, **2017,** *117*, 3420-3444.
- Wide range redox states of expanded Porphyrinoids. Madan D Ambhore, **Ashokkumar Basavarajappa** and V. G. Anand, *Chemical Communication*, **2019**, *55*, 6763—6766.

CHAPTER I
Introduction

I.1. Porphyrinoids - Annulene perspective

Annulenes are a class of conjugated monocyclic hydrocarbons formally made up of alternating single and double bonds identified with the general formula $(C_2H_2)_n$. The size of the rings is indicated by prefixing the annulene, a number enclosed in square brackets, representing the number of atoms in the ring. According to this, cyclobutadiene is considered as [4]annulene, and benzene as [6]annulene.[1-2] Major support to the understanding of the nature of cyclic conjugated compounds came from Hückel rule predicted that the molecules whose conjugated systems having (4*n*+2) π-electrons would have aromatic character. The analogous molecules with 4nπ electrons, which did not follow Hückel's (4n+2) π rule for aromaticity, were earlier named as "pseudoaromatic." However, both theoretical and experimental studies suggested that, for at least some members of the 4nπ series cyclic systems, delocalization of π-electrons leads to strong destabilization of the molecule, in comparison to the stabilization for aromaticity. Because of this reason, in 1965, Ronald Breslow coined the term "antiaromatic" to define such systems.[3]

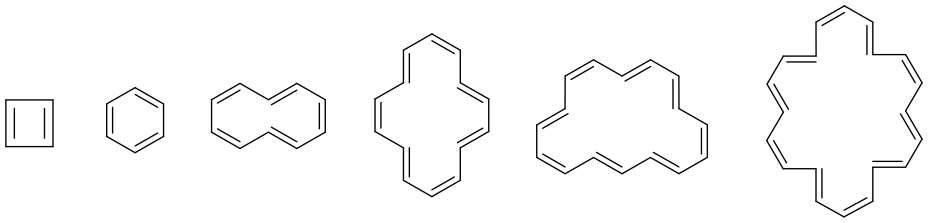

Scheme I.1: Structures of annulenes having either 4nπ and (4n+2) π electrons.

To test these speculations experimentally, in 1960s Sondheimer and co-workers synthesised an impressive array of annulenic structures containing 12, 14, 16, 18, 20, 24 and 30 carbon atoms. A range of annulenes, both the 4nπ and (4n+2) π series, were successfully synthesized and characterized comprehensively through NMR spectroscopy.[1] Quite often aromaticity or antiaromaticity is a signature of π-electron delocalization. One important consequence of π-electron delocalization is the ability to sustain either diamagnetic ring current or paramagnetic ring current in applied magnetic field. Such a diamagnetic or paramagnetic ring current can be easily detected by the NMR spectroscopy. Aromatic annulenes displayed diatropic ring current effects, in which the inner protons were shielded and the outer protons were deshielded. Conversely, annulenes containing 4nπ electrons should sustain a paramagnetic ring current. So paratropic ring current effects were observed in NMR spectrum with stark reversing of the shielding and deshielding effects on the protons. Increasing the

cyclic conjugation pathway in the system assists the conformational flexibility, and hence, the molecule can have more than one stable conformer. At higher temperatures, the ^{1}H NMR spectra of all the relatively stable annulenes examined so far revealed only a singlet. This difficulty was overcome by lowering the temperature. Hence, the diatropic and paratropic ring current effects on its protons were observed only at low temperature.[4] At lower temperature, the NMR spectra of the aromatic annulene systems [14]annulene, [18]annulene,[5] and [22]annulene are typical of diatropic systems, consisting of outer proton signals at low field (δ 10.61, 12.99, and 10.4-11.2 ppm, respectively) and inner proton signals at high field (δ 2.12, 0.72, and 0.35-1.5 ppm, respectively).[6] On a similar note, the low-temperature spectra of the antiaromatic annulene systems [16]annulene and [24]annulene are typical of paratropic systems, consisting of outer proton signals at high field (δ -0.56 and -2.9 to -1.2 ppm, respectively), and inner proton signals at low field (δ 4.67 and 5.27 ppm, respectively).[7-8] Due to the inherent conformational flexibility that disrupts the conjugation pathway, ring currents in these systems became progressively weaker upon increasing the size of the ring. Next higher order annulenes having 28π electrons or more were also synthesized, but their ^{1}H NMR spectrum could not be measured due to the very poor solubility in most of the common organic solvents.[9]

Work on monocyclic annulenes declined in the 1970s, giving way to studies of bridged and heteroatom derivatives. Increasingly, annulenes were being synthesised to explore the idea of aromaticity, and bridging the rings evolved as an effective method for providing rigidity to annulenes conducive for π- electron delocalisation. Whilst the smaller [*n*]annulenes ($6 < n \leq 16$) did not adopt planar structures due to steric interactions between inner protons, the larger annulenes had to confront conformational flexibility to remain sufficiently planar for this π-delocalisation to happen.[1-2, 10] However, the internal steric crowding of hydrogen atoms in di-*trans*-[10]annulene, **I.3**, was eliminated by replacing the 1- and 6-hydrogen atoms by one atom (or group) connected to both the 1- and 6-positions.[10] Using this strategy any annulene could be bridged.

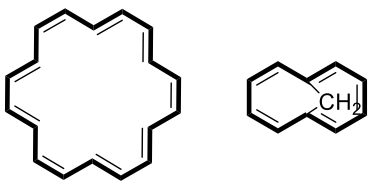

I.7 I.8

Scheme I.2: Structures of [18]annulene and bridged [10]annulene.

[18]annulene, **I.7** and 1,6-methano[10]annulene, **I.8**, are the classic examples for [4n+2]annulenes and their bridged variants, respectively (Scheme **I.2**). Both of these annulenes fulfil the spectral and structural conditions for aromaticity, but the rigid bridged [10]annulene displayed benzenoid properties. As a consequence of its conformational flexibility, **I.7** is a highly reactive molecule that is more likely to polymerize than to undergo electrophilic substitution reactions.[11]

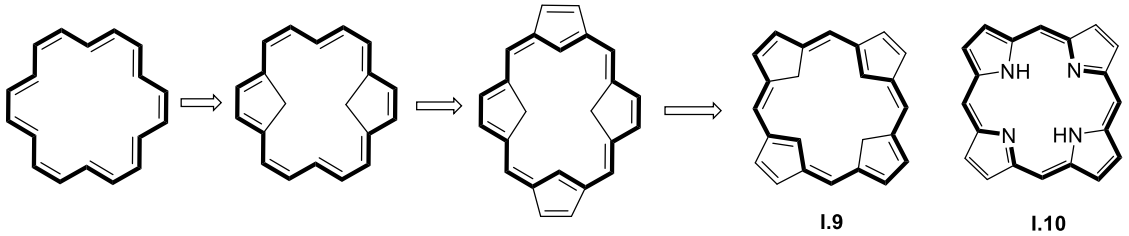

I.9 I.10

Scheme I.3: Bridging [18]annulene to get porphyrin analogue.

Various bridging schemes can be visualized for **I.7** and many were reported to be stable and aromatic compounds amenable to synthesis. One of the most effective ways of imposing rigidity on **I.7** while retaining planarity is the successive addition of two internal CH_2-bridges and two external CH=CH bridges into **I.7.** This transformation leads to the bridged [18]annulene or tetracyclopentadienic hydrocarbon **I.9,** which might be regarded as the parent structure of porphyrin, **I.10** (Scheme **I.3**). In the medium annulenes, especially the [10] and [14]annulenes, the presence of bridging atoms eliminates the crowding caused by the inner hydrogen atoms, thus favouring planarity and aromaticity. This concept has been well demonstrated by Vogel and co-workers by the preparation and properties of 1,6-imino[10]annulene, **I.11,** and its 14π-homologue syn-1,6:8,13-diimino[14]annulenes, **I.12**.[12] These imino bridged [4n+2]annulenes comparable with porphyrin, **I.10** in ^{1}H NMR spectroscopic terms, especially with respect to ring current effects (Scheme **I.4**). So this analogy confirms that the conjugation pathway in porphyrin is similar to that of 18π annulene with two carbons being replaced by two nitrogens. Hence the name aza annulenes.[13] Also

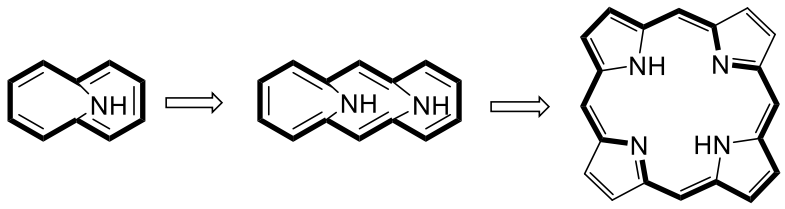

I.11 I.12 I.10

Scheme I.4: Imino bridged [4n+2]annulenes and porphyrin or aza annulene.

the rigidity of porphyrin backbone facilities the ring current effects due to the global delocalization of π electrons and the concept of Huckel rule can be extended to higher porphyrin homologues also.

I.2. Isophlorins

Isophlorin, **I.14** is a 20π macrocycle with four pyrrole units. The concept of isophlorin was first highlighted by Robert Burns Woodward in 1960 as an unstable intermediate during the synthesis of chlorophyll. The isophlorin was proposed as a probable intermediate during the mechanistic pathway for the synthesis of porphyrin.[14] The condensation of four pyrrole units with aldehyde in acidic conditions forms an unconjugated tetrapyrrole porphyrinogen, **I.13**.[15-16] At the beginning, the porphyrinogen, **I.13**, undergoes four-electron oxidation to the intermediate isophlorin, **I.14** which subsequently undergoes two-electron oxidation to yield the aromatic porphyrin, **I.10**. The isophlorin is structurally related to porphyrin, but differs in its conjugation pathway (Scheme **I.5**). The change in conjugation pathway results in marked difference in its electronic and magnetic properties. Nitrogen doped carbon skeleton withstand effective delocalization of π-electrons from the overlapping sp^2 orbitals,[16] as experimentally demonstrated for porphyrin. Conversely, isophlorin's conjugated pathway comprises of carbon atoms alone. Even though delocalization of π-electrons seems to be apparent for **I.14**, the resultant effect has not been experimentally verified until date due to its inherent instability under ambient conditions.[17]

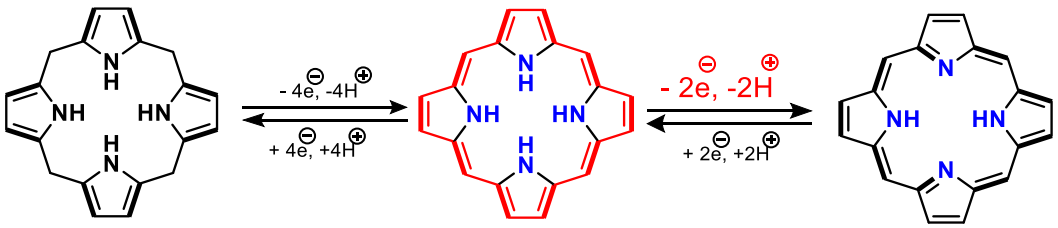

Scheme I.5: Oxidation of porphyrinogen into a porphyrin through isophlorin.

The pyrrole nitrogen's can undergo deprotonation with a one-step two-electron transfer reaction resulting in the reduced stability of isophlorin **I.14**. The presence of four hydrogen atoms in the centre of the macrocycle can cause ample repulsive forces to deviate the macrocycle from planar conformation. Any transformation to reduce this strain should be facile, and hence, the oxidation of **I.14** to **I.10** is quite rapid at ambient temperature. Not surprisingly, the hypothetical tetrapyrrole, **I.14**, remains a synthetic challenge to date.

I.3. Synthesis of Isophlorins

The synthesis of a stable isophlorin was attempted by various groups to study their intriguing properties of stable antiaromatic system. An earlier attempt in synthesizing this 20π macrocycle includes pioneering works of Vogel and co-workers. Inspired by the successful synthesis of annulenes, they represented the porphyrin and isophlorin as structural analogues of 18π and 20π annulenes, respectively. Vogel used non pyrrolic heterocyclic units such as furan/thiophene/selenophene or N-substituted pyrrole for synthesizing modified isophlorins.[13] These substituted heterocycles provide additional structural rigidity and also prevents the proton coupled electron-transfer to oxidize the antiaromatic isophlorin to the aromatic porphyrin.

I.3.1. Isophlorin Dications

In 1982, Frank and co-workers reported the oxidized product of the tetra-N-methyl isophlorin as a 18π dication **I.16**.[18] Later Vogel's group synthesised the antiaromatic 20π isophlorin, **I.17**, by controlled two-electron reduction of the dication **I.16**, having modified core using 0.15 M solution of anthracene-sodium in THF as the reducing agent at −78 °C (Scheme **I.6**).[19] The resultant 20π tetra-N-methyl isophlorin product was crystallized from an ethanol/hexane mixture as air sensitive brown needles. Because of the steric hindrance caused by the four methyl groups inside the macrocycle is forced to adopt nonplanar conformation. Hence all the methyl groups are either above (or below) the mean plane of the macrocycle or alternative pyrroles necessarily in syn, anti, syn, anti-orientation. X-ray crystallographic analysis revealed the alternate syn and anti-conformation of the four pyrrole rings, leading to the loss of the planar conformation. Unfortunately, the first successful synthesis of 20π isophlorin was diminished by its non-antiaromatic characteristics due to the structure induced loss of antiaromaticity.

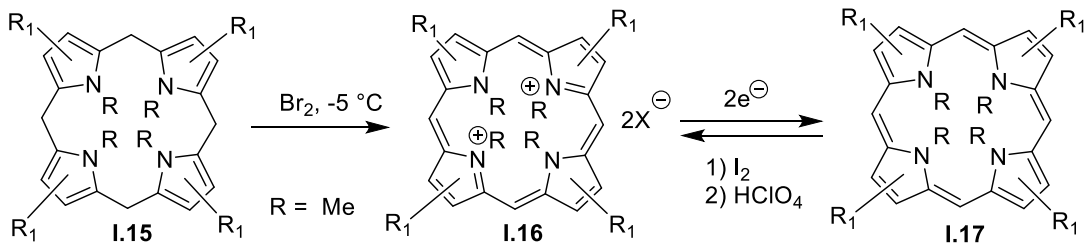

Scheme I.6: Oxidation of N-tetramethyl porphyrinogen to isophlorin through its dication.

Due to the comparable aromatic features and structural similarity with pyrrole, the chalcogen family of heterocycles were employed as building blocks instead of pyrrole to synthesize the stable 20π macrocycle (Scheme **I.7**). Vogel's group employed different approaches to synthesize isophlorins from thiophene/furan/selenophene by replacing all the pyrrole rings of a porphyrin.[20-23] These macrocycles displayed resemblance to the porphyrin and were anticipated to stabilize 20π electrons conjugated pathway in their neutral form. But, they undergo facile two-electron ring oxidation to form a 18π porphyrin dication as their perchlorate salts. The molecular structure confirmed displacement of the thiophene rings from the mean plane of the macrocycle due to the relatively large Van der Waal radius of sulphur when compared to oxygen. Structural characterization of the porphyrinogen **I.18** and the porphyrin dication **I.19** showed the transformation to planar from a nonplanar conformation, proving the global π-conjugation in the dication **I.19**.

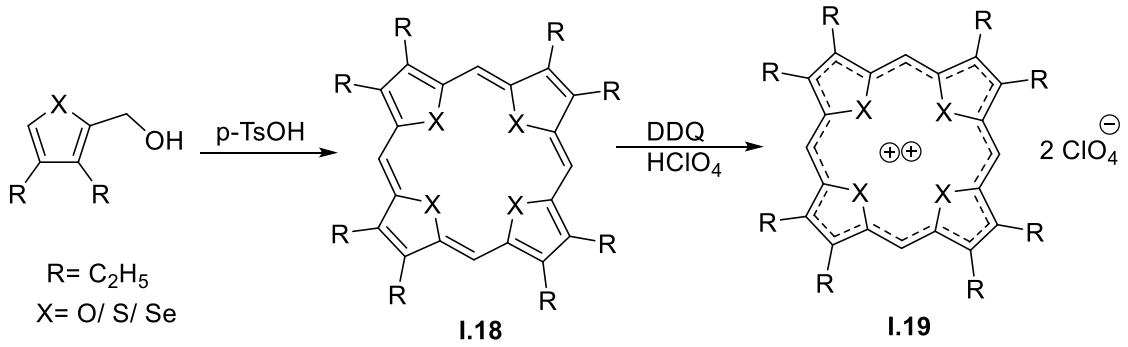

Scheme I.7: Synthesis of 18π porphyrin dications.

During the oxidation of **I.18** to its corresponding porphyrin dication, **I.19**, the macrocycle did not account for loss of its hydrogens in the process of aromatization. Its tendency for oxidation to a dication by mineral acids is analogous to the chemical property of metals. Therefore, Vogel compared the isophlorin to a "pseudo metal" for its ability to undergo ring oxidation with mineral acids.[23] The isophlorin, **I.21** in the presence of perchloric acid reduces the quinone to phenol, in support of two-electrons oxidation of the macrocycle. Thus, it suggests the possibility of two-electron reduction of the dication back to the neutral macrocycle. The isolated dication, **I.20**, when treated with potassium metal in THF solution underwent the expected reduction further by four electrons to yield the unexpected aromatic 22π tetraoxaporphyrin dianion, **I.22** (Scheme **I.8**).[13] Controlling the reduction process was quite difficult, so the two-electron oxidation of dianion was achieved by passing molecular oxygen at very low temperature. The resultant product tetraoxaisophlorin, **I.21** was crystallized as air sensitive black crystals. Its proton NMR spectrum displayed two sharp

signals at δ −0.64 and 1.98 ppm for the *meso* and furan protons, respectively. The significant upfield chemical shifts for the protons of the furan rings and the *meso* carbon atoms justified the strong paratropic ring current effects expected of an antiaromatic macrocycle. Even though this tetraoxaisophlorin, **I.21**, was not stable under ambient conditions, successful synthesis provided ample confidence to attempt the synthesis of these elusive antiaromatic isophlorins.

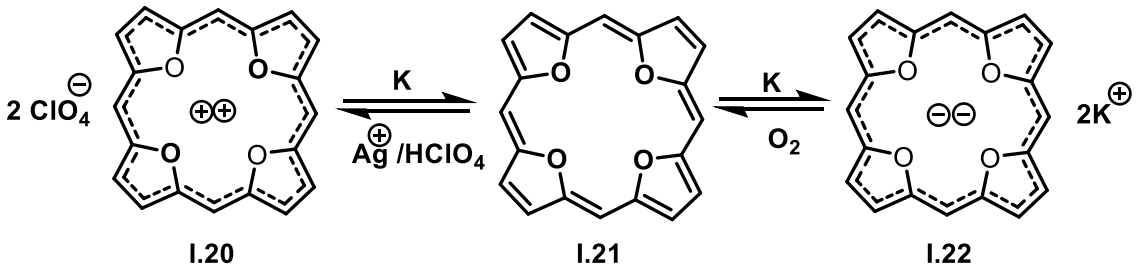

Scheme I.8: Reduction of tetraoxaisophlorin dication into tetraoxaisophlorin and dianion.

I.3.2. Mononuclear Metal Complexes of Isophlorin

Initial attempts at synthesis of isophlorins were mainly based on β-substituted heterocyclic units. With advances in synthetic organic chemistry, accesses to *meso* phenyl substituted porphyrins have increased remarkably. The *meso* substituents effect did not influence the stability of metal complexes, but it affects the reactivity of a metal containing β-substituted as well as *meso* substituted porphyrin complexes. By taking this as an advantage, Vaid and co-workers synthesized isophlorin metal complexes from suitable metal complexes of porphyrins. The antiaromatic 20π [Si(IV)- (tetraphenylisophlorin)](THF)$_2$, **I.24**, was synthesised from [Si(IV)(TPP)Cl$_2$], **I.23**, using sodium amalgam in THF as an air sensitive dark orange crystals (Scheme **I.9**).[24] X-ray diffraction analysis showed a ruffled structure of the isophlorin complex because of the smaller size of Si(IV) in comparison to the cavity of the porphyrin. Due to the presence of four covalent bonds instead of usual two covalent bonds and two dative bonds, the distance between nitrogen and silicon in isophlorin complex, **I.24** was shortened in comparison to the same in porphyrin complexes of silicon. Efforts from the same group resulted in the synthesis of germanium(IV) isophlorin complex by two electron reduction of a germanium porphyrin complex.[25] Direct synthesis of isophlorin−metal complexes relatively requires substantial efforts in comparison with porphyrin−metal complexes. Therefore, by using indirect methods few other dinuclear complexes of isophlorins like dicarbon complex of a isophlorin from a cobalt(II) complex of porphyrin[26] and borene complex of porphyrin were synthesized.[27]

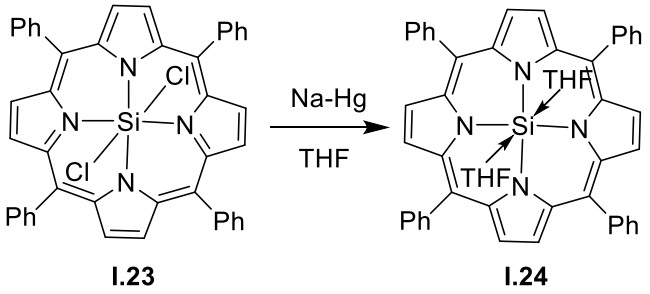

Scheme I.9: Reduction of Si(IV) Porphyrin into Si(IV) Isophlorin.

I.3.3. Stable Isophlorins

Despite the above mentioned macrocycles, the synthesis of pyrrole based isophlorins is still challenging. Chen and co-workers serendipitously discovered the tetra pyrrole isophlorin, **I.26** while reducing a *meso* tetraphenyl porphyrin Cu(II) complex, **I.25,** using zinc powder at room temperature.[28] The strong electron withdrawing trifluoromethyl substituents on the β positions of the pyrrole were enough to boost the macrocycle's electron deficient nature (Scheme **I.10**). X-ray diffraction analysis revealed a saddle-like conformation for the macrocycle, induced by larger out of the plane distortion by trifluoromethyl substituted pyrroles. The nonplanar structure of isophlorin, **I.26** is mainly due to the steric hindrance caused by four hydrogens in the macrocyclic cavity. Both spectroscopic evidence and structural details revealed the structure induced loss of antiaromaticity in the 20π macrocycle.

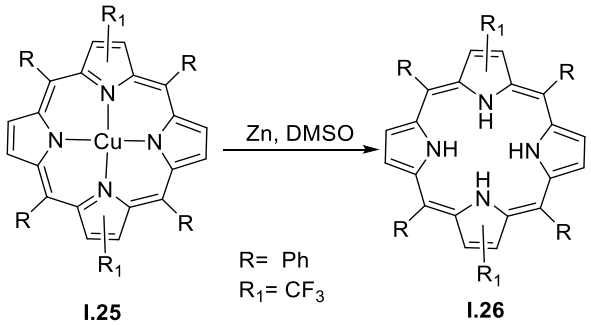

Scheme I.10: Reduction and demetallation of Cu(II) Porphyrin into 20π Isophlorin.

Substituting the nitrogens by other chalcogen atoms can avoid the steric crowding in the center of the cavity. Yet, the synthesised tetrafuran/ thiophene isophlorin were unstable and undergo facile two-electron oxidation into their analogous aromatic dications. Two-electron oxidation of the 20π isophlorin can be minimised by using appropriate electron withdrawing substituents on the macrocycle, as seen for the tetrapyrrole isophlorin, **I.26**. By taking this as an advantage, the tetraoxaisophlorin, **I.27** was synthesised using electron withdrawing pentafluorophenyl group as the *meso* substituent.[29] A singlet at δ 2.49 ppm was observed for

the furan β-hydrogens in the ^{1}H NMR spectrum due to the strong paratropic ring current effect expected of a 4nπ cyclic system. X-ray diffraction analysis of **I.27** showed an absolute planar macrocycle. In an alternative and modified synthetic procedure, furan was reacted with thiophene diol to obtain the dithia-dioxa-isophlorin, **I.28** (Scheme **I.11**). Both spectroscopic evidence and structural details confirmed the antiaromatic character of this core modified 4nπ isophlorin. Unlike the oxidation of tetraoxa isophlorin, **I.21**, to its corresponding dication, **I.20,** neither **I.27** nor **I.28** revealed any such tendency to undergo oxidation to form 18π aromatic species. Addition of strong oxidation agents like DDQ, TFA, or iodine did not oxidize these macrocycles to their respective dications, substantiating its strong stability under ambient conditions, in spite of being antiaromatic in nature. Structurally alike macrocycles synthesized with thiophene did not show expected paratropic ring current effects which was later attributed to its non-planar structure confirmed from its molecular structure.[30]

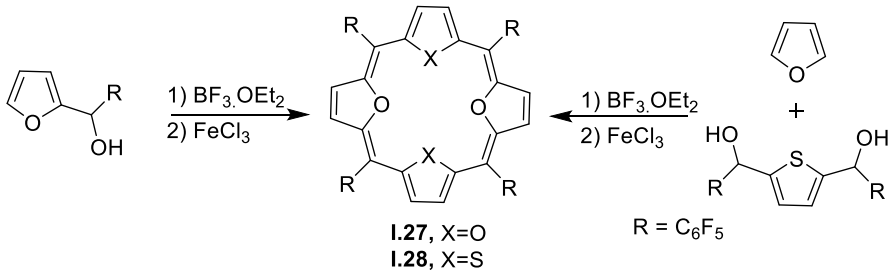

Scheme I.11: Synthesis of *meso*-pentafluorophenyl tetraoxa and dioxa−dithia Isophlorins.

I.4. Expanded Isophlorinoids

Expanding the π–conjugation of core-modified isophlorin is a well-known strategy to synthesize large 4nπ macrocycles. Even though it seems comparable to analogous porphyrinoids, π-delocalised macrocycles synthesised by interlinking the heterocyclic units through bridging carbon atoms whose π-electrons flow only through the carbon atoms are considered as expanded isophlorins.[17] These 4nπ macrocyclic systems are anticipated to have altered properties compared to their aromatic counterparts. The absence of pyrroles units can prevent the amine- imine inter-conversion thus stabilizing the π-conjugation pathway which supports an annulene like cyclic systems.

A 30π hexa furan, **I.29**, and the 40π octa furan, **I.30**, were synthesised by reacting furan with pentafluoro benzaldehyde, under acidic conditions (Scheme **I.12**).[31] Both the macrocycles exhibited complementary ring current effects. The ^{1}H NMR spectrum for hexa furan, **I.29** displayed diatropic ring current effect to confirm its aromatic characteristics. Its molecular

structure revealed the ring inversion of alternate furan units. On the other hand, paratropic ring current effect was observed for octa furan macrocycle, **I.30** and the molecular structure, determined from X-ray diffraction analysis confirmed a planar structure with symmetrical inversions of alternate furan rings. Generally neutral expanded porphyrinoids with eight or more heterocycles coil into a twisted conformation due to their highly fluxional nature. However, the octafuran macrocycle, **I.30**, represents the only example to exhibit a planar topology for a true octaphyrin. By using different synthetic protocol, a series of 30π core modified expanded isophlorins with furan/thiophene/selenophene were synthesized and characterized. These molecules displayed varied structural features based on the topology and number of ring inversions.[32]

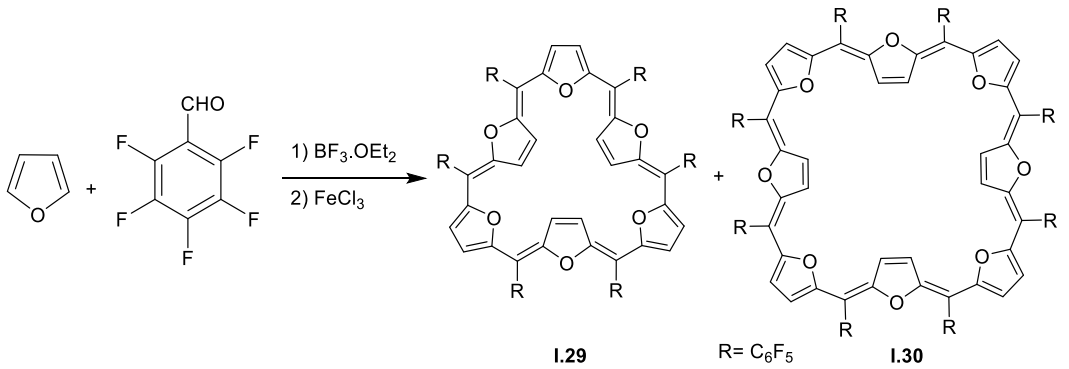

Scheme I.12: One pot synthesis of 30π hexa furan and the 40π octa furan expanded isophlorins.

Apart from the insertion of additional heterocyclic rings to expand the length of the π–conjugated network of isophlorin, additional *meso* carbon bridges can also be employed. Though such examples are very few, yet they significantly improve the unexplored chemistry

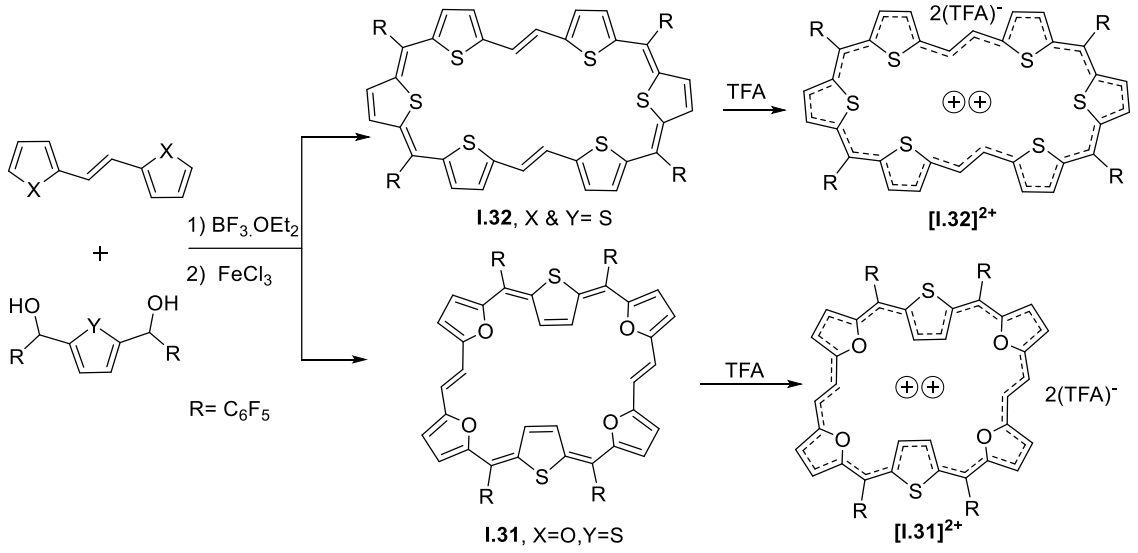

Scheme I.13: Synthesis of ethylene bridged 32π Expanded Isophlorins.

of antiaromatic systems. Inserting two additional *meso* carbons into an isophlorin framework can change the π-count from (4n+2)π to 4nπ systems and vice versa. The synthesis of ethylene linked expanded isophlorins, **I.31** and **I.32**, was carried out by the condensation of bis-thiophene ethylene or bis furan ethylene with appropriate diols of thiophene/ furan/selenophene in acidic condition followed by in situ oxidation (Scheme **I.13**).[33] As expected, the addition of two meso carbons converted the aromatic 30π macrocycle to the antiaromatic 32π expanded isophlorin. The expected paratropic ring current effects were observed in the ^{1}H NMR spectrum at low temperatures and single crystal X-ray diffraction analysis confirmed the planar structure of this macrocycle. This 32π macrocycles undergoes characteristic and reversible two-electron ring oxidation to form 30π dicationic species.[34]

I.5. Redox Active Octaphyrins

The Octaphyrin, **I.33** can show multiple π frameworks varying from 32π to 40π electrons. However, the twisted 36π and 38π are the most predominant configurations observed for the eight pyrrole cyclic structures. In contrast to this, Osuka and co-workers successfully showed ring inversion induced planar conformation for the 36π octaphyrin dianion, **I.35**.[35] With the addition of 40 equiv. of a strong base such as TBAF, they observed only the mono deprotonated octaphyrin, **I.34**, which displayed the characteristic features of a Mobius band. The subsequent addition of large excess of TBAF (7000 equiv) caused the bis deprotonation and resulting dianion, **I.35**, uncoiled to form a planar structure (Scheme **I.14**). X-ray

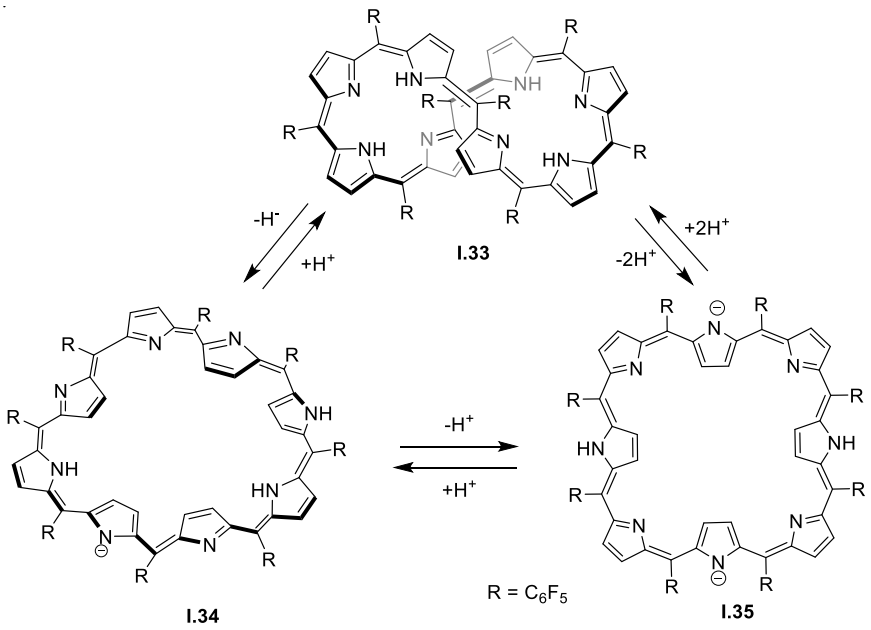

Scheme I.14: Deprotonation of 36π octaphyrin into its planar isophlorin dianion.

diffraction analysis of **I.35** displayed four alternate pyrrole ring inversion, similar to that observed for 40π octa furan, **I.30**.

Core modified expanded porphyrins can be envisaged, by replacing pyrrole rings of macrocycle with other heterocycles, in the octaphyrin framework. Latos and co-workers reported core modified octaphyrins, containing alternate pyrroles and thiophene units with eight *meso* positions.[36] Accordingly, two different core modified octaphyrins having figure-of-eight conformations, with 36π and 38π electrons in their conjugation pathway were observed. These two octaphyrins were inter-convertible between themselves through proton-coupled electron transfer redox reactions. The 36π tetrathiaoctaphyrin, was reduced to 38π octaphyrin, with sodium borohydride and upon oxidation with *p*-chloranil, the 38π octaphyrin was quantitatively dehydrogenated to 36π octaphyrin. Apart from the redox states explained above, two more additional redox states 34π and 40π, can be foreseen for octaphyrin. For an octaphyrin, four discrete species with 34π, 36π, 38π and 40π electrons were observed through redox inter-conversions using a combination of both proton coupled electron-transfer (PCET) and electron-transfer (ET) processes.[37] 36π octaphyrin, **I.37**, was oxidized quantitatively with Meerwein salt to yield 34π dicationic macrocycle, **I.36** and shows the expected diatropic ring current effects in its ^{1}H NMR spectrum. Single crystal X-ray diffraction analysis displayed an unpredicted planar conformation with all the pyrrole rings were found to be inverted similar to the 40π octa furan, **I.30**. Reduction of dication, **I.36** with zinc dust and aqueous ammonium chloride resulted in highly reduced 40π octaphyrin, **I.39**. Single crystal X-ray diffraction studies revealed altered planar topology from a square to a rectangular geometry

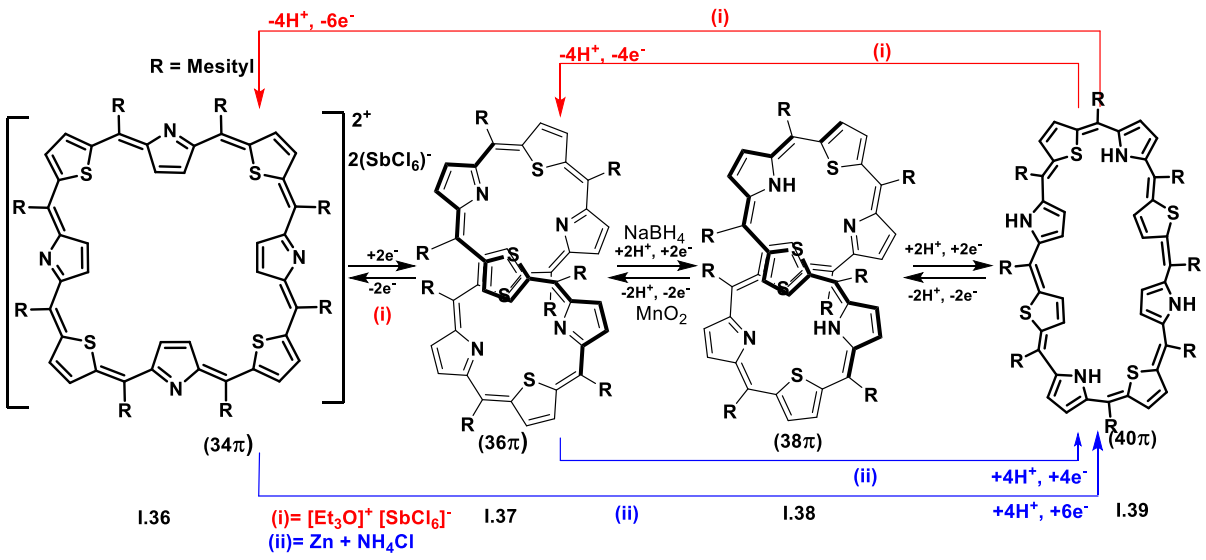

Scheme I.15: Four reversible redox states of tetrathiaoctaphyrin.

for the octaphyrin. This topological modification was observed along with an unusual ring inversion of the heterocyclic rings. On top of the reversible six-electron redox, even four-electron reversible redox between **I.37** and **I.39** was established by using the MnO_2/(Zn + NH_4Cl) couple (Scheme **I.15**).

I.6. Cyclic Oligothiophenes

Cava and co-workers synthesised sulfur bridged annulenes by a new synthetic methodology through McMurry coupling of dialdehydes of thiophene and its oligomers.[38] By employing intermolecular McMurry coupling of 2,5-thiophenedicarboxaldehyde, three thiophene containing trisulfide, **I.40** and the four thiophene containing tetrasulfide, **I.41**, were synthesised (Scheme **I.16**). Both cyclic structures represent a typical annulene-like π-framework with cis ethylene bridges in between the thiophenes. Trisulfide, **I.40** accounts for 18π-electrons with six methine bridges between the three thiophene units and can be considered as smallest of the isophlorin macrocycle. However, its ^{1}H NMR spectrum did not disclose significant diatropic ring currents as predicted of (4n+2)π systems. X-ray diffraction analysis revealed nonplanar structure in which all the three thiophene units deviated from mean plane of the macrocycle. The higher homologue tetrasulfide, **I.41** also did not exhibit any ring current effects, even though it accounted for 4nπ electrons.

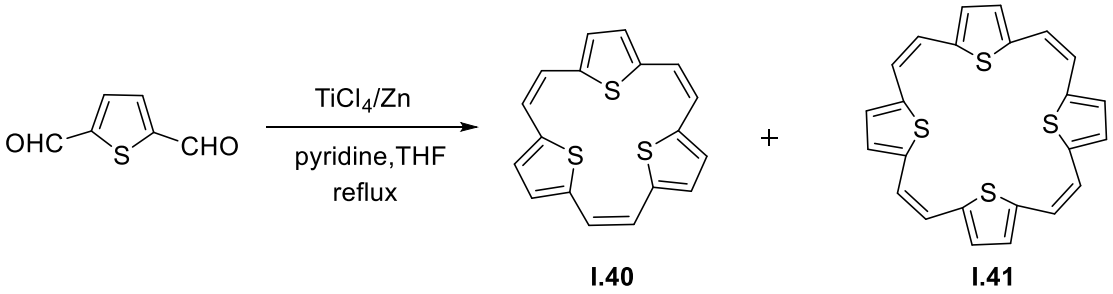

I.40 **I.41**

Scheme I.16: McMurry coupling products of thiophene dialdehyde.

Similarly, the dialdehyde of bithiophene was cyclised at high dilution condition to synthesize 20π and 30π macrocycles, **I.42** and **I.44**, respectively (Scheme **I.17**). 20π tetrathiophene, **I.42**, shows structural resemblance to porphycene, but no ring current effects were observed in ^{1}H NMR spectra. Hexathiophene, **I.44**, can be viewed as structural isomer of 30π expanded isophlorin **I.29**, since both contain six thiophene rings and six *meso* carbon atoms. In contrast to **I.29**, the chemical shift values are much more upfield shifted to indicate the lack of diatropic ring current effects. Further, the cyclization of terthiophene dialdehyde under McMurry reaction conditions yielded the 28π hexathiophene, **I.43**, with two ethylene bridges

(Scheme **I.17**). This moderately stable annulene was found to be non-antiaromatic in nature. However, this macrocycle was successfully oxidized by the addition of sulfuric acid to its corresponding dication. The isolated dication revealed downfield chemical shift values for all its protons in the ^{1}H NMR spectra, suggesting the diatropic ring current effects expected of the 26π system. These neutral sulfur bridged annulenes obviously lack effective delocalization of π electrons and hence exhibited benzenoid like features instead of annulenoid characteristics, despite complete conjugation in the macrocycles.

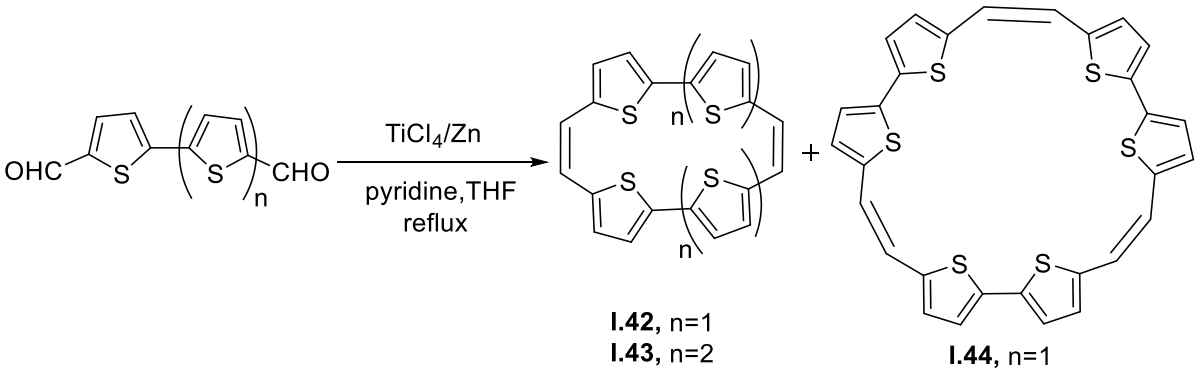

Scheme I.17: McMurry coupling products of bithiophene and terthiophene dialdehyde.

Bauerle and co-workers reported the synthesis of conjugated cyclothiophenes bearing twelve, fourteen and sixteen thiophene units.[39] They have proposed a metal templated approach in which platinum metal was used for synthesis of conjugated cyclo [8-18] thiophenes in higher yields. In this highly effective synthesis, they converted the alkylated oligothiophenes to stannylated intermediate via their corresponding dibromo derivative and later coupled with equimolar amounts of Pt^{II} complex. Finally, the metal was removed through reductive elimination of Pt with C-C bond formation to yield the desired oligothiophene macrocycles. The ^{1}H NMR spectrum of these cyclic oligothiophenes did not display any ring current

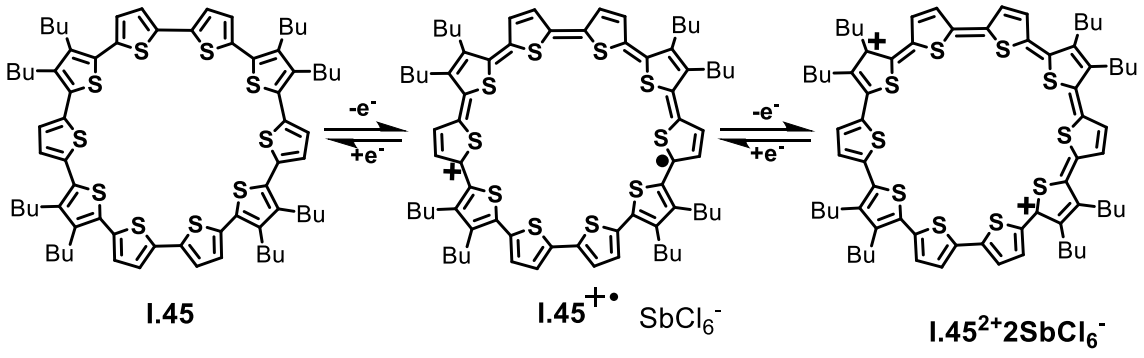

Scheme I.18: Oxidation of cyclo[10]thiophene into its radical cation and dication.

effects indicating the benzenoid character of the macrocycles. These cyclo(n)thiophenes showed unusal electronic states upon oxidation, as demonstrated by absorption and ESR spectroscopy. The cyclo[10]thiophene, **I.45** undergoes one electron oxidation upon addtion of thianthrenium hexachloridoantimonate(V) ($ThiSbCl_6$) to yield the radical cation species (Scheme **I.18**). Further oxidation with more equivalents of $ThiSbCl_6$ resulted in formation of dication species.[40]

In a parallel study, Iyoda's group has explored shape persistent π-expanded oligothiophenes (Scheme **I.19**). Their synthetic approach comprised of Sonogashira and McMurry coupling reactions and acetylene linked thiophenes as precursors.[41] The planarity of these giant macrocycles was maintained due to the proper combination of linking thiophenes with acetylene and ethylene bridges in order the release the strain. Nevertheless, the electronic absorption spectrum for these macrocycles displayed only negligible red shifts in absorption values compare to their increased π-count, suggesting lack of effective conjugation between the adjacent thiophene units. Similar to cyclo(n)thiophenes, oxidised species of these macrocycles also shows interesting characteristics. The 6-mer, **I.46** upon oxidation with $Fe(ClO_4)_3$ formed a dication with 34π-electrons and exhibited large diatropic ring current effect in its ^1H NMR spectrum. In contrast, the 52π dication obtained by the oxidation of 9-mer, **I.47** revealed biradical cationic character instead of Hückel-type cyclic conjugation.[42]

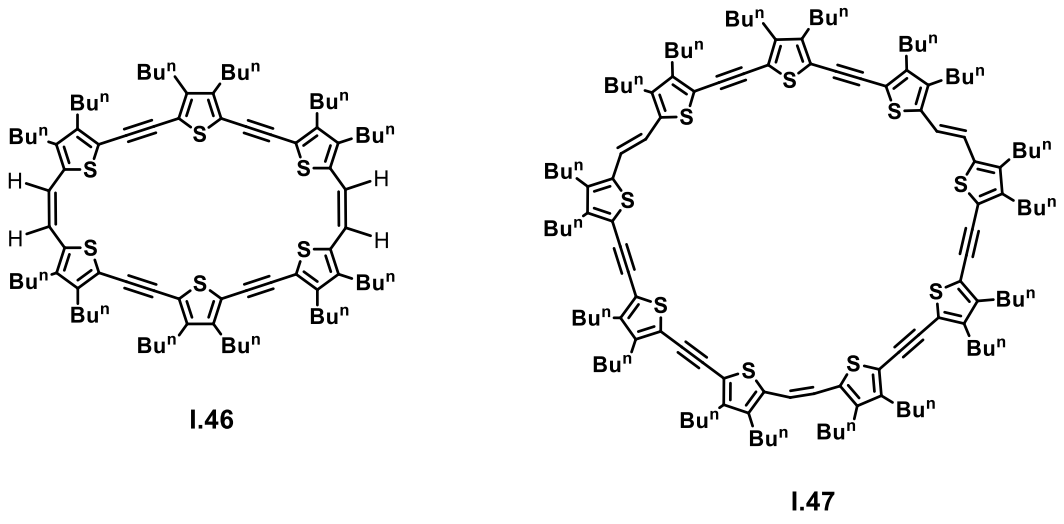

I.46 **I.47**

Scheme I.19: Acetylene and ethylene bridged cyclo(n)thiophenes.

I.7. π-Conjugated Organic Radicals

An expanded macrocycle formed by the insertion of an additional thiophene and a *meso* carbon to the parent tetrathia isophlorin will be forced to accommodate a sp^3 *meso* carbon

which interrupts the continuous flow of the π electrons. However, the pentapyrrolic systems have an uninterrupted π circuit because of the pyrrole's nitrogen ability to alter between amine and imine form. This π framework suffers a major transformation upon replacing all the pyrrole rings by other heterocycles, such as furan/ thiophene/selenophene. Unlike pyrrole, these chalcogens do not sustain a double bond with α carbon in the heterocyclic unit (Scheme **I.20**). This is apparent by the incomplete conjugation of expanded isophlorins with an odd number of heterocyclic rings having equal number of meso carbon bridges.[17]

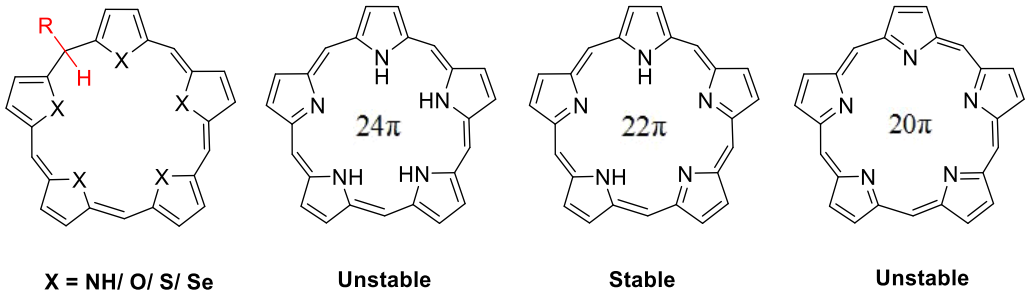

Scheme I.20: Different conjugation pathways for pentaheterocyclic systems.

The acid catalyzed reaction of pyrrole with pentafluoro benzaldehyde, yielded a variety of expanded porphyrins bearing five to twelve pyrrole units.[43] As mentioned previously, all the macrocycles were fully conjugated due to the pyrrole's nitrogen ability to shuttle between amine and imine form. Under similar reaction conditions, thiophene reacts with pentafluoro benzaldehyde to give expanded isophlorinoids having four to ten thiophene units.[44] In contrast to the speculation that expanded isophlorins with odd number of heterocyclic units having equal number of *meso* carbon bridges cannot favour complete conjugation, it came to light that pentathiophene, **I.48** was an absolutely conjugated 25π radical. This stable neutral radical's molecular structure was confirmed through X-ray diffraction analysis. It displayed a planar structure with the unpaired electron delocalized all over the macrocycle. **I.48** demonstrated amphoteric behaviour with suitable redox reagents through single electron transfer (SET) reactions (Scheme **I.21**). It undergoes one electron oxidation into an antiaromatic 24π cation, **I.50**, as well as one electron reduction to an aromatic 26π anion, **I.49**. Both the macrocycles were found to retain its planar structure as confirmed from X-ray diffraction analysis. The expected diatropic and paratropic ring current effects were observed in their ^{1}H NMR spectrum for the aromatic anion and the antiaromatic cation respectively. The synthetic reports on such a stable neutral radical are not very common.[45]

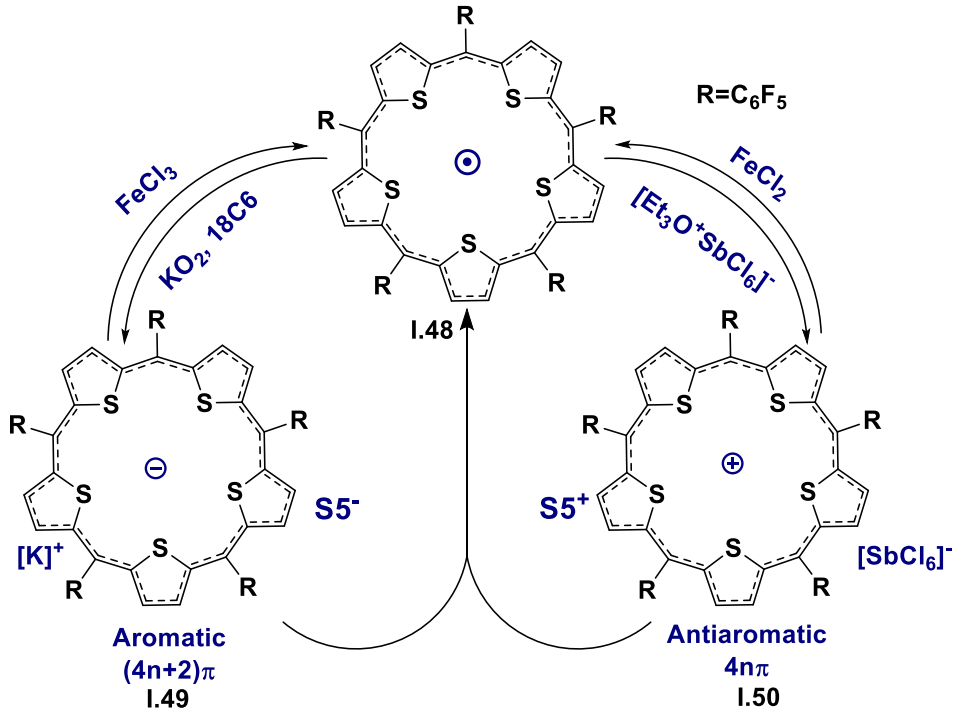

Scheme I.21: Single electron transfer reactions of neutral cyclic pentathiophene radical.

In 1900, Gomberg reported the synthesis of the first ever organic radical, triphenylenemethane and the quest to identify such stable π-conjugated radicals still persist.[46] However, organic molecules with a radical behaviour are short-lived species and very reactive. Yet, few π-conjugated organic radical molecules have displayed a tendency to be stable which is so far assumed based on the Clar's aromatic sextet rule. A classic example is phenalenyl, **I.51**, neutral three-ring triangular hydrocarbon radical, in which one of the 13 π-electrons is unpaired and delocalized among the six carbon atoms.[47] The parent phenalenyl is stable only in oxygen-free solutions and forms a dimer due to the σ-bond-formation reactions. Substituted phenalenyls investigated through X ray diffraction analysis forms π dimers depending on the steric bulk of substituents, which can partially or completely suppress σ

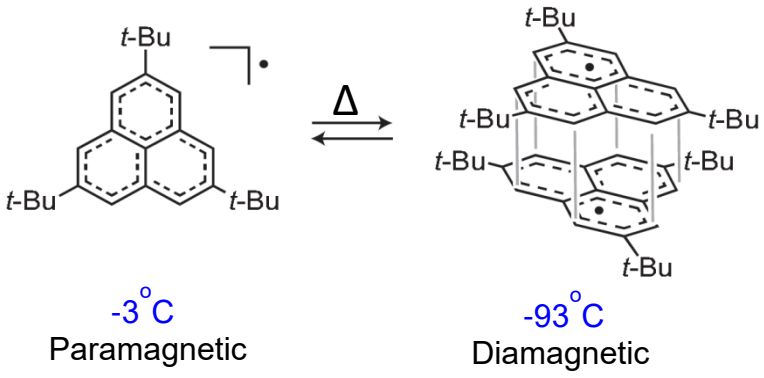

Scheme I.22: π dimerization of phenalenyl radical.

dimerization (Scheme **I.22**).[48-50] Most of π-conjugated radicals reported like triangulene and heteroatom incorporated polycyclic aromatic hydrocarbon radicals suffer because of these kind of dimerization.[51-52]

I.8. 3D (anti)aromaticity and 3D Conjugated Molecules

Aromaticity and antiaromaticity are the important factors which governs the electronic and spectral properties of 2D π-conjugated organic molecules. However, the same concepts were rarely studied in 3D π-conjugated molecules. The basic 3D molecular structures having π-conjugation are limited since the synthesis of these kinds of molecules has been hampered owing to the multistep syntheses, preorganization of monomer units, non-availability of general methods and overall poor yields. Shinokubo and co-workers showed the three-dimensional aromaticity emerging from the close stacking of two antiaromatic π-conjugated macrocycles. They synthesised a cyclophane, **I.52**, employing bithiophene linkers that connect two norcorrole macrocycles (Scheme **I.23**).[53] X-ray diffraction analysis revealed two antiaromatic norcorrole units adopt a stacked face-to-face geometry with an inter planar distance (3.09 Å) shorter than the sum of the van der Waals radii of two sp^2- hybridized carbon atoms (3.4 Å) involved. The close proximity of the two norcorrole units exhibits significant three-dimensional aromaticity that arises from molecular-orbital interactions between the two π-conjugated antiaromatic systems. In ^{1}H NMR analysis, the presence of a diatropic ring current effect confirms the three-dimensional aromaticity in the norcorrole cyclophane, **I.52**. The same group recently reported one more cyclophane, **I.53** containing two antiaromatic norcorrole units tethered with two flexible alkyl chains.[54] This cyclophane, **I.53** displayed crystal polymorphism with three different molecular structures and the similar three-dimensional aromaticity like **I.52**.

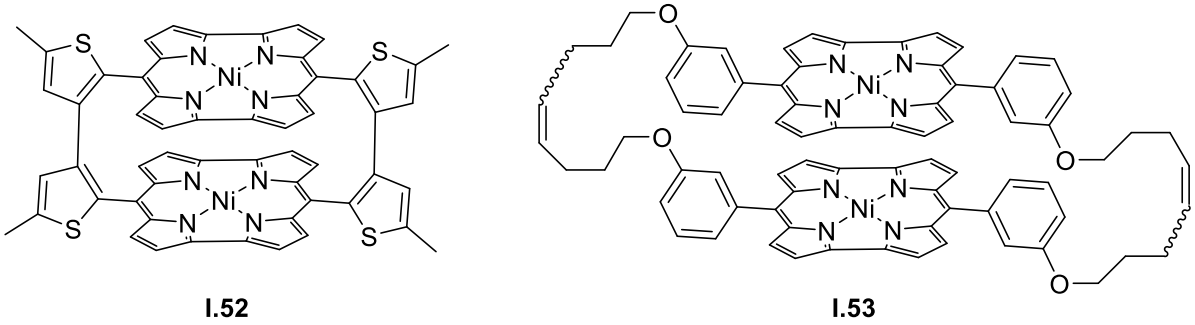

I.52 **I.53**

Scheme I.23: Structures of Norcorrole cyclophanes having 3D aromaticity.

Recently an all thiophene fully conjugated diradicaloid molecular cage was reported and its global aromaticity and antiaromaticity was explored at different oxidation states. The synthesized diradicaloid cage **I.54,** comprises of 12 conjugated thiophene units and eight methine linkages.[55] It was chemically oxidised by two, four and six equivalents of $NO.SbF_6$ to give the corresponding dication, tetracation and hexacation respectively. Different types of aromaticity were exhibited by these cages as tabulated below, subject to the symmetry, number of π-electrons and spin state (Scheme **I.24**).

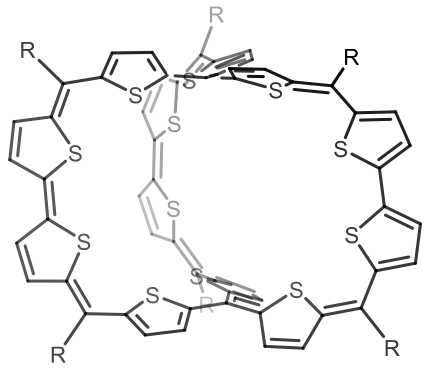

I.54 **R= Mesityl**

Neutral	(4n+2)π Huckel Aromaticity
Dication	4nπ Baird Aromaticity
Tetracation	4nπ 3D global antiaromaticity
Hexacation	(4n+2)π 3D global l Aromaticity

Scheme I.24: All thiophene molecular cage and its aromaticity at different oxidation states.

Sessler and co-workers serendipitously identified a 3D Carbaporphyrin Cage, **I.55,** molecule during the synthesis of cabaporphyrin macrocycle from the condensation of tetrapyrrole precursor and pentafluorobenzaldehyde.[56] ^{1}H NMR spectroscopy inferred the non-aromatic character for this cage molecule, **I.55.** In contrast, after oxidation with trifluoroacetic acid, the cage gained 3D global aromaticity. Itami and co-workers reported all-benzene carbon nanocages, **I.56,** 3D cage-shaped conjugated hydrocarbons comprising of only sp^2-carbons. The [n.n.n] carbon nanocages, **I.56**, contains three [n]paraphenylene bridges coupled by two benzene-1,3,5-triyl bridgeheads.[57] Yamago and co-workers reported a 3D, spherical π-

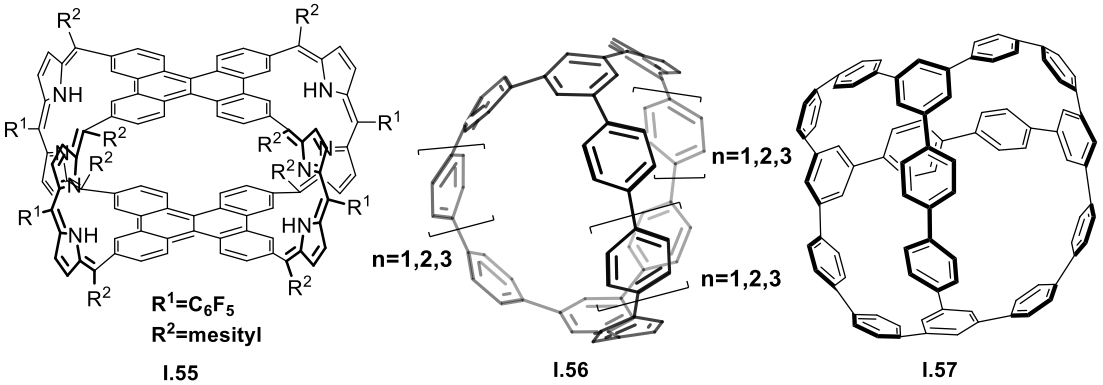

I.55 **I.56** **I.57**

Scheme I.25: Structures of 3D Carbaporphyrin Cage and all benzene carbon nanocages.

conjugated molecule, **I.57**, in which all the sp^2-carbons of 1,4- disubstituted and 1,3,5-trisubstituted benzenes are covalently bonded to give a ball-like molecule.[58] The synthesis involved the formation of assembly of four molecules of a stannylated trisubstituted benzene derivative creating an octahedral shaped hexanuclear platinum complex from which reductive elimination of platinum gave the 3D π-conjugated molecule, **I.57** (Scheme **I.25**).

I.9. Conclusions

From the examples discussed above, it is evident that the isophlorin chemistry has unveiled the diversity in terms of structure and reactivity. The synthesis of stable 20π isophlorins and their expanded derivatives contradicts the so-called instability of antiaromatic structures. The nature of heteroatoms and substituents on the *meso* carbons plays a pivotal role in giving stability to the isophlorins. The diverse structural topographies of these antiaromatic molecules such as planar, figure-of-eight and ruffled geometries demonstrate the significance of planarity even in 4nπ systems. A ruffled and figure-of-eight conformation shows the structure induced loss of paratropic ring current effects. On the other hand, heterocyclic ring inversion prevents winding of the macrocycle into a nonplanar geometry. These anti-aromatic 4nπ systems show dissimilar reactivity with oxidizing agents in comparison to the aromatic systems. Reversible two-electron oxidation of isophlorins to their corresponding aromatic dications has been the hallmark of these 4nπ systems. There are number of unexplored features of antiaromatic isophlorinoids, which ideally could be revealed in parallel to porphyrinoids. In this context, this thesis describes the synthesis, structural characterization and redox properties of expanded isophlorinoids derived from thiophene subunits. Majority of the expanded isophlorins composed of ethenylene and ethynylene links with varying number of thiophene units have disadvantages like laborious and multistep synthesis approach and lack of effective conjugation of the π circuit. So attempts were made using a very few ethenylene and ethynylene bridges and ring inverted heterocyclic unit like α-α coupled thiophene to synthesise a true anti-aromatic expanded isophlorins. Further, development of novel synthetic protocol for the synthesis 3D isophlorinoid cage molecules will be described in the following chapters.

I.10. References

1. Sondheimer, F., *Acc. Chem. Res.* **1972,** *5,* 81-91.
2. Spitler, E. L.; Johnson, C. A.; Haley, M. M., *Chem. Rev.* **2006,** *106,* 5344-5386.

3. Breslow, R., *Acc. Chem. Res.* **1973,** *6,* 393-398.

4. Sondheimer, F., *Pure. Appl. Chem.* **1963**, *7*, 363.

5. Sondheimer, F., *Chem. Soc., Spec. Publ.,* **1967**, *21*, 75.

6. McQuilkin, R. M.; Metcalf, B. W.; Sondheimer, F., *J. Chem. Soc. D: Chem. Commu.,* **1971,** 338-339.

7. Oth, J. F. M.; Gilles, J. M., *Tetrahedron. Lett.* **1968,** *9,* 6259-6264.

8. Calder, I. C.; Sondheimer, F., *Chem. Comm.* **1966,** 904-905.

9. Sondheimer, F.; Robert A. W., *Found. Conf. Chem. Res.,* **1968**, *12*, 125.

10. Vogel, E.; Roth, H. D., *Angew. Chem., Int. Ed.* **1964,** *3,* 228-229.

11. Vogel, E., *Pure. Appl. Chem.,* **1990**, *62*, 557.

12. Vogel, E.; Pretzer, W.; Böll, W. A., *Tetrahedron. Lett.* **1965,** *6,* 3613-3617.

13. Vogel, E., *Pure. Appl. Chem.,* **1993,** *65,* 143.

14. Woodward, R. B., *Angew. Chem.* **1960,** *72,* 651-662.

15. Ghosh, A., *Angew. Chem., Int. Ed.* **2004,** *43,* 1918-1931.

16. Narita, A.; Wang, X.-Y.; Feng, X.; Müllen, K., *Chem. Soc. Rev.* **2015,** *44,* 6616-6643.

17. Reddy, B. K.; Basavarajappa, A.; Ambhore, M. D.; Anand, V. G., *Chem. Rev.* **2017,** *117,* 3420-3443.

18. Franck, B., *Angew. Chem., Int. Ed.* **1982,** *21,* 343-353.

19. Pohl, M.; Schmickler, H.; Lex, J.; Vogel, E., *Angew. Chem., Int. Ed.* **1991,** *30,* 1693-1697.

20. Haas, W.; Knipp, B.; Sicken, M.; Lex, J.; Vogel, E., *Angew. Chem., Int. Ed.* **1988,** *27,* 409-411.

21. Vogel, E.; Rohrig, P.; Sicken, M.; Knipp, B.; Herrmann, A.; Pohl, M.; Schmickler, H.; Lex, J., *Angew Chem Int Edit* **1989,** *28,* 1651-1655.

22. Vogel, E.; Frode, C.; Breihan, A.; Schmickler, H.; Lex, J., *Angew. Chem., Int. Ed.* **1997,** *36,* 2609-2612.

23. Vogel, E.; Haas, W.; Knipp, B.; Lex, J.; Schmickler, H., *Angew. Chem., Int. Ed.* **1988,** *27,* 406-409.

24. Cissell, J. A.; Vaid, T. P.; Rheingold, A. L., *J. Am. Chem. Soc.* **2005,** *127,* 12212-3.

25. Cissell, J. A.; Vaid, T. P.; Yap, G. P., *J. Am. Chem. Soc.* **2007,** *129,* 7841-7.

26. Vaid, T. P., *J. Am. Chem. Soc.* **2011,** *133,* 15838-41.

27. Weiss, A.; Hodgson, M. C.; Boyd, P. D. W.; Siebert, W.; Brothers, P. J., *Chem. Eur. J.* **2007,** *13,* 5982-5993.

28. Liu, C.; Shen, D.-M.; Chen, Q.-Y., *J. Am. Chem. Soc.* **2007,** *129,* 5814-5815.

29. Reddy, J. S.; Anand, V. G., *J. Am. Chem. Soc.* **2008,** *130,* 3718-3719.

30. Kon-no, M.; Mack, J.; Kobayashi, N.; Suenaga, M.; Yoza, K.; Shinmyozu, T., *Chem. Eur. J.* **2012,** *18,* 13361-71.

31. Reddy, J. S.; Mandal, S.; Anand, V. G., *Org. Lett.* **2006,** *8,* 5541-5543.

32. Reddy, J. S.; Anand, V. G., *J. Am. Chem. Soc.* **2009,** *131,* 15433-15439.

33. Gopalakrishna, T. Y.; Reddy, J. S.; Anand, V. G., *Angew. Chem., Int. Ed.* **2013,** *52,* 1763-1767.

34. Gopalakrishna, T. Y.; Anand, V. G., *Angew. Chem., Int. Ed.* **2014,** *53,* 6678-6682.

35. Cha, W.-Y.; Soya, T.; Tanaka, T.; Mori, H.; Hong, Y.; Lee, S.; Park, K. H.; Osuka, A.; Kim, D., *Chem. Comm.* **2016,** *52,* 6076-6078.

36. Sprutta, N.; Latos-Grażyński, L., *Chem. Eur. J.* **2001,** *7,* 5099-5112.

37. Ambhore, M. D.; Basavarajappa, A.; Anand, V. G., *Chem. Comm.* **2019,** *55,* 6763-6766.

38. Hu, Z. Y.; Atwood, J. L.; Cava, M. P., *J. Org. Chem.* **1994,** *59,* 8071-8075.

39. Krömer, J.; Rios-Carreras, I.; Fuhrmann, G.; Musch, C.; Wunderlin, M.; Debaerdemaeker, T.; Mena-Osteritz, E.; Bäuerle, P., *Angew. Chem.* **2000,** *39,* 3481-3486.

40. Zhang, F.; Götz, G.; Mena-Osteritz, E.; Weil, M.; Sarkar, B.; Kaim, W.; Bäuerle, P., *Chem. Sci.* **2011,** *2,* 781-784.

41. Nakao, K.; Nishimura, M.; Tamachi, T.; Kuwatani, Y.; Miyasaka, H.; Nishinaga, T.; Iyoda, M., *J. Am. Chem. Soc.* **2006,** *128,* 16740-7.

42. Iyoda, M.; Tanaka, K.; Shimizu, H.; Hasegawa, M.; Nishinaga, T.; Nishiuchi, T.; Kunugi, Y.; Ishida, T.; Otani, H.; Sato, H.; Inukai, K.; Tahara, K.; Tobe, Y., *J. Am. Chem. Soc.* **2014,** *136,* 2389-2396.

43. Shin, J.-Y.; Furuta, H.; Yoza, K.; Igarashi, S.; Osuka, A., *J. Am. Chem. Soc.* **2001,** *123,* 7190-7191.

44. Gopalakrishna, T. Y.; Reddy, J. S.; Anand, V. G., *Angew. Chem., Int. Ed.* **2014,** *53,* 10984-10987.

45. Morita, Y.; Nishida, S. In Stable Radicals; John Wiley & Sons: 2010.

46. Gomberg, M., *J. Am. Chem. Soc.* **1900,** *22,* 757-771.

47. Goto, K.; Kubo, T.; Yamamoto, K.; Nakasuji, K.; Sato, K.; Shiomi, D.; Takui, T.; Kubota, M.; Kobayashi, T.; Yakusi, K.; Ouyang, J., *J. Am. Chem. Soc.* **1999,** *121,* 1619-1620.

48. Morita, Y.; Ohba, T.; Haneda, N.; Maki, S.; Kawai, J.; Hatanaka, K.; Sato, K.; Shiomi, D.; Takui, T.; Nakasuji, K., *J. Am. Chem. Soc.* **2000,** *122,* 4825-4826.

49. Koutentis, P. A.; Chen, Y.; Cao, Y.; Best, T. P.; Itkis, M. E.; Beer, L.; Oakley, R. T.; Cordes, A. W.; Brock, C. P.; Haddon, R. C., *J. Am. Chem. Soc.* **2001,** *123,* 3864-3871.

50. Suzuki, S.; Morita, Y.; Fukui, K.; Sato, K.; Shiomi, D.; Takui, T.; Nakasuji, K., *J. Am. Chem. Soc.* **2006,** *128,* 2530-2531.

51. Ueda, A.; Wasa, H.; Suzuki, S.; Okada, K.; Sato, K.; Takui, T.; Morita, Y., **2012,** *51,* 6691-6695.

52. Ravat, P.; Blacque, O.; Juríček, M., *J. Org. Chem.* **2020,** *85,* 92-100.

53. Nozawa, R.; Kim, J.; Oh, J.; Lamping, A.; Wang, Y.; Shimizu, S.; Hisaki, I.; Kowalczyk, T.; Fliegl, H.; Kim, D.; Shinokubo, H., *Nat. Comm.* **2019,** *10,* 3576.

54. Kawashima, H.; Ukai, S.; Nozawa, R.; Fukui, N.; Fitzsimmons, G.; Kowalczyk, T.; Fliegl, H.; Shinokubo, H., *J. Am. Chem. Soc.* **2021,** *143,* 10676-10685.

55. Ni, Y.; Gopalakrishna, T. Y.; Phan, H.; Kim, T.; Herng, T. S.; Han, Y.; Tao, T.; Ding, J.; Kim, D.; Wu, J., *Nat. Chem.* **2020,** *12,* 242-248.

56. Ke, X.-S.; Kim, T.; He, Q.; Lynch, V. M.; Kim, D.; Sessler, J. L., *J. Am. Chem. Soc.* **2018,** *140,* 16455-16459.

57. Matsui, K.; Segawa, Y.; Itami, K., *J. Am. Chem. Soc.* **2014,** *136,* 16452-16458.

58. Kayahara, E.; Iwamoto, T.; Takaya, H.; Suzuki, T.; Fujitsuka, M.; Majima, T.; Yasuda, N.; Matsuyama, N.; Seki, S.; Yamago, S., *Nat. Comm.* **2013,** *4,* 2694.

CHAPTER II

Synthesis of (4n+1)π Isophlorin Radical and Redox Properties

II.1. Introduction

By replacing one of the pyrrole units or *meso* carbon atoms by other substituents, variety of porphyrins and expanded porphyrins were synthesised.[1] Among the range of substituents used, an acetylene−cumulene moiety presents the unique structural pattern to the porphyrinoid skeleton (scheme **II.1**).[2-4] Though, the annulene−cumulene unit have been successfully incorporated into aromatic porphyrinoids and expanded porphyrinoids, examples of including acetylene−cumulene moieties to the antiaromatic isophlorins are very rare.[5] Even in the reported ethyne porphyrins, incorporation of -C≡C- was not straight forward and it could be achieved only through multiple synthetic steps. The reported porphyrinoids with acetylene−cumulene units in their conjugation pathway display different electronic and coordination properties than parent porphyrinoids. Therefore, synthesis of acetylene embedded isophlorins with minimal synthetic steps will be challenging and they have the potential to exhibit different ligating, electronic and redox properties.

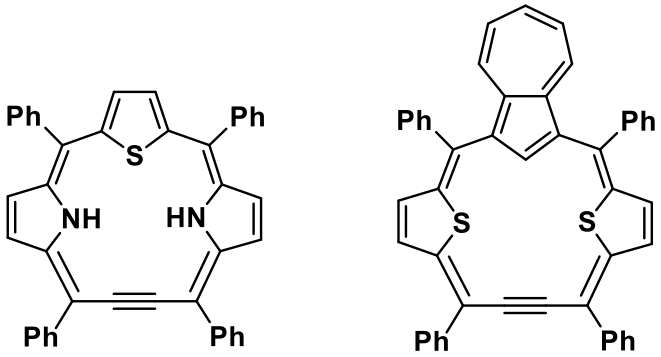

Scheme II.1: Acetylene−cumulene containing poprphyrinoids.

A variety of expanded isophlorins can be synthesised by simply expanding the π-conjugated skeleton of the macrocycle. These expanded macrocycles rigid structural framework and effective conjugation provides a unique opportunity to study the effect of double and triple bonds in antiaromatic molecules. Along with the insertion of additional heterocyclic rings to expand the π network of isophlorin, π conjugation pathway can be extended by replacing few of the *meso* carbon atoms with acetylene linkages. Iyoda and co-workers have reported the synthesis of macrocycles composed of ethenylene and ethynylene links with varying number of thiophene units between twelve and thirty in a given macrocyclic framework (scheme **II.2**).[6-7] These macrocycles required functionalized precursor units and were cyclized through a Wittig type condensation. Irrespective of such extended conjugation, none of these molecules could display effective delocalization of π-electrons. The reason was evident from their electronic absorption spectrum, as they displayed only a small increment in red shifts

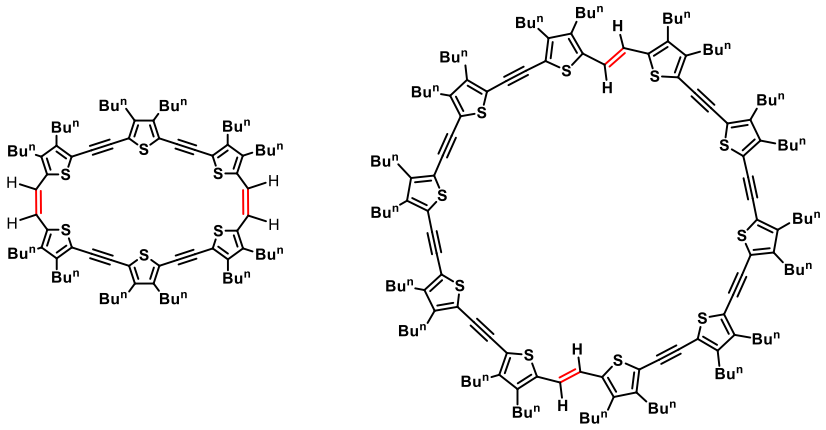

Scheme II.2: Ethenylene and ethynylene inserted oligothiophene macrocycles.

relative to their increased π-conjugation path way. The synthetic procedure used for the above mentioned macrocycles is very tedious due to the multistep synthetic approach. Therefore, synthesising expanded isophlorins with effective conjugation by increasing *meso* links by employing simpler synthetic methodology from easy to make precursors is still a challenging task. Therefore, a synthetic methodology was designed such that acetylene bridge between the thiophene units was introduced in one of the precursors by using modified sonogashira coupling reaction 1,2-di(thiophen-2-yl)ethyne, **II.1** was synthesised.[8]

II.2 Synthesis

Ethylene bridged expanded 32π isophlorins can be synthesised by adopting a modified Rothemund-type synthesis, from 1,2-di(thiophen-2-yl)ethene and diols of five-membered heterocycles.[9] In a process similar to this, acetylene bridged bis-thiophene, **II.1** was condensed with diol of thiophene **II.2**,[10] under dilute conditions (Scheme **II.3**). An equimolar concentration of thiophene diol and the corresponding acetylene bridged thiophene were dissolved in 100 ml dry dichloromethane and degassed with argon for ten minutes. Then, a catalytic amount of boron trifluoride diethyl etherate ($BF_3.OEt_2$) was added through a syringe under dark. After stirring for an hour, two equivalents of DDQ were added and stirring

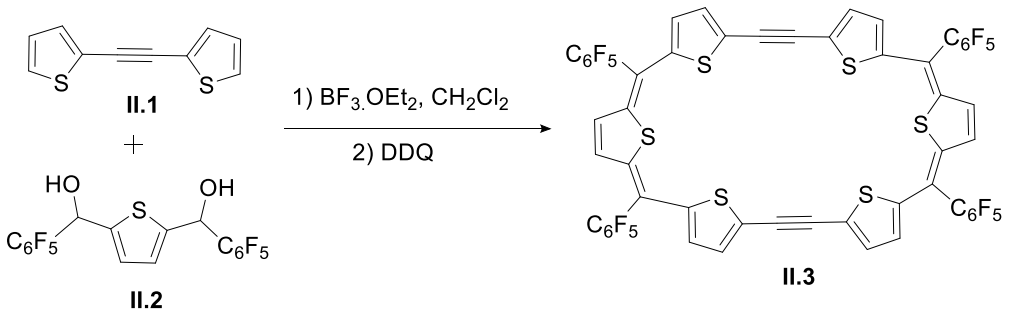

Scheme II.3: Synthesis of 32π expanded isophlorins.

continued for an additional two hours. Then, few drops of triethyl amine were added and the resultant solution was passed through a short basic alumina column. In contrast, the MALDI-TOF/TOF mass spectrum of this reaction mixture (fig. **II.1**) revealed *m/z* value corresponding to 1516.5691 instead of the expected macrocycle, **II.3** (*m/z* 1255.8944). Yet, the mixture was concentrated and further purified by silica gel column chromatography using CH_2Cl_2/hexane as eluent.

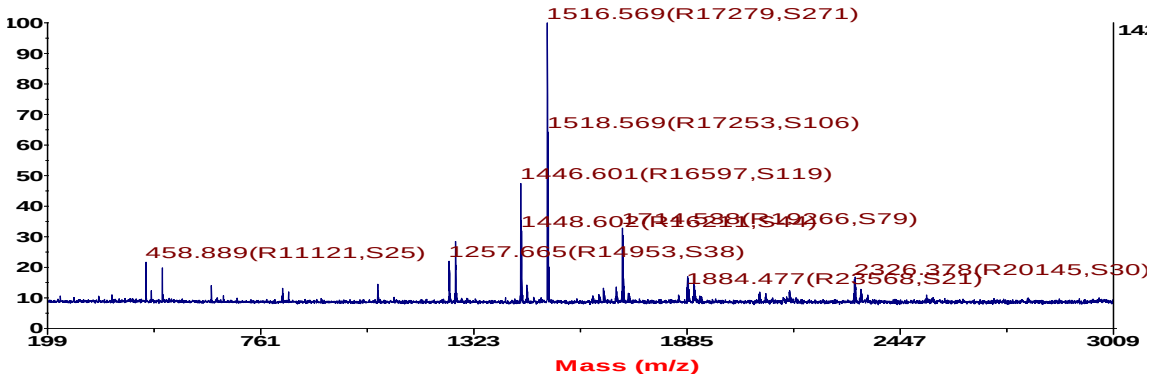

Figure II.1: MALDI TOF-TOF spectrum of reaction mixture.

II.3. Isolation and Characterization of radical macrocycle

The product, **II.4,** in its high resolution mass spectrum displayed an *m/z* value of 1516.8701 instead of the expected 1255.8944. It suggested the formation of higher membered macrocycle than the expected 32π macrocycle. As no such acetylene precursors have been employed in condensation reactions for expanded porphyrnoids, it could be suspected that the acetylene precursor's reactivity for the formation of unexpected product. Yet, the isolated product formed pink coloured solution when dissolved in common organic solvents. It displayed intensive colour perhaps due to the extensive conjugation and was found to absorb in the visible region at 546 nm (ε = 50330) (fig. **II.2**)

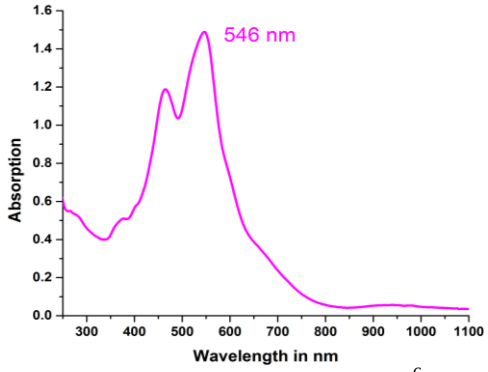

Figure II.2: Uv-visible absorption spectrum of 10^{-6} M solution of **II.4** in $CHCl_3$.

^{1}H NMR spectroscopy is an ideal analytical tool to elucidate the structure of the compound. But, surprisingly, the ^{1}H NMR spectrum did not show any signal corresponding to the

isolated product either at room temperature or even at low temperature. The absence of NMR signals even at low temperature suggests the possibility of paramagnetic nature of the product. Electron Paramagnetic Resonance (EPR) spectrum recorded at room temperature and at 77 K displayed a broad singlet with g = 2.0036, confirming the formed product as an organic radical (fig. **II.3**).

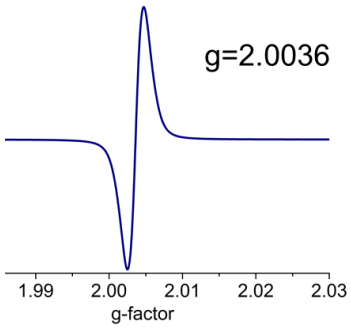

Figure II.3: Electron Paramagnetic Resonance (EPR) spectrum of **II.4.**

To confirm the molecular structure of **II.4**, good quality crystals of the isolated product were grown in chloroform-methanol solvent system employing solvent diffusion method. From single crystal X-ray diffraction analysis, an unprecedented molecular structure with cyclopentathiophene core was revealed for the isolated macrocycle (fig. **II.4**). The unexpected product, **II.4**, was having totally seven thiophene units with five pentafluorophenyl meso substituents. Among the seven thiophene units, sulfur atoms of the five thiophenes pointed towards the center of the macrocycle and two remaining thiophene units were tethered orthogonally to the cyclopentathiophene core through an unprecedented fused five membered carbon ring. All the meso pentafluorophenyl rings were found near

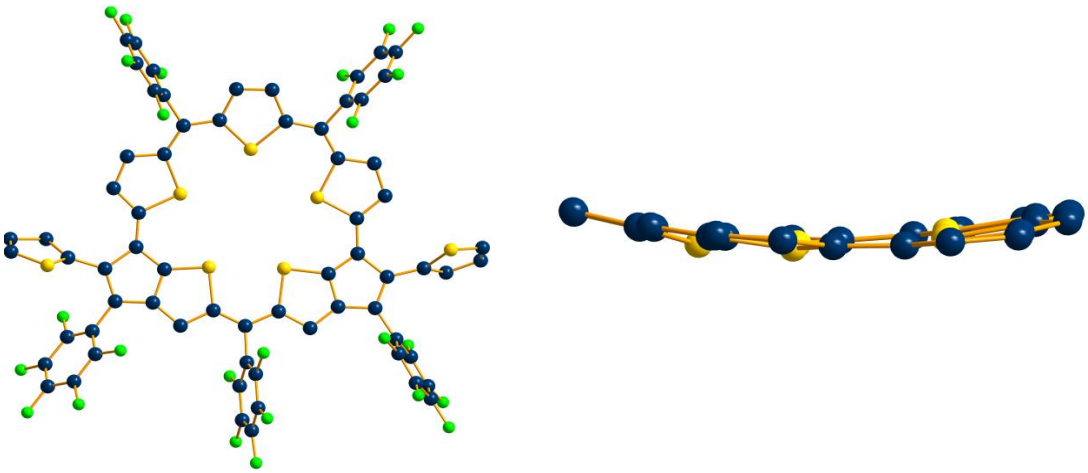

Figure II.4: Molecular structure of **II.4** top view (left) and side view (right).

orthogonal with respect to the plane of the macrocycle defined by the five meso carbon atoms. Molecular structure of **II.4** shows a slight deviation from absolute planar conformation along the molecular plane defined by the five *meso* carbons. This molecular structure with a fused planar pentaphyrin type system is the first example for the class of fused porphyrinoid radical with five heterocyclic units.

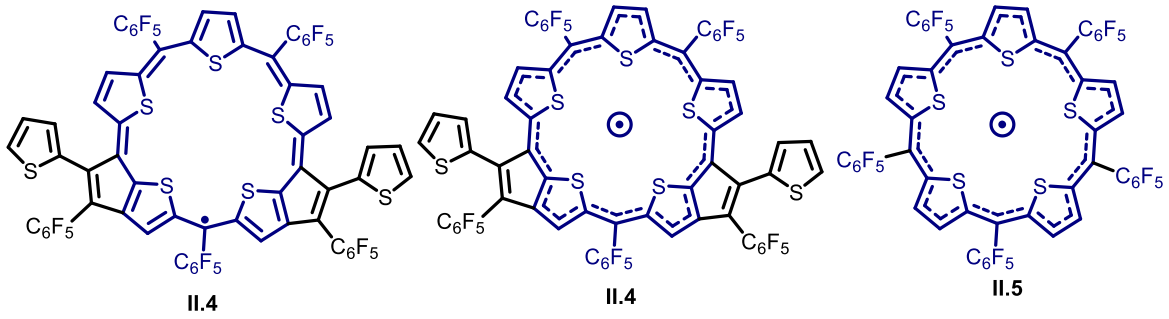

Scheme II.4: Structures of radical macrocycles **II.4** and **II.5.**

The paramagnetic behaviour of molecule, **II.4**, is mainly attributed to the cyclic pentathiophene 25π electrons core unit. The pentathiophene macrocycle, **II.5**, was identified as an absolutely conjugated stable neutral radical exhibited a planar structure with the unpaired electron delocalized all over the macrocycle (scheme **II.4**). It also demonstrated amphoteric properties with appropriate redox reagents through single electron transfer (SET) reactions.[11] Similar to **II.4**, the newly isolated macrocycle, **II.4**, also demonstrated effective delocalization of 25π electrons along its conjugated framework and doesn't belong to either aromatic (4n+2)π, nor antiaromatic 4nπ type of molecules. Computational calculations further support the delocalisation of unpaired electron in the cyclic pentathiophene core. The spin density diagram obtained from unrestricted DFT calculations (UB3LYP/6-31G (d,p))

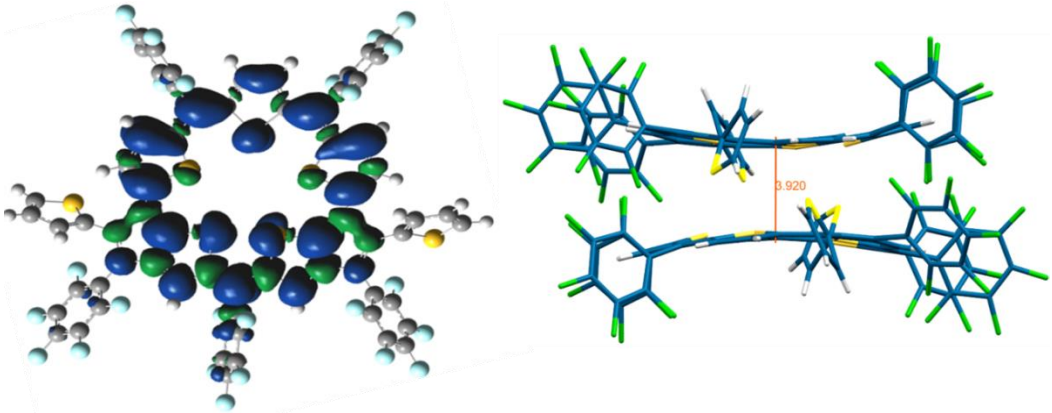

Figure II.5: Spin density diagram of **II.4** and sandwich type of crystal packing with weak π-π interaction.

shows the delocalization of electron spin density only over pentathiophene cyclic system. The crystal packing displays a sandwich type of very weak π-π interaction with an inter planar distance of 3.96 Å between two molecules (fig. **II.5**). But this π-π interaction is not strong enough to antiferromagnetically couple the two unpaired electrons as observed in the case of dimer of phenyalene radical at lower temperatures.[12] This can be partially attributed to the poor π-π interaction due to the near orthogonal orientation of the meso pentaflurophenyl groups.

II.4. Redox properties of neutral radical

Being a neutral radical, it can be expected that such systems will be responsive to one electron redox reactions. In fact, the 25π open-shell molecule **II.5** undergoes one electron oxidation reaction to form 24π cation as well as one electron reduction to yield the 26π anion. Further, these oxidation and reduction processes were reversible in nature.[11] These obtained cation and anion acts as mutual redox couple and upon mixing because of the comproportionation reaction forms stable neutral radical **II.5**. Due to a very identical core structure, a similar redox reaction can be expected from **II.4**. Preliminary cyclic voltammetric studies for the **II.4** revealed two oxidation waves at +0.63 V and +1.30 V, along with two reduction waves at -0.55 V and -0.91 V. All these potentials were further confirmed by differential pulse voltammetry (fig. **II.6**). Further to examine the distinct oxidised and reduced species, spectroelectrochemical measurements were recorded for the electrochemically oxidized and reduced species.

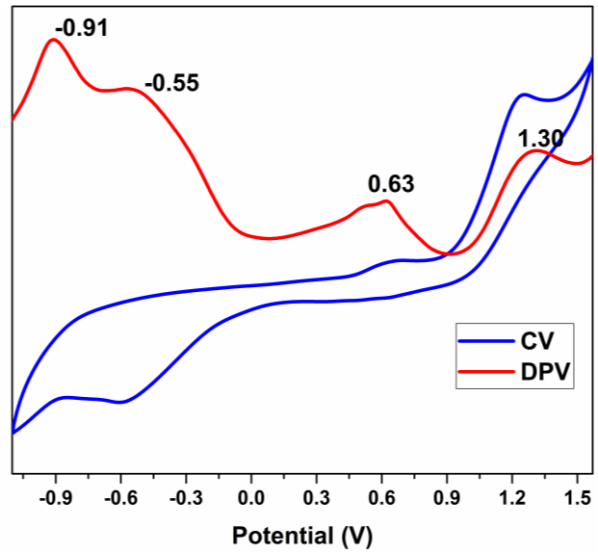

Figure II.6: Cyclic voltammogram (CV, blue) and differential pulse voltammogram (DPV, red) of **II.4** in CH_2Cl_2 (with 0.1 M Bu_4NPF_6 as the supporting electrolyte).

Changes in the absorption were monitored through electrochemical oxidation and reduction of **II.4** at two different potentials as observed in the cyclic voltammogram. At a reduction potential of -0.63 V, a red shifted absorption maximum at 626 nm and a low energy band at 870 nm was observed (fig. **II.7**). Upon applying an oxidation potential of +0.8 V, the absorption maxima of the parent neutral radical molecule progressively disappeared and a blue shifted, intense sharp peak was observed at a lower wavelength value of 497 nm.

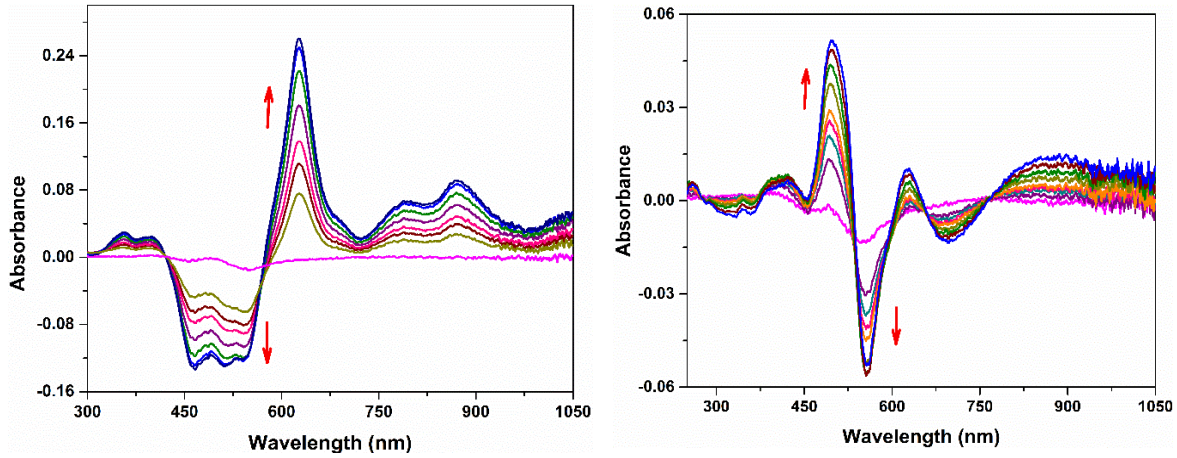

Figure II.7: Changes in absorption spectra of **II.4** upon applying a potential of -0.63 V (left) and 0.8 V (right), respectively.

In support of the spectroelectrochemical studies, suitable redox reagents were employed to confirm the redox behaviour of **II.4** by synthesising corresponding 24π antiaromatic monocation and 26π aromatic monoanion species. At first, a one-electron reduction of **II.4** was attempted with potassium superoxide in the presence of 18-crown-6 (scheme **II.5**). Addition of potassium superoxide to a solution of **II.4** in DMSO, imparts a subtle colour change from pink to blue. The blue coloured solution of **[II.4]**$^-$ revealed an intense and a red shifted broad absorption at 622 nm with a low energy band at 870 nm suggesting the aromatic characteristics of the formed anion macrocycle (fig. **II.8**). A new peak that was detected in

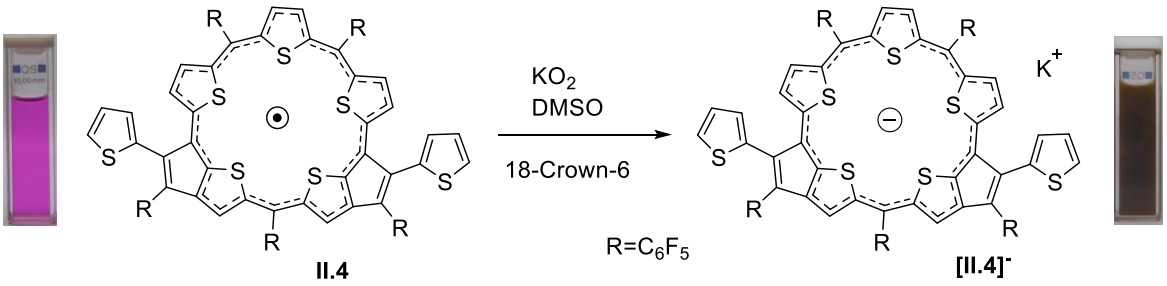

Scheme II.5: One electron reduction of **II.4.**

the absorption spectra upon chemical reduction was similar to that found in electro-reduction of the neutral radical macrocycle. Therefore, it confirmed the formation of anionic species in both chemical and electrochemical processes.

Similarly, one-electron oxidation of **II.4** was attempted using various oxidising agents like Meerwein's salt,[13] $NOBF_4$ and trifluoroacetic acid, but none of these reactions could yield the anticipated antiaromatic cation, **[II.4]**$^+$ (scheme **II.6**). Thiophene based conjugated oligomers and cyclic systems are well known to undergo one or multiple electron oxidations to form respective cations. The well-known oxidising agents like Meerwein salt and many antimony based salts oxidise the conjugated thiophenes into radical cations and dications depending on the stability of oxidising species.[14-15] It is suspected that the cyclic radical **II.4** bearing two free thiophene units was also prone to these types of oxidations and hence interferes in the ring oxidation. Therefore, upon addition of oxidising agents to **II.4**, it can lead to multiple oxidation reactions like ring oxidation to form cation **[II.4]**$^+$ or/and along with oxidation of two free thiophene oxidation. Such multicharged species are expected to be quite reactive have been observed to discourage irreversible redox reactions.[16] Particularly, cyclic voltammetry studies also revealed a relatively unstable oxidized species. Therefore, this could be the possible reason for **II.4** not forming the expected 24π stable oxidised product **[II.4]**$^+$ under ambient conditions in the solution state.

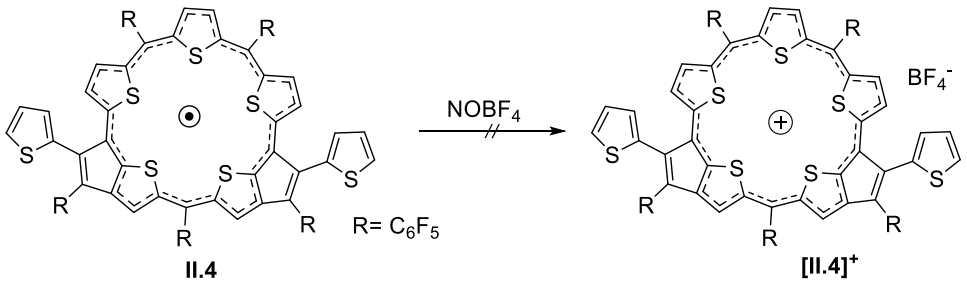

Scheme II.6: One electron oxidation of **II.4.**

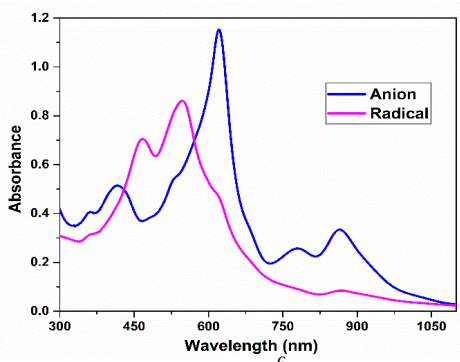

Figure II.8: Uv-visible absorption spectrum of 10^{-6} M solution of **II.4** and **[II.4]**$^-$ in DMSO.

II.5. Quantum mechanical calculations

To quantify the aromaticity and anti-aromaticity of three oxidation states of **II.4**, quantum mechanical calculations were carried out with the Gaussian09 rev D program.[15] All the calculations were performed by Density Functional Theory (DFT) with Becke's three-parameter hybrid exchange functional and the Lee-Yang-Parr correlation functional (B3LYP) and 6-31G(d,p) basis set for all the atoms that were used in the calculations. The molecular structure obtained from single crystal X-Ray diffraction analysis was used to optimise the geometry of molecules. Upon comparing the relative energies of optimised geometries of **[II.4]**$^-$ and **[II.4]**$^+$**,** the **[II.4]**$^-$ showed lower energy than the **[II.4]**$^+$ by 8.83 eV indicating that **[II.4]**$^-$ is favoured energetically. Lately, quantum chemical calculations have greatly supported the experimentally observed ring current effects. Nucleus Independent Chemical Shift (NICS) has been extensively used to quantify the strength of π-electron delocalization.[17] Schleyer and co-workers proposed the notion of NICS for π conjugated cyclic structures, and it has been useful to analyse and interpret the ring current effects in porphyrin and isophlorin molecules. In contrast to the familiar NMR chemical shift convention, the signs of the computed values are reversed (table **II.1**).

Table II.1: NICS values and corresponding aromaticity.

NICS Values	Ring Currents
Negative	Aromatic
Positive	Antiaromatic
Around zero	Non aromatic/antiaromatic

Using optimized geometries, NICS values were calculated with gauge independent atomic orbital (GIAO) method. The global ring centers for the NICS (0) values were labelled at the non-weighted mean centres of the macrocycles. The calculated NICS (0) value of δ 1.9 ppm for radical molecule, **II.4** suggests it is neither aromatic, nor antiaromatic type of molecule. Surprisingly, this value is quite low compared to the NICS (0) value of δ +11.5 ppm estimated for **II.5**. In fact, this can be attributed to the relatively non-planar geometry of the macrocycle which is perhaps induced by the two fused five membered rings to the meso carbons. A rather high positive NICS (0) value of δ +17.5 ppm was calculated for **[II.4]**$^+$, suggesting the strong antiaromatic nature. A negative NICS (0) value of δ -7 ppm, confirmed

the aromatic property of **[II.4]**$^{-}$. These calculated NICS (0) values trend were matching the previously reported redox species of cyclic pentathiophne radical **II.5**.

Herges and co-workers have developed the theory of Anisotropy of the Induced Current Density (ACID) to quantify electronic delocalization as a general method for π-conjugated cyclic systems.[18] Later, Sundholm and many others have assessed the magnetically induced current densities from density functional theory.[19] It provides the direction and strength of the current arising from the delocalization of π-electrons and also the direction of the current. This method has been used for a variety of porphyrins and isophlorins to signify the aromatic and antiaromatic pathways in (4n+2)π and 4nπ systems, respectively. ACID plots were obtained by using the continuous set of gauge transformations (CSGT) method, and the found results were plotted using POVRAY 3.7 software. In AICD plot, aromatic molecules show clockwise ring currents whereas antiaromatic molecules displays anticlockwise ring currents. The anion molecule **[II.4]**$^{-}$ showed clockwise ring currents suggesting the aromatic nature, whereas cationic form **[II.4]**$^{+}$ clearly exhibited anti-clockwise delocalization of π-electrons (fig. **II.9**). Along with the direction of ring currents, these plots also help in determining the path of the π-electrons delocalization. In cation molecule, **[II.4]**$^{+}$ the flow of electron was observed only through the carbon skeleton.

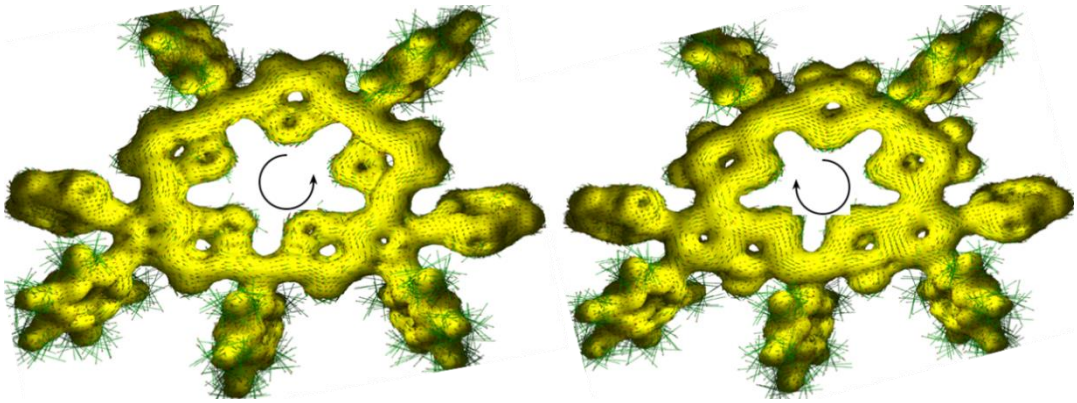

Figure II.9: AICD plot of **[II.4]**$^{+}$ (left), **[II.4]**$^{-}$ (right).

To simulate the steady-state absorption spectra, time-dependent TD-DFT calculations were employed on the optimized structures. Simulated absorption spectra for macrocycles **II.4**, its reduced species **[II.4]**$^{-}$ and oxidised species **[II.4]**$^{+}$ were matched with the experimental results (fig. **II.10** & **II.11**).

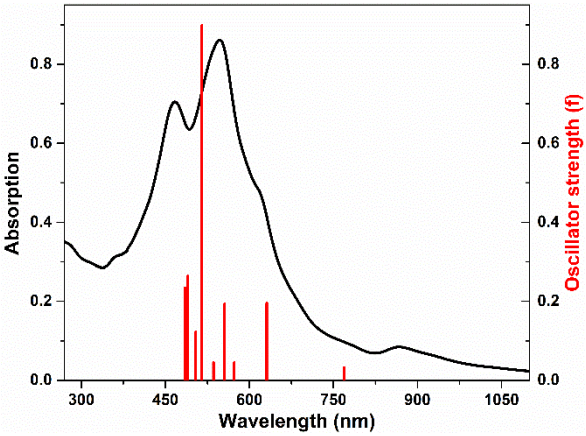

Figure II.10: The steady state absorption spectra (black line) of **II.4** recorded in $CHCl_3$ along with the theoretical vertical excitation energies (red bar) obtained from TD-DFT calculations carried out at the B3LYP/6-31G(d,p) level.

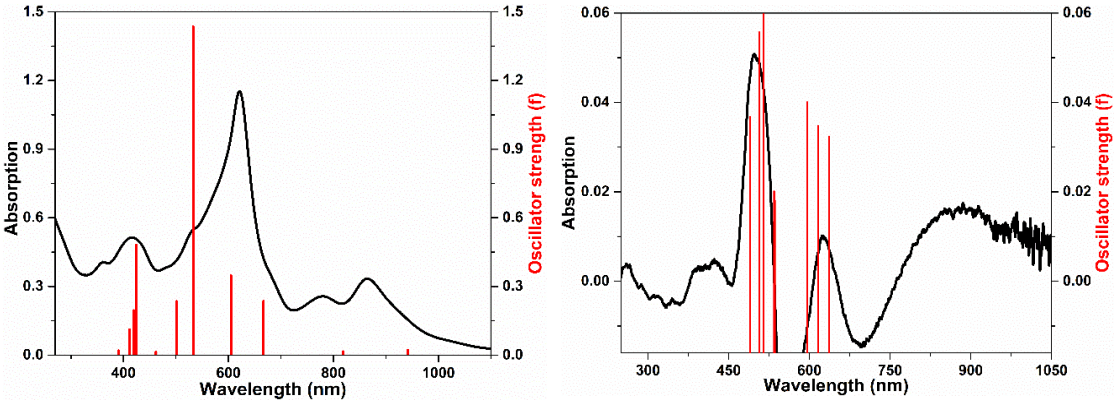

Figure II.11: The steady state absorption spectra (black line) of **[II.4]**$^-$ (left) and **[II.4]**$^+$ (right) recorded in $CHCl_3$ along with the theoretical vertical excitation energies (red bar) obtained from TD-DFT calculations carried out at the B3LYP/6-31G(d,p) level.

II.6. Synthesis β-methyl substituted macrocycles

Careful observation of the molecular structure of **II.4** revealed that one of the β-positions of the thiophene was involved in the formation of rare fusion of five membered rings with a porphyrinoid. To study the formation of this fused five membered ring and to elucidate the mechanism, thiophene β-positions were substituted with methyl groups and macrocycles were synthesised. Firstly thiophene diol, **II.8**, with both the β-positions were substituted with methyl group was synthesised. 3,4-dimethyl thiophene, **II.6** was formylated using n-butyl lithium and DMF to obtain **II.7** with 65% yield. It was further subjected to reduction using freshly prepared Grignard reagent (C_6F_5MgBr) to obtain β-methylated thiophene diol, **II.8** (scheme **II.7**).

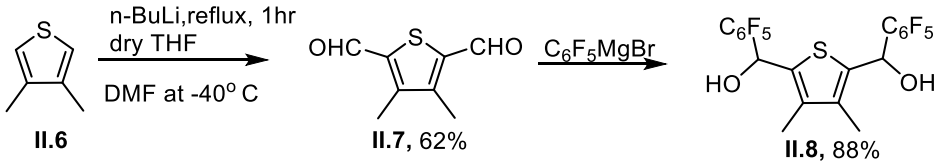

Scheme II.7: Synthesis of β-methylated thiophene diol **II.8**.

This diol, **II.8** was condensed with the acetylene bridged bis-thiophene, **II.1**, using similar reaction conditions (scheme **II.8**) as mentioned in Scheme- **II.3**. Surprisingly, the MALDI-TOF/TOF mass spectrum of this reaction mixture did not reveal any *m*/*z* values corresponding to expected radical and for any other macrocyclic products similar to **II.3**. This reaction unhesitatingly supported the participation of thiophene β-hydrogens of the diol in the formation of unexpected product, **II.4**.

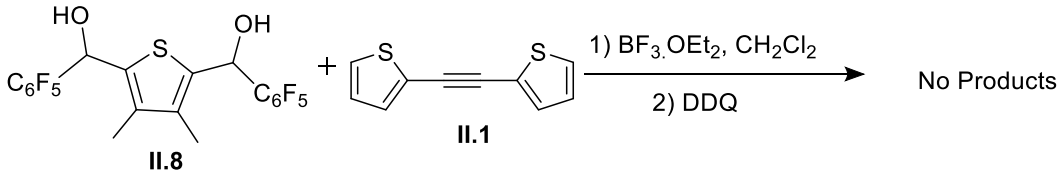

Scheme II.8: Condensation reaction between β-methylated thiophene diol, **II.8** and 1,2-di(thiophen-2-yl)ethyne, **II.1**.

In an alternative strategy, the second precursor 1,2-di(thiophen-2-yl)ethyne β-positions were substituted with methyl groups. Using palladium catalysed coupling reaction[8] methyl substituted bisthienylethyne, **II.10** was synthesised from 2-iodo-3-methyl thiophene, **II.9** and trimethylsilylacetylene (scheme **II.9**).

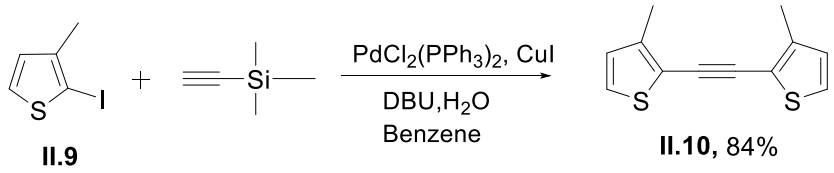

Scheme II.9: Synthesis of β-methylated bisthienylethyne **II.10**.

The resultant methylated bisthienylethyne, **II.10**, was condensed with thiophene diol, **II.2**, employing identical reaction condition as described for scheme-**II.3**. Interestingly, the MALDI-TOF/TOF mass spectrum of this reaction mixture revealed *m*/*z* value corresponding to tetra methylated radical molecule, **II.11** similar to **II.4** as expected (fig. **II.12**). The results from these reactions provide sufficient proof that the β-carbons of thiophene diol were involved in the formation of five membered fused ring. Further, it could also be deduced that

out of seven thiophene units present in the molecule, four thiophene rings were from acetylene bridged bis-thiophene monomer unit (scheme **II.10**).

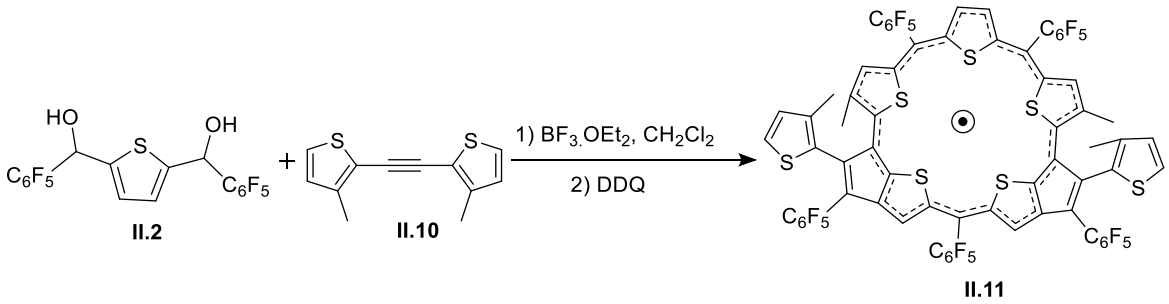

Scheme II.10: Condensation reaction between thiophene diol and methylated bisthienylethyne.

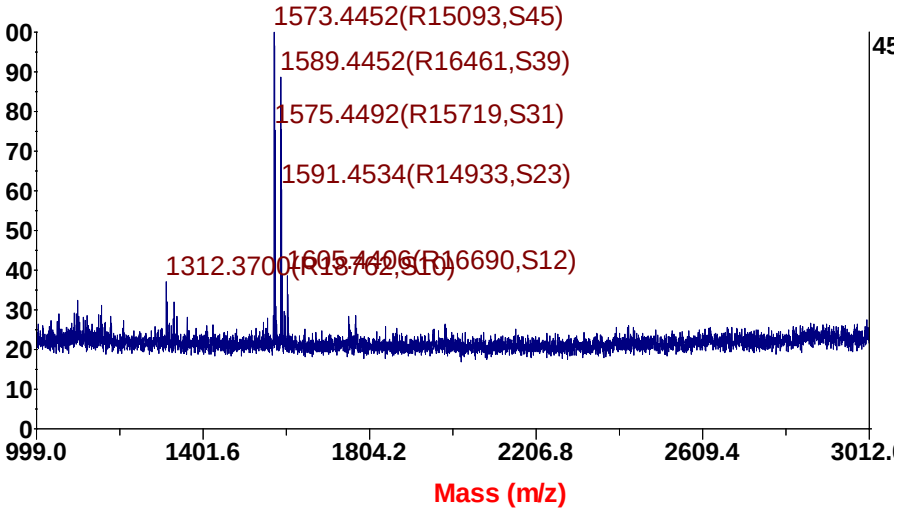

Figure II.12: MALDI TOF-TOF spectrum of reaction mixture.

II.7. Plausible Mechanism

Based on the reactions performed, a plausible mechanism was proposed analogous to the reaction of acetylene with a carbo cation. Generally, carbocations formed from the alcohols upon reacting with acid can react with alkynes (scheme **II.11**).[20]

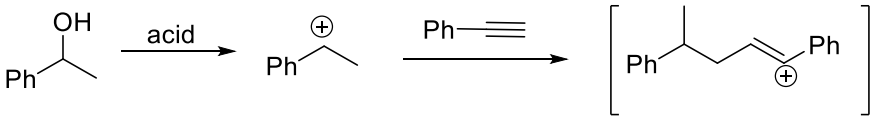

Scheme II.11: Reaction between carbocation and alkynes.

During the first step of cyclisation reaction, the thiophene diol, **II.2** reacts with boron trifluoride diethyl etherate ($BF_3.OEt_2$) to form the intermediate carbocation. This carbocation reacts with the acetylene bridged bis-thiophene, **II.1**, and forms rearranged carbocation **II.A**. This rearranged carbocation, **II.A** is expected to form a highly unstable four membered ring,

II.B because of the involvement of sulphur lone pair electrons. This intermediate, **II.B** upon rearrangement forms a carbocation **II.C**, which during the oxidation process loses hydrogen to from the five membered ring as observed in the final product **II.4** (scheme **II.12**).

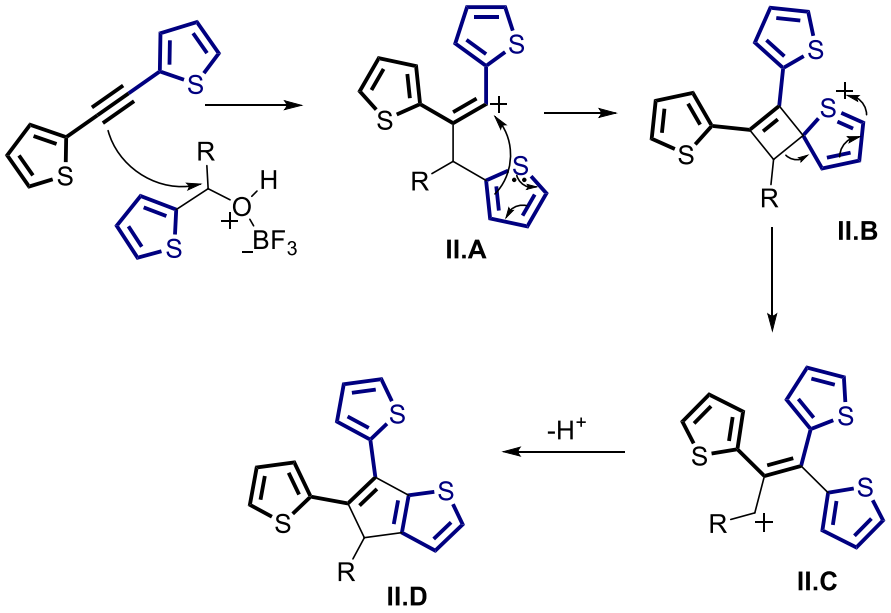

Scheme II.12: A plausible mechanism for the formation of five membered ring.

The scheme **II.12** shows the formation of five membered ring on one side and similar reactions can be expected on other side also to form intermediate **II.E**. This intermediate undergoes scrambling type reaction which is well known in porphyrinoid chemistry[21] to yield final radical molecule **II.4** (scheme **II.13**).

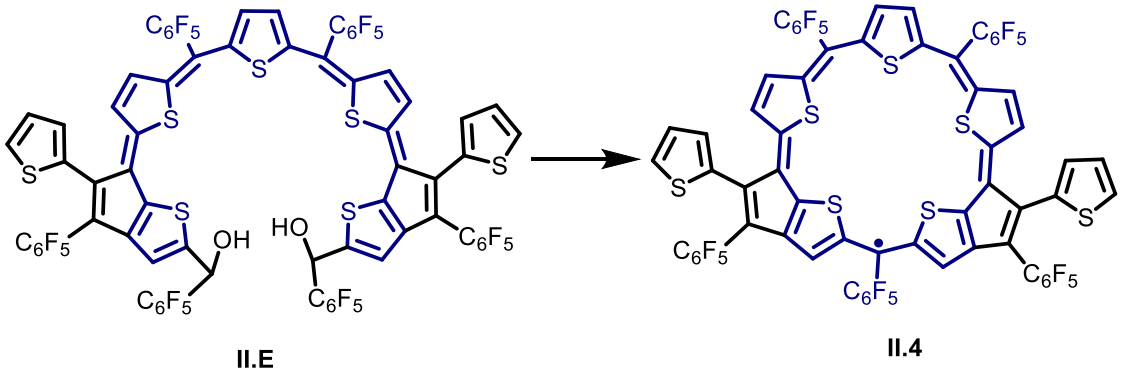

Scheme II.13: A plausible scrambling reaction to form macrocycle **II.4**.

II.8. Conclusions

A neutral 25π conjugated radical macrocycle, **II.4**, was successfully isolated during the synthesis of acetylene bridged antiaromatic macrocycles from thiophene precursors. The unpredicted reactivity of the acetylene precursor is supposed to be the possible reason for the

formation of unexpected product. In porphyrinoids, pyrrole's ability to inter-convert the nitrogen between imine and amine forms enables macrocycles with odd number of carbon atoms to attain complete conjugation. Whereas, thiophene based macrocycles with odd number of carbon atoms in their cyclic π-conjugated pathway can stabilize a neutral radical under similar circumstances. The molecular structure of the unexpected radical molecule, **II.4**, was obtained through single crystal X-ray diffraction analysis. This radical molecule consists of pentathiophene core and this core is responsible for the paramagnetic behaviour of the macrocycle. Further, one-electron oxidation and reduction reactions were performed to identify the respective cationic antiaromatic and anionic aromatic macrocycles. All these cation, anion and neutral macrocycles redox properties were studied through cyclic voltammetry and spectroelectrochemically. These observed redox properties were also supported by computational studies. A plausible mechanism has been proposed for the unexpected formation of the radical molecule based on the reactions performed using β-methylated thiophene monomers. This π-conjugated radical macrocycle displays a property like to that of metals with many oxidation states. Yet, more such macrocycles would be essential to generalize the reactivity of π-conjugated radical system.

II.9. Experimental section

All reagents and solvents were of commercial reagent grade and were used without further purification except where noted. Dry CH_2Cl_2 was obtained by refluxing and distillation over P_2O_5. Column chromatography was performed on basic alumina, silica gel and gel permeation chromatography with Bio-Beads S-X100 (BIO-RAD). ^{1}H NMR spectra were recorded on a JEOL 400 MHz and BRUKER 400 MHz spectrometers. Chemical shifts (δ) are reported in parts per million (ppm). Electronic spectra were recorded on a Perkin-Elmer λ-35 ultraviolet−visible (UV−vis) spectro-photometer. High Resolution Mass spectra were obtained using WATERS G2 Synapt Mass Spectrometer. Single-crystal X-ray diffraction analysis data were collected at 100K with a BRUKER KAPPA APEX II CCD Duo diffractometer (operated at 1500 W power: 50 kV, 30 mA) using graphite-monochromated Mo Kα radiation (λ = 0.71073 Å). In case of disordered solvent molecules, the contributions to the scattering arising from the disordered solvents in the crystal were removed by use of the utility SQUEEZE in the PLATON software package. Cyclic voltammetry (CV) and Differential pulse voltammetry (DPV) measurements were carried out on a BAS electrochemical system using a conventional three-electrode cell in dry CH_2Cl_2 containing 0.1 M tetrabutylammonium hexafluorophosphate ($TBPF_6$) as the supporting electrolyte.

Measurements were carried out under an Ar atmosphere. A glassy carbon (working electrode), a platinum wire (counter electrode), and Ag/Ag^+ (reference electrode) were used.

Density Functional Theory (DFT) Calculations

Quantum mechanical calculations were performed with the Gaussian09 (rev-D) program suite using a High Performance Computing Cluster facility of IISER PUNE. All calculations were carried out by Density functional theory (DFT) with Becke's three-parameter hybrid exchange functional and the Lee-Yang-Parr correlation functional (B3LYP) and 6-31G(d,p) basis set for all the atoms were employed in the calculations. The molecular structures obtained from single crystal analysis were used to obtain the geometry optimized structures. To simulate the steady-state absorption spectra, the time-dependent TD-DFT calculations were employed on the optimized structures. Molecular orbital contributions were determined using GaussSum 2.2.Program package. The global ring centres for the NICS (0) values were designated at the non-weighted mean centres of the macrocycles. The NICS (0) value was obtained with gauge independent atomic orbital (GIAO) method based on the optimized geometries. Anisotropy of the current-induced density (ACID) calculation was done to visualize delocalized π electrons. The ACID plots can directly display the magnitude and direction of the induced ring current when an external magnetic field is applied orthogonal to the macrocycle plane. Current density plots were obtained by employing the continuous set of gauge transformations (CSGT) method to calculate the current densities, and the results were plotted using POVRAY 3.7 for Windows.

Synthetic Procedure and Characterisation

Macrocycle II.4:

A mixture of bisthienylethyne, **II.1**, (190 mg, 1 mmol) and thiophene diol, **II.2** (476 mg, 1 mmol) were stirred in 100 mL of dry dichloromethane. The solution was purged with argon for 10 min. and shielded from light. $BF_3.OEt_2$ (122μL, 1 mmol) was added and stirring continued for 2h. Then, DDQ (567 mg, 2.5 mmol) was added and the mixture was stirred for an additional two hours. Finally solution was passed through short pad of basic alumina column. This mixture was concentrated and further purified by silica gel column chromatography using CH_2Cl_2/Hexane as eluent.

Characterisation of macrocycle II.4:
Yield- 5%

HR-MS (ESI-TOF): *m*/*z* = 1516.8701 (found), 1516.8741 (calcd. For $C_{67}H_{14}F_{25}S_7$).

UV-Vis ($CHCl_3$): λ_{max} nm (ε) L mol^{-1} cm^{-1} = 463 (42670), 546 (50330).

EPR: g= 2.0026.

Crystal data: $C_{67}H_{14}F_{25}S_7$, (*M*r 1516.87), monoclinic, space group *P 2₁/n*, a = 19.39(3), b = 18.92(6), c = 19.84(7) Å, α= 90, β= 116.69(3), γ= 90, V = 6507(40) $Å^3$, Z = 4, T = 100(2) K, D_{calcd} = 1.648 cm^{-3}, R_1 = 0.0971 (3160), R_w (all data) = 0.1122(3809), GOF = 2.64.

3,4-dimethylthiophene-2,5-dicarbaldehyde, II.7:

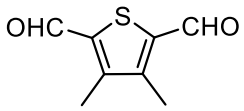

Dilithiated thiophene was prepared by the addition of butyllithium (22.32 mmol, 13.95 ml) at room temperature to a mixture of TMEDA (22.32 mmol, 3.34 ml), 3,4-dimethyl thiophene, **II.6** (8.92 mmol, 0.98 ml) and hexane (20 ml). The temperature of the mixture was allowed to rise to 50 ^oC and the conversion was completed by refluxing the mixture for 30 min. Then, THF (10 ml) was added, the solution was cooled to -40 ^oC and excess DMF (26.78 mmol, 2.06 ml) was added over a 10 min. period. The temperature of the system was gradually raised to room temperature and stirring was continued for 30 min. The suspension was then poured into a mixture of 30% HCl (25 ml) and H_2O (70 ml) at -20 ^oC under vigorous stirring. Saturated $NaHCO_3$ solution was slowly added until the aqueous layer had reached pH 6. The organic layer was separated and the aqueous layer extracted with Et_2O. The organic solution was dried over Na_2SO_4, the solvent removed in vacuum, and further purified using 100-200 mesh silica gel column using 20% ethyl acetate in hexane to yield dimethylated thiophene 2,5 dicarbaldehyde, **II.7** in 62% yields.

NMR Data: ^{1}H NMR (400MHz, $CDCl_3$, 298K): δ 10.16 (s, 2H), 2.53 (s, 6H).

(3,4-dimethylthiophene-2,5-diyl)bis((perfluorophenyl)methanol), II.8:

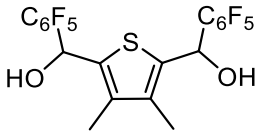

To the stirred solution of **II.7**, (5.95 mmol, 1 g in 15 ml THF) under argon atmosphere at 0 ^oC, freshly prepared 2.5 equivalents of Grignard reagent (C_6F_5MgBr, 14.88 mmol) was added. Stirring was continued for 2 h to attain room temperature, the reaction mixture was quenched with saturated NH_4Cl solution. The organic layer was extracted with Et_2O and

combined organic layer was washed with water and brine solution. After drying over Na_2SO_4, the solvent was evaporated under vacuum and purified by recrystallization using dichloromethane-hexane to yield compound **II.8** in 88% yields.

NMR Data: ^{1}H NMR (400MHz, $CDCl_3$, 298K): δ 6.44 (d, *J* = 8 Hz, 2H), 2.24 (d, *J* = 8 Hz, 2H), 2.16 (s, 6H).

1,2-bis(3-methylthiophen-2-yl)ethyne, II.10:

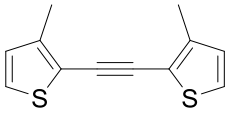

A 100 mL round bottom flask was purged with dry argon, and charged with $PdCl_2(PPh_3)_2$ (188 mg, 6 mol%), CuI (84 mg, 10 mol%) and starting material iodide, **II.9** (4.46 mmol). Septum is parafilmed after solids were added. While stirring, dry benzene (24.0 mL, starting material is 0.20 M in dry benzene) sparged with dry argon is added by syringe. Argon-sparged DBU (3.99 mL, 6 equiv) is then added by syringe, followed by a purge of the reaction flask with argon. Ice-chilled trimethylsilylethynylene (315 μL, 0.50 equiv) is then added by syringe, followed immediately by distilled water (32 μL, 40 mol%). The reaction flask is covered in aluminum foil and left stirring at a high rate of speed for 18 h, at the end of which the reaction mixture is partitioned in ethyl ether and distilled water (50 mL each). The organic layer is washed with 10% HCl (3 x 75 mL), saturated aqueous NaCl (1 x 75 mL), dried over Na_2SO_4, gravity-filtered and the solvent removed in vacuum. The crude product is purified by silica gel column chromatography to yield **II.10** in 84% yields. The spectroscopic data matches with the data already reported in literature.[22]

NMR Data: ^{1}H NMR (400 MHz, $CDCl_3$, 298K): δ 7.35 (d, *J* = 4 Hz, 2H), 6.77 (d, *J* = 4 Hz, 2H), 2.26 (s, 6H)

II.10. References

1. Lash, T. D., *Eur. J. Org. Chem.* **2007,** *2007,* 5461-5481.
2. Jux, N.; Koch, P.; Schmickler, H.; Lex, J.; Vogel, E., *Angew. Chem., Int. Ed.* **1990,** *29,* 1385-1387.
3. Martire, D. O.; Jux, N.; Aramendia, P. F.; Martin Negri, R.; Lex, J.; Braslavsky, S. E.; Schaffner, K.; Vogel, E., *J. Am. Chem. Soc.* **1992,** *114,* 9969-9978.
4. Weghorn, S. J.; Lynch, V.; Sessler, J. L., *Tetrahedron. Lett.* **1995,** *36,* 4713-4716.

5. Nojman, E.; Berlicka, A.; Szterenberg, L.; Latos-Grazynski, L., *Inorg Chem* **2012,** *51*, 3247-60.

6. Nakao, K.; Nishimura, M.; Tamachi, T.; Kuwatani, Y.; Miyasaka, H.; Nishinaga, T.; Iyoda, M., *J. Am. Chem. Soc.* **2006,** *128*, 16740-7.

7. Iyoda, M.; Tanaka, K.; Shimizu, H.; Hasegawa, M.; Nishinaga, T.; Nishiuchi, T.; Kunugi, Y.; Ishida, T.; Otani, H.; Sato, H.; Inukai, K.; Tahara, K.; Tobe, Y., *J. Am. Chem. Soc.* **2014,** *136*, 2389-96.

8. Mio, M. J.; Kopel, L. C.; Braun, J. B.; Gadzikwa, T. L.; Hull, K. L.; Brisbois, R. G.; Markworth, C. J.; Grieco, P. A., *Org. Lett.* **2002,** *4*, 3199-3202.

9. Gopalakrishna, T. Y.; Reddy, J. S.; Anand, V. G., *Angew. Chem., Int. Ed.* **2013,** *52*, 1763-7.

10. Reddy, J. S.; Anand, V. G., *J. Am. Chem. Soc.* **2008,** *130*, 3718-3719.

11. Gopalakrishna, T. Y.; Reddy, J. S.; Anand, V. G., *Angew. Chem., Int. Ed.* **2014,** *53*, 10984-10987.

12. Suzuki, S.; Morita, Y.; Fukui, K.; Sato, K.; Shiomi, D.; Takui, T.; Nakasuji, K., *J. Am. Chem. Soc.* **2006,** *128*, 2530-2531.

13. Rathore, R.; Kumar, A. S.; Lindeman, S. V.; Kochi, J. K., *J. Org. Chem.* **1998,** *63*, 5847-5856.

14. Ohmae, T.; Nishinaga, T.; Wu, M.; Iyoda, M., *J. Am. Chem. Soc.* **2010,** *132*, 1066-74.

15. Frisch, M. J.; Trucks, G. W.; Schlegel, H. B.; Scuseria, G. E.; Robb, M. A.; Cheeseman, J. R.; Scalmani, G.; Barone, V.; Petersson, G. A.; Nakatsuji, H.; Li, X.; Caricato, M.; Marenich, A. V.; Bloino, J.; Janesko, B. G.; Gomperts, R.; Mennucci, B.; Hratchian, H. P.; Ortiz, J. V.; Izmaylov, A. F.; Sonnenberg, J. L.; Williams; Ding, F.; Lipparini, F.; Egidi, F.; Goings, J.; Peng, B.; Petrone, A.; Henderson, T.; Ranasinghe, D.; Zakrzewski, V. G.; Gao, J.; Rega, N.; Zheng, G.; Liang, W.; Hada, M.; Ehara, M.; Toyota, K.; Fukuda, R.; Hasegawa, J.; Ishida, M.; Nakajima, T.; Honda, Y.; Kitao, O.; Nakai, H.; Vreven, T.; Throssell, K.; Montgomery Jr., J. A.; Peralta, J. E.; Ogliaro, F.; Bearpark, M. J.; Heyd, J. J.; Brothers, E. N.; Kudin, K. N.; Staroverov, V. N.; Keith, T. A.; Kobayashi, R.; Normand, J.; Raghavachari, K.; Rendell, A. P.; Burant, J. C.; Iyengar, S. S.; Tomasi, J.; Cossi, M.; Millam, J. M.; Klene, M.; Adamo, C.; Cammi, R.; Ochterski, J. W.; Martin, R. L.; Morokuma, K.; Farkas, O.; Foresman, J. B.; Fox, D. J. *Gaussian 16 Rev. C.01*, Wallingford, CT, 2016.

16. Vogel, E.; Pohl, M.; Herrmann, A.; Wiss, T.; König, C.; Lex, J.; Gross, M.; Gisselbrecht, J. P., *Angew. Chem., Int. Ed.* **1996,** *35*, 1520-1524.

17. Schleyer, P. v. R.; Maerker, C.; Dransfeld, A.; Jiao, H.; van Eikema Hommes, N. J. R., *J. Am. Chem. Soc.* **1996,** *118,* 6317-6318.

18. Geuenich, D.; Hess, K.; Köhler, F.; Herges, R., *Chem. Rev.* **2005,** *105,* 3758-3772.

19. Valiev, R. R.; Fliegl, H.; Sundholm, D., *J. Phys. Chem. A* **2013,** *117,* 9062-9068.

20. Jefferies, L. R.; Cook, S. P., *Tetrahedron.* **2014,** *70,* 4204-4207.

21. Geier Iii, G. R.; Littler, B. J.; Lindsey, J. S., *J. Chem. Soc. Perkin Trans. 2.* **2001,** 701-711.

22. Tanaka, Y.; Koike, T.; Akita, M., *Chem. Comm.* **2010,** *46,* 4529-4531.

CHAPTER III

Anti-aromatic Isophlorin-Fullerene Non-Covalent Interactions

III.1. Introduction

π-conjugated network of isophlorin, is an appealing template for the design and synthesis of new 4nπ macrocycles. Core modified and expanded isophlorins have been characterized as stable 4nπ macrocycles with electronic and redox properties those are not observed in aromatic systems.[1] They display characteristic and reversible two-electron ring oxidation corresponding to their aromatic dication where as expanded porphyrins show redox reactions which are generally proton-coupled electron transfer reactions. Invariably large π-conjugated macrocycles have a tendency to twist and adopt nonplanar conformations like figure of eight or multiple twists due to their flexible nature (scheme **III.1**).[2-4]

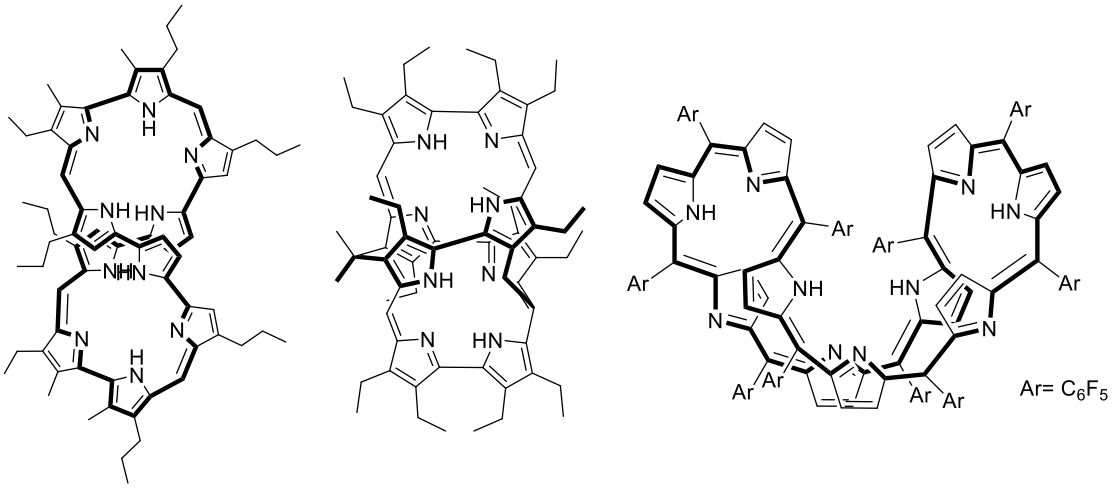

Scheme III.1: Structures of nonplanar expanded porphyrins.

Giant porphyrinoids adopt non-planar figure-eight conformations and are well studied examples for non-aromatic macrocycles. Relative to aromatic systems, the experimental evidence reported for large antiaromatic systems are very limited. Because of this structural induced loss of ring current effects, expanded porphyrinoids and isophlorinoids are devoid of aromatic and antiaromatic characteristics. Despite many efforts, there are hardly few strategies reported to sythesise planar expanded isophlorins.[5-6] However, its unstable nature under ambient conditions has limited the exploration of its chemistry as a model antiaromatic system. Even though customized synthetic protocols have met with limited success to enhance the stability of an isophlorin core[7-8] yet there is enough scope to explore novel precursors and synthetic methodologies for larger 4nπ macrocycles. Accordingly, a few successful modifications have been reported to isophlorin skeleton for synthesizing few stable antiaromatic macrocycles.[9-10]

The length of the π–conjugated network can be increased by either introducing additional heterocyclic units or by adding more number of *meso* carbon bridges to get expanded isophlorins with altered optical and electronic properties. One of the main strategies employed is replacing the *meso* carbon bridges with ethylene linkages to get higher homologues of isophlorins.[11] A variety of 32π-antiaromatic expanded isophlorins, **III.1** and **III.2**, were synthesised by replacing two methine carbon bridges by an equal number of ethylene bridges.[6] These anti-aromatic macrocycles displayed remarkable structural diversity and susceptible to reversible two-electron ring oxidation to yield stable aromatic dications.

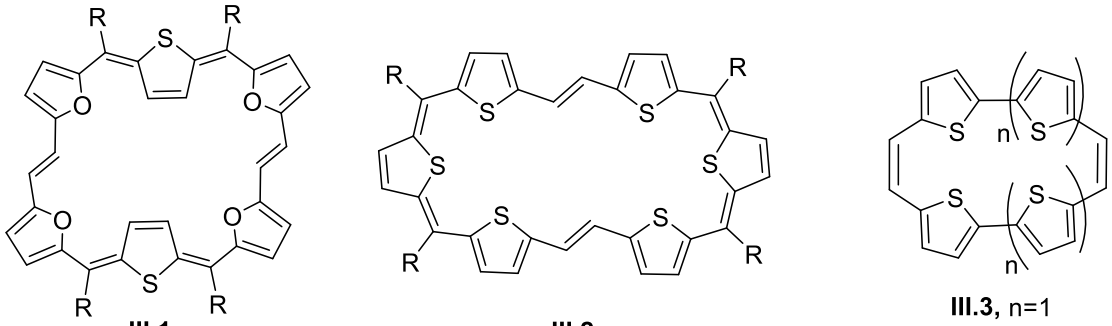

Scheme III.2: 32π Expanded Isophlorins and ethylene bridged isophlorins.

Cava and co-workers reported the synthesis of thiophene macrocycles, **III.3** and **III.4**, having ethylene bridges by McMurry coupling of dialdehydes derived from thiophene and its oligomers (scheme **III.2**).[11] Later ,giant cyclic oligothiophene macrocycles individually reported by Bauerle and Iyoda were found to be non-anti aromatic in nature.[12-13] So far, the 40□ octafuran macrocycle, **III.5** represents the only example to exhibit a planar topology for a true octaphyrin.[14] Otherwise, most of the methods significantly alter the stoichiometric composition of an octaphyrin to sustain a planar topology.[15] Synthesis of expanded antiaromatic isophlorins with eight heterocyclic rings and an equal number of *meso* carbons are not very common due to their inherent flexibility and structure induced loss of antiaromaticity. Among the reported 40π isophlorins, only **III.5** displayed a planar structure with antiaromatic behaviour. The core modified isophlorin, **III.6,** adopts a non-planar figure-of-eight conformation[16] whereas **III.7** was reported during the reduction of core modified isophlorin containing alternate pyrroles and thiophene units with eight *meso* positions (scheme **III.3**).[17] The isoelectronic structure for these 40π isophlorins are not known in the literature. However, many planar expanded 4nπ and (4n+2)π systems have been synthesised by less number of *meso* carbons and a greater number of directly linked heterocyclic unit links.[13, 18] The isophlorins **III.10**, and **III.12**, can be envisaged as an isoelectronic structure

for 40π isophlorins with two ethylene bridges and two bithiophene units. The presence of rigid bithiophene unit induces the planarity into the macrocycle.

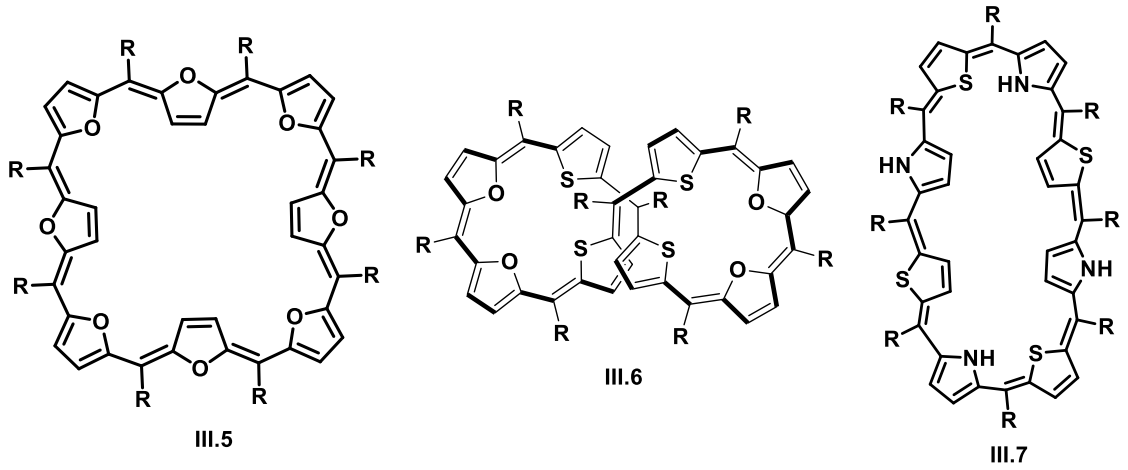

Scheme III.3: 40π expanded antiaromatic isophlorins.

III.2. Synthesis of (III.10)

Similar to the synthesis of porphyrin isomers reported by Vogel and co-workers,[19] the expanded isophlorins can also be structurally modified to obtain 40π expanded isophlorins. It can be envisaged that these structural isomers can be synthesized with a direct α-α bond between the adjacent thiophene units in addition to the bridging meso carbons. The requisite precursors are easy to synthesize and have already been employed in a variety of porphyrinoids and isophlorinoids.[6] A synthetic strategy followed the modified Rothemund type synthesis, which consists of condensing bithiophene diol,[15] **III.8** with *E*-ethylene bridged bis(thiophene), **III.9** in dichloromethane under dilute conditions (scheme **III.4**). Then, a catalytic amount of boron trifluoride etherate ($BF_3.OEt_2$) was added under dark, followed by oxidation with DDQ in open air atmosphere. The MALDI-TOF/TOF mass

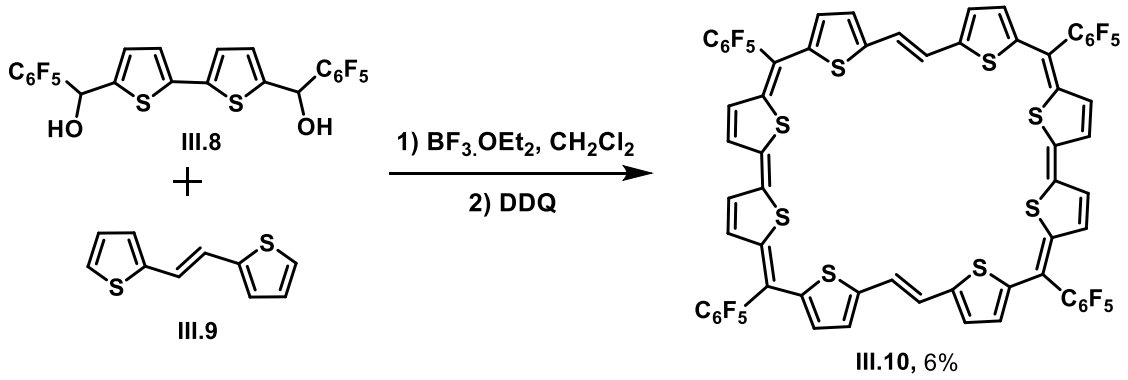

Scheme III.4: Acid catalysed synthesis of 40π Expanded Isophlorins **III.10.**

spectrum of this reaction mixture revealed the formation of the expected ethylene bridged, 40π expanded isophlorin, **III.10**, as the major product. The reaction mixture was passed through a short basic alumina column and further concentrated in rotary evaporator. Upon further purification through silica gel column chromatography with CH_2Cl_2/hexane as eluent, a pink coloured band was isolated in 7% yields and the isolated product corresponded to the expanded 40π isophlorin macrocycle, **III.10**. The major product octathiophene, **III.10**, isolated from the reaction displayed an *m/z* value of 1423.8971 in its high-resolution mass spectrum, confirmed the composition of this macrocycle. This core modified 40π isophlorin was found to be highly soluble in most of the common organic solvents. Due to the extended

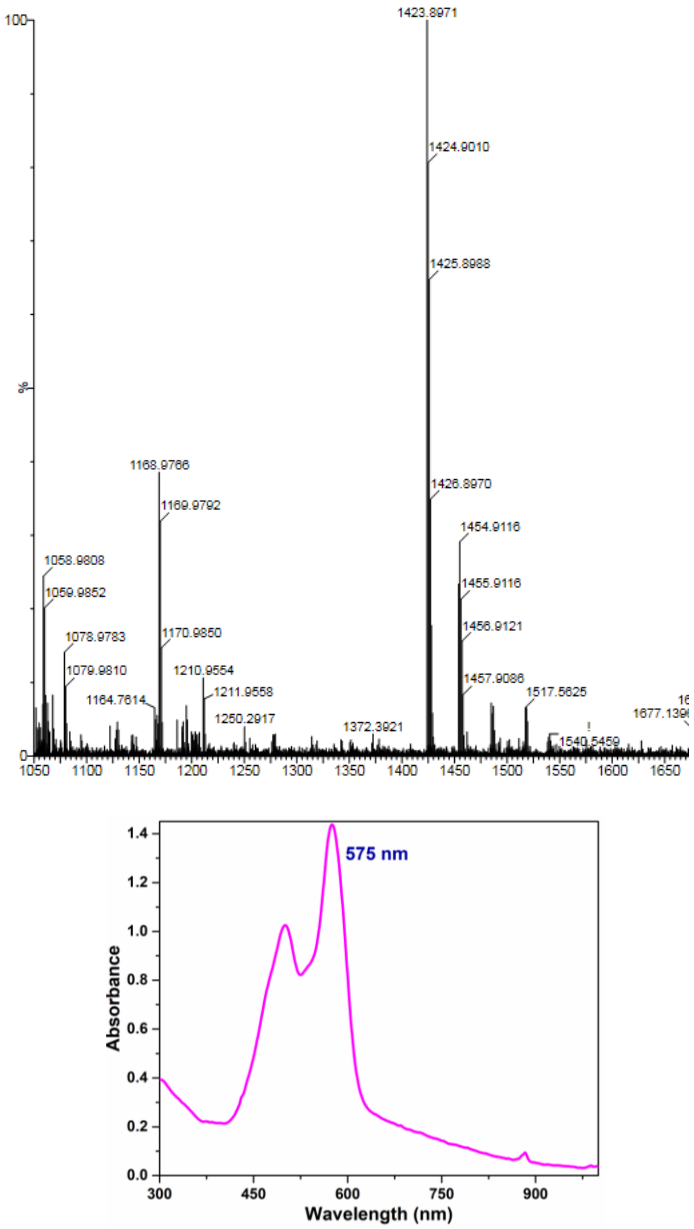

Figure III.1: HRMS spectrum of **III.10** (top) and UV -Vis absorption spectrum of 10^{-6} M solution of **III.10** in dichloromethane (bottom).

conjugation, **III.10** absorbs in the visible region of the electromagnetic spectrum and found to have multiple absorptions at 575 nm and 498 nm with very high extinction co-efficient (fig. **III.1**). The extension of the delocalized π electrons network was also well confirmed by the large red shifted absorptions in comparison to the 20π isophlorin derivatives.

III.3. ^{1}H NMR Studies of (III.10)

Macrocycle **III.10,** accounts for a formal count of 40π electrons along its conjugated path and hence expected to be antiaromatic in nature. Accordingly, its ^{1}H NMR spectrum was expected to display a paratropic ring current effect which is characteristic of antiaromatic 4nπ systems. The octathiophene, **III.10,** displayed four different signals at room temperature suggestive of a highly symmetrical structure for the macrocycle in solution state (fig. **III.2**).

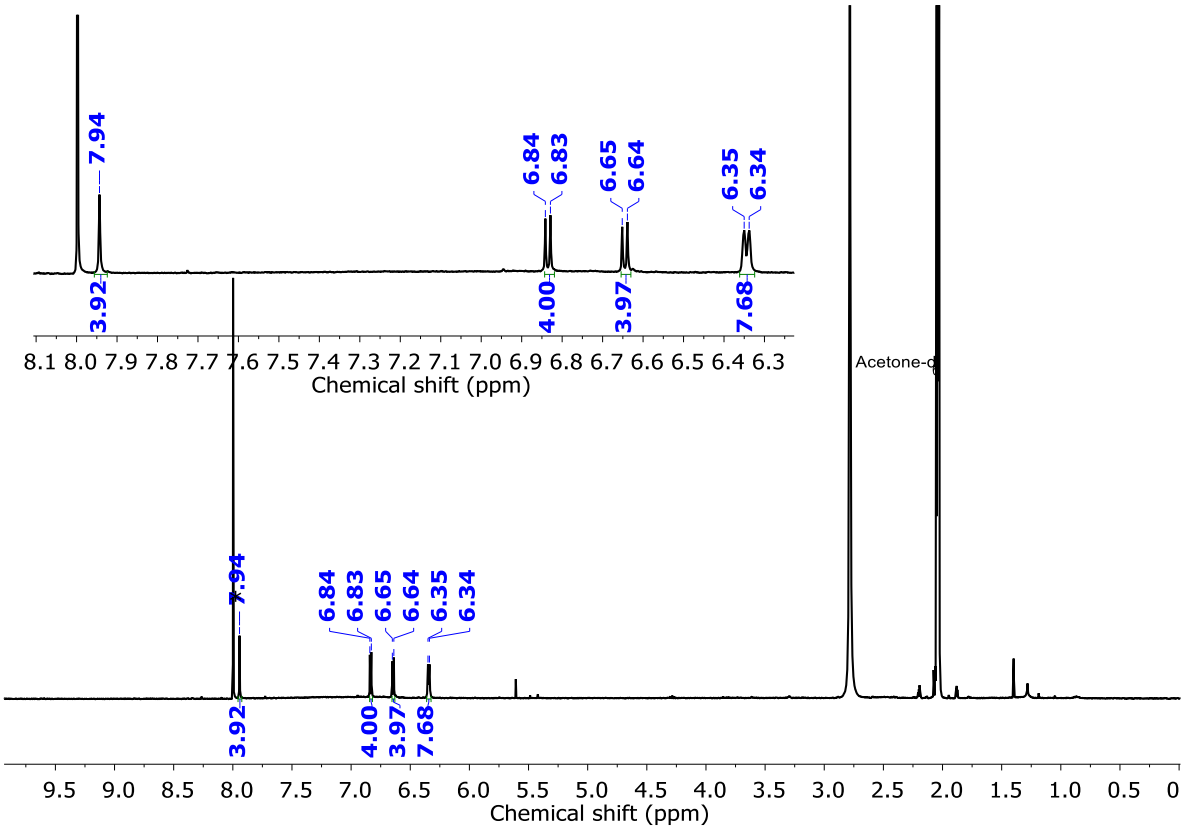

Figure III.2: ^{1}H NMR spectrum of **III.10** in acetone-d_6 at 300K

All the thiophene protons were found to resonate as a three doublets at δ 6.86 and 6.66 ppm corresponding to an equal number of protons whereas, the doublet at δ 6.36 ppm corresponded to twice the number of protons. As expected for a 4nπ system, the protons of the ethylene bridge must experience ring current effects and hence expected to resonate at different chemical shift values. But a singlet was observed for the proton of the ethylene bridged carbons at δ 7.95 ppm. The observed chemical shifts does not support significant

paratropic ring current effects as expected for 4*n*π macrocycles hints the passible fluxional behaviour of **III.10**. The proton at δ 7.95 ppm expected to resonate as two signals corresponding to the protons of inside and outside the macrocycle. The alleged solution-state dynamics involving fast flipping of the two carbon atoms result in a time averaged spectrum similar to that of annulenes. In a similar 32π macrocycle, the ethylene bridge protons were found to resonate as a singlet at room temperature, but could be distinguished by ring current effects only at lower temperatures.[20] Therefore, variable temperature ^{1}H NMR spectra (fig. **III.3**) were recorded to confirm the fluxional behaviour of the macrocycle. As expected the intensity of the signal at δ 7.95 ppm decreased gradually upon lowering temperature. However, this singlet did not split into two signals, even at 203 K, which suggested the rapid flipping of the ethylene bridge proton even at low temperatures. Whereas, the thiophene proton signals displayed minor variation in their chemical shift values. This is largely attributed to the fluxional behaviour of larger ring size 40π macrocycle, **III.10**, in the solution state. ^{19}F NMR spectra revealed three different signals at δ -138.5 ppm, -152.86 ppm, and -160.56 ppm corresponding to ortho, meta and para substituted fluorines of pentafluoro groups at room temperature.

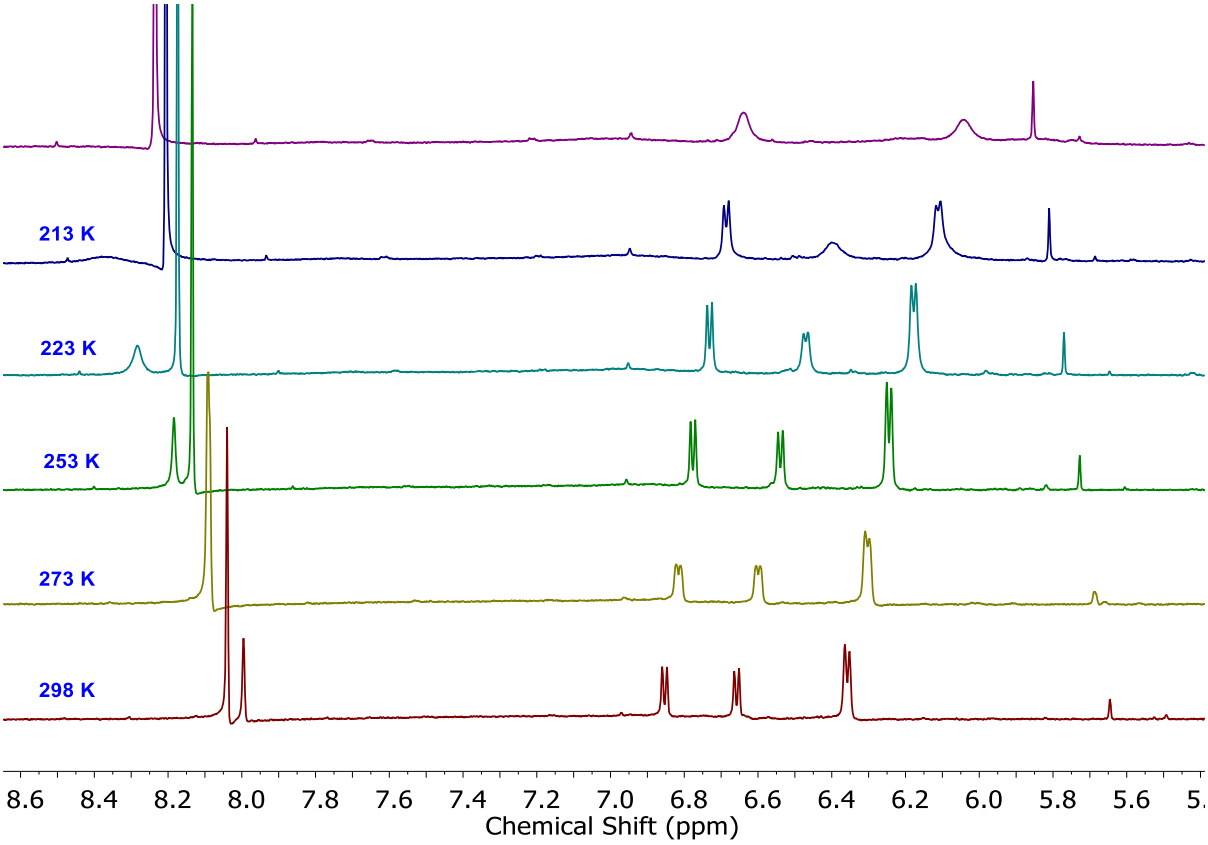

Figure III.3: Variable temperature ^{1}H NMR spectra of **III.10** in acetone-d_6.

III.4. Synthesis of (III.12)

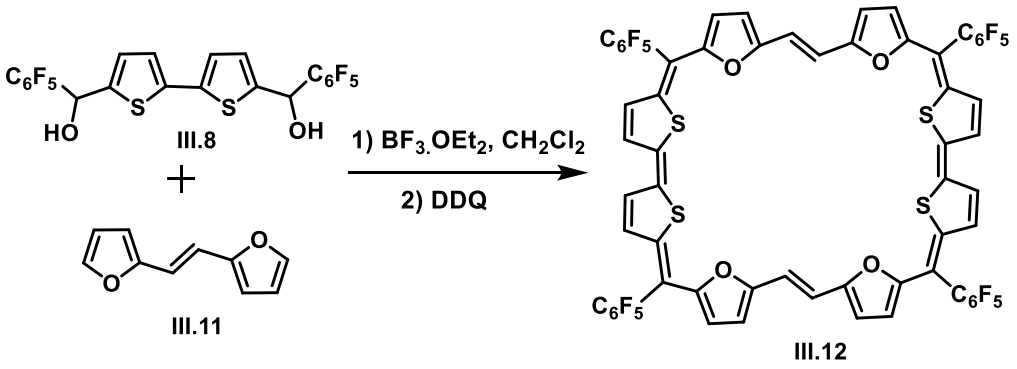

Scheme III.5: Acid catalysed synthesis of 40π expanded Isophlorins **III.12.**

Based on the structural variation upon substituting thiophene with furans, an attempt was made to replace the E-ethylene bridged bis(thiophene) with bisfuran units (scheme **III.5**). Replacement of four thiophenes in 40π octathiaisophlorin, **III.10**, with furan lead to the formation of isoelectronic species of core modified isophlorin **III.6**. Anticipating a structural analogue of **III.10**, condensation of bithiophene diol, **III.8** with E-ethylene bridged bisfuran, **III.11** was carried out under similar reaction conditions as described in scheme **III.4**. Formation of the desired macrocycle, **III.12,** was identified from the MALDI-TOF/TOF mass spectrum of the reaction mixture. It was further purified from the reaction mixture through silica gel column chromatography, using CH_2Cl_2/hexane as eluent, as a pink coloured band with 6% yields.

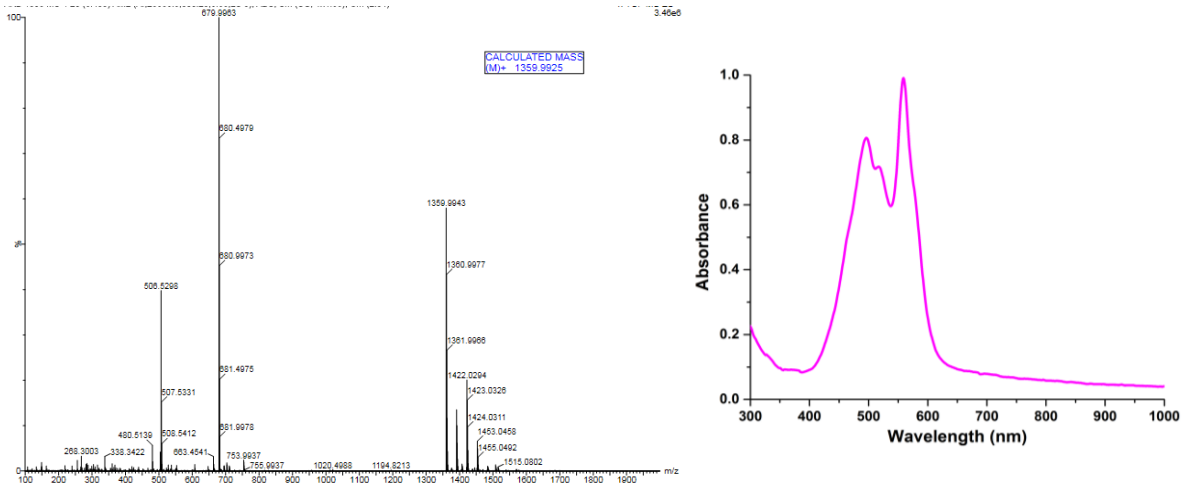

Figure III.4: HRMS spectrum of **III.12** (left) and UV -Vis absorption spectrum of 10^{-6} M solution of **III.12** in dichloromethane (right).

High-resolution mass spectrometric (HRMS) analysis of **III.12,** displayed an m/z value of 1359.9943, confirmed the composition of this macrocycle. This macrocycle accounts for 40π electrons along its conjugated pathway and due to this extended conjugation, it displayed multiple absorptions at 558 nm and 495 nm with very high extinction co-efficient in the absorption spectrum (fig. **III.4**). These absorptions are quite intense and also red shifted compared to the earlier reported ethylene bridged 32π isophlorins, clearly in support of effective and extended conjugation.

III.5. ^{1}H NMR Studies of (III.12)

III.12 displayed a well resolved ^{1}H NMR spectrum at room temperature with chemical shifts in the region between δ 5.6 ppm and 10.18 ppm (fig. **III.5**). Overall, seven doublets were observed and the signals at δ 5.6, 5.72, 6.26 ppm corresponded to twice the number of protons compared to other signals. However the observed numbers of signals were sufficiently larger than expected in the region between 11.00-5.00 ppm. This indicates the relatively less symmetrical structure for the macrocycle, **III.12**, in comparison to **III.10**. Variable temperature ^{1}H NMR experiments were performed (fig. **III.6**) to evaluate the fluxional behaviour of the macrocycle. Upon reducing the temperature to 183 K, more numbers of signals were observed, clearly suggesting the fluxional behaviour and an altered conformation of the macrocycle when the ethylene bridged thiophene subunits are replaced by furans in **III.10.**

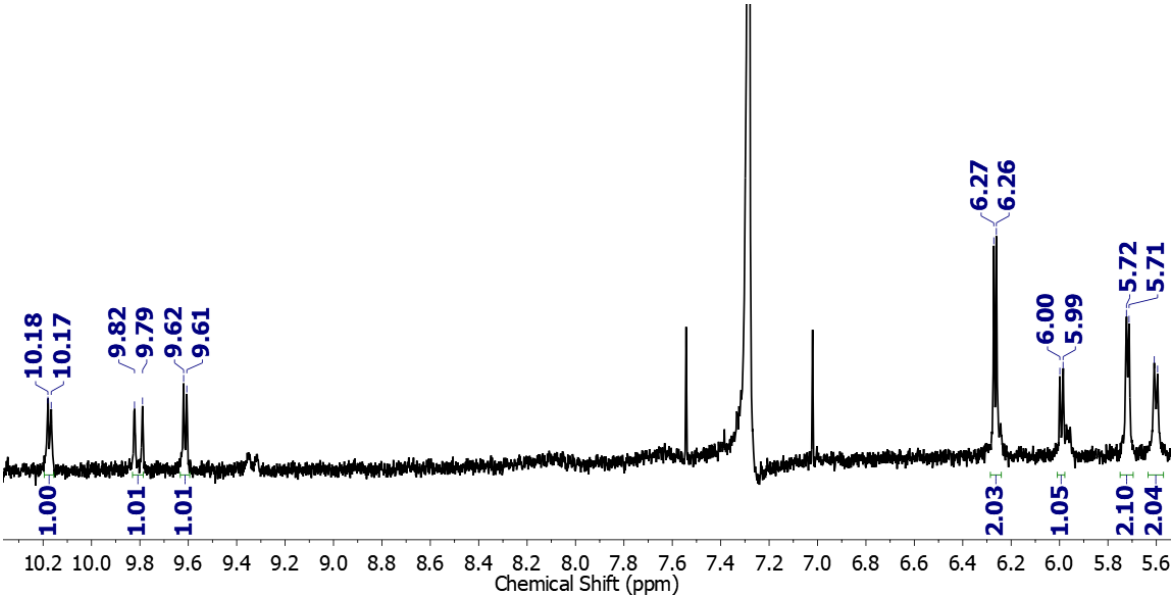

Figure III.5: ^{1}H NMR spectrum of **III.12** in $CDCl_3$ at 300 K.

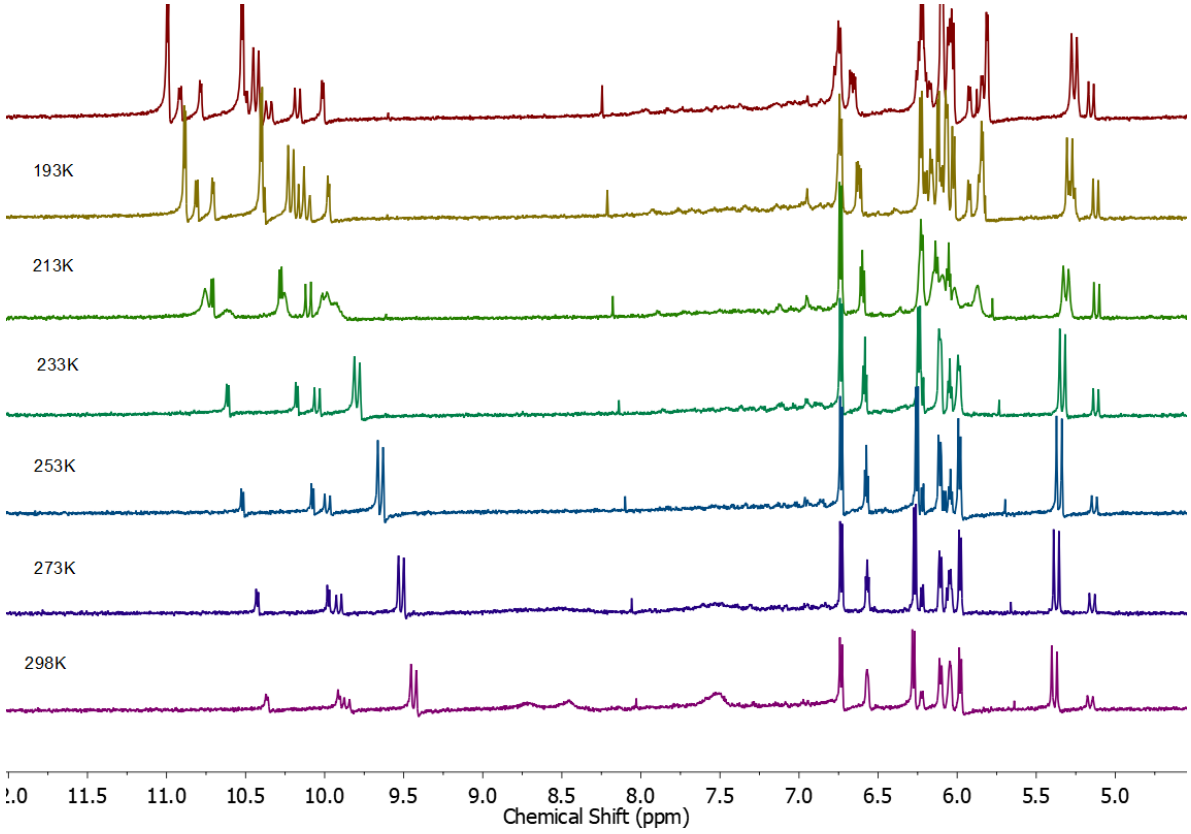

Figure III.6: Variable temperature ^{1}H NMR spectra of **III.12** in acetone-d_6.

III.6. Single Crystal X-ray Diffraction Studies

Since NMR studies could not provide unambiguous structural analysis, the efforts made to grow single crystals of these macrocycles **III.10** and **III.12**, with various organic solvents to determine the absolute conformation in solid state went futile. Then the concept of co-crystallization with fullerene C_{60} was utilised to determine molecular structure of macrocycles Supramolecular assemblies of π-conjugated molecules and fullerene are well studied because of their attractive photophysical, photochemical, and/or electrochemical properties and because of these interesting properties many molecules have been synthesized to host fullerene.[21-22] Despite having flat surface, porphyrin and its derivatives aids well as a good receptor for fullerene. A number of multi porphyrin arrays, metallo porphyrins and contracted porphyrins (subporphyrin) and isophlorins have been synthesized with well confined cavity for better binding affinity of fullerene.[23-24] In spite of much effort, only few porphyrins show strong π-π interactions in solution. Hence, most hosts contain multi-porphyrin arrays connected to a scaffold that forms a binding pocket for effective fullerene binding. Although this approach was very effective at succeeding high binding affinities, it adds considerable

synthetic challenges. Still, creating a simple, unfunctionalized porphyrinoid or isophlorinoid system that improves binding affinity of fullerene effectively, remains a challenge.

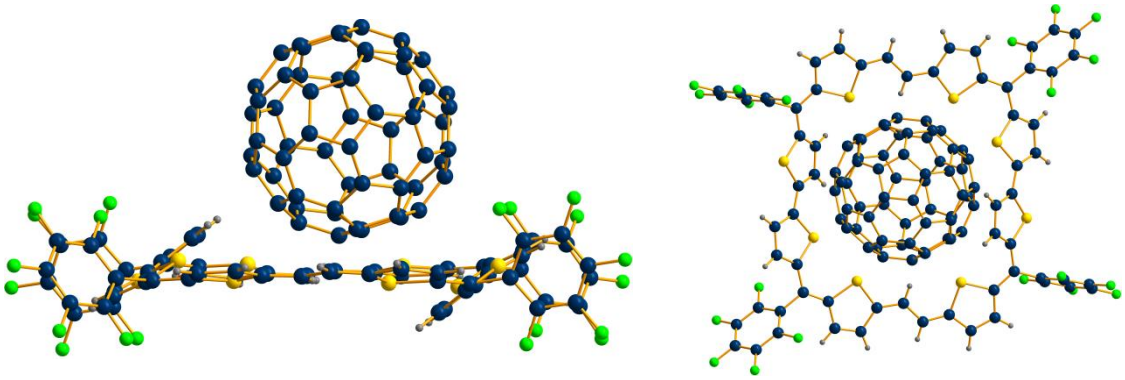

Figure III.7: Supramolecular complex of isophlorin **III.10** and $\mathbf{C_{60}}$ side view (left) and top view (right).

From an earlier report, C_{60} fullerene is known to bind to antiaromatic 20π tetraoxa isophlorin.[25] Expecting the formation of supramolecular complex, fullerene C_{60} and **III.10** were mixed in a 1:1 ratio in toluene at room temperature. This solution was undisturbed for few days to co-crystallize fullerene with the 40π octathiophene macrocycle. After a few days, dark block shaped crystals were observed in the solution. The single crystal X-ray diffraction analysis of these crystals revealed the formation of the co-crystallized product (fig. **III.7**). The isophlorin, **III.10** molecular structure revealed a rectangular shape for the macrocycle with inversion of only two thiophene rings, located diagonally opposite to each other. This solid state structure obtained for **III.10** is completely different than the solution state structure as observed from its ^{1}H NMR spectrum at room temperature. The notable feature of the crystal structure is its near-planar conformation for a 40π macrocycle. Both the ethylene bridges in this macrocycle retained *E* conformation similar to that of the monomer (*E*)-1,2-di(thiophen-2-yl)ethene. Along with ring inversion, the bithiophene units of **III.10** were found to be deviated by 32.55° from the mean macrocyclic plane defined by four meso carbons. Two C_{60} spheres were located exactly above and below the macrocycle, making a 1:2 complex of isophlorin and C_{60}, where macrocycle was sandwiched by two fullerene units (fig. **III.8**). Because of the π-π interactions, the close contacts observed between the macrocycle and closest carbons of both C_{60} were 1.39 Å. These values are extremely short compared to reported π-π stacking values in literature.[25] The close contacts between isophlorins and fullerenes were mainly due to the van der Waals attraction of the fullerene curved π surface to the isophlorin anti-aromatic π surface. A few other interactions between

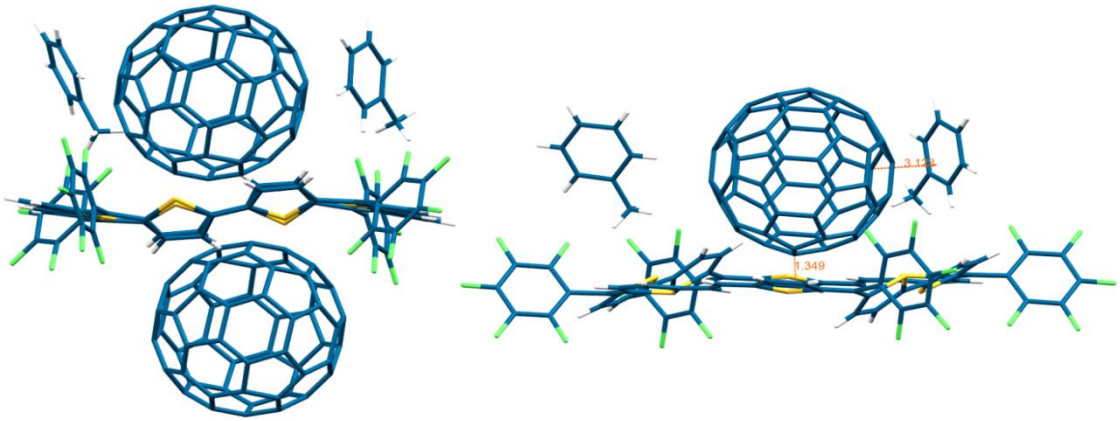

Figure III.8: 1:2 complex of isophlorin **III.10** with fullerene (left) and interaction of C_{60} with solvent molecules and isophlorin **III.10** (right).

macrocycle and C_{60} are noteworthy. Two toluene solvent molecules were also observed on each side of C_{60} molecule and one of the toluene is having π-π interactions with C_{60} at a distance of 3.14 Å. The distance between inverted bithiophene units and nearest carbon atoms of C_{60} is 3.174 Å. These distances are which are shorter than the sum of van der Waals radii suggest the π-π interactions between supramolecular complex of macrocycle and C_{60} in the solid state. The packing diagram of supramolecular complex of isophlorin and C_{60} shows a linear type of packing of repeating units containing only one 1:2 host guest complex (fig. **III.9**). Surprisingly fullerene-fullerene interactions also were observed along with the other

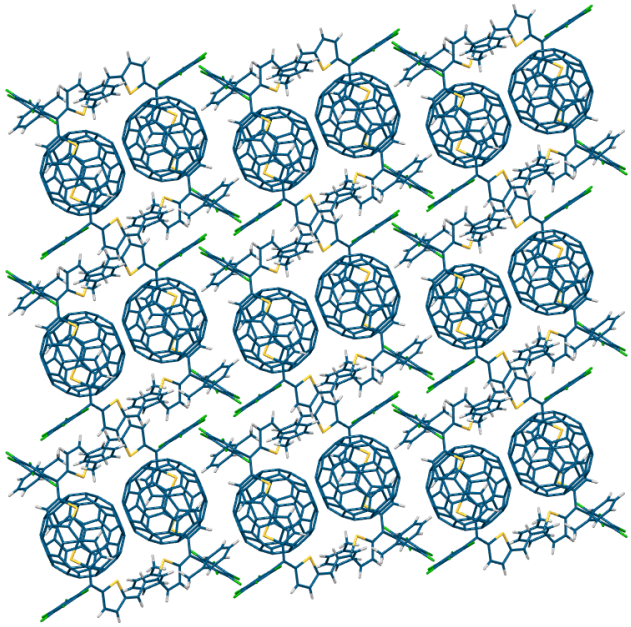

Figure III.9: Linear type packing diagram between fullerene and isophlorin **III.10**.

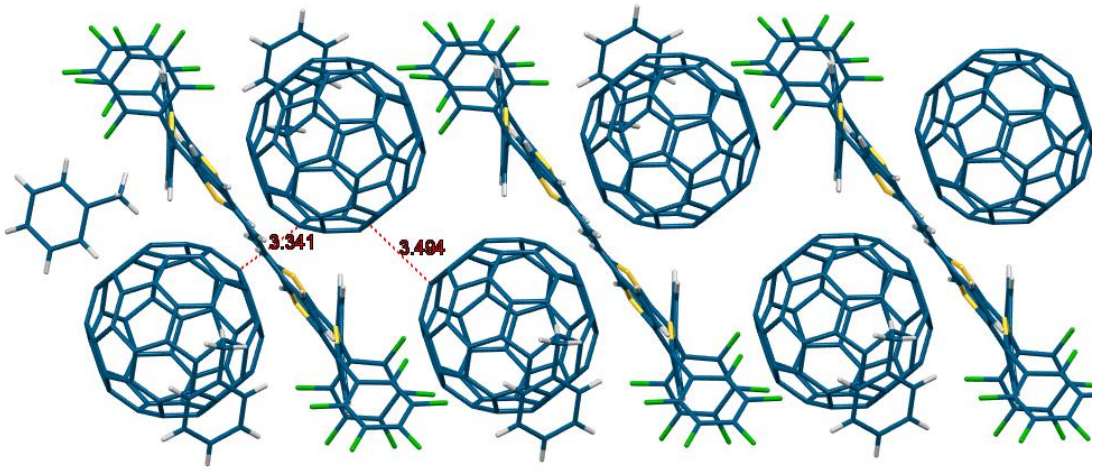

Figure III.10: Packing diagram showing shorts contact between fullerens.

short contacts. Each fullerene sphere was found to exhibit short contacts with two neighbouring fullerenes and the distance between nearest carbon atoms of fullerene were found to be 3.31 Å and 3.49 Å (fig. **III.10**). The short contacts 2.94 Å, 2.95 Å and 3.02 Å were observed between *ortho*-F atoms of the *meso*- pentafluorophenyl ring and nearest carbon atoms of fullerene, suggest the significant contribution of C-F interaction in the complexation.

III.7. Redox properties

As 4nπ isophlorinoids are well documented to exhibit reversible two-electron oxidations, hence it was expected that the 40π octathiophene can also be oxidized to its corresponding 38π aromatic dication. Hence, cyclic voltammetry and differential pulse voltammetry

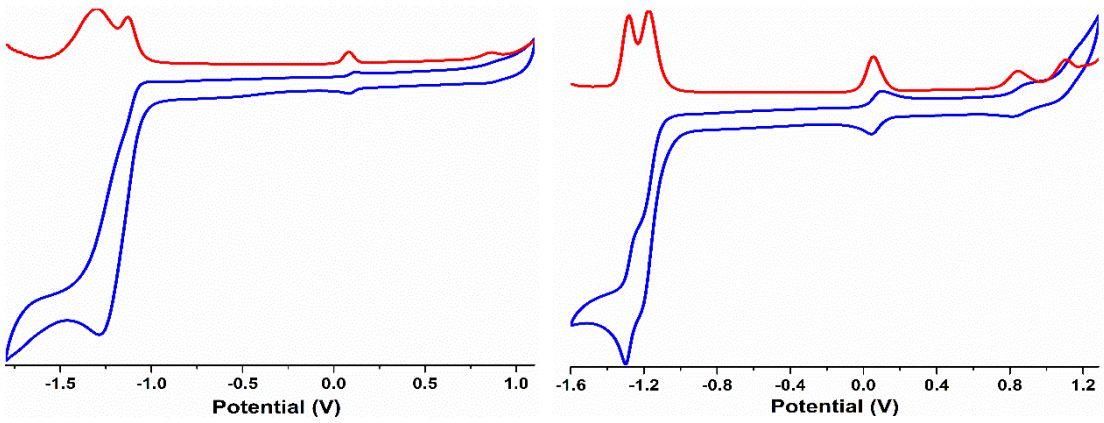

Figure III.11: Cyclic voltammogram (CV, blue) and differential pulse voltammogram (DPV, red) of **III.10** (left) and **III.12** (right) in CH_2Cl_2 (with 0.1 M Bu_4NPF_6 as the supporting electrolyte).

measurements were performed to examine the electrochemical properties of antiaromatic macrocycles. Cyclic Voltamogram of **III.10** (figure **III.11**) revealed the redox properties with two reduction waves at -1.25 and -1.46 V and two reversible oxidation waves at + 0.04 and + 0.83 V. The core modified isophlorin, **III.12**, also displayed similar signals in its cyclic voltammogram supporting reversible redox nature of these expanded isophlorins. All these potentials were further established by differential pulse voltammogram.

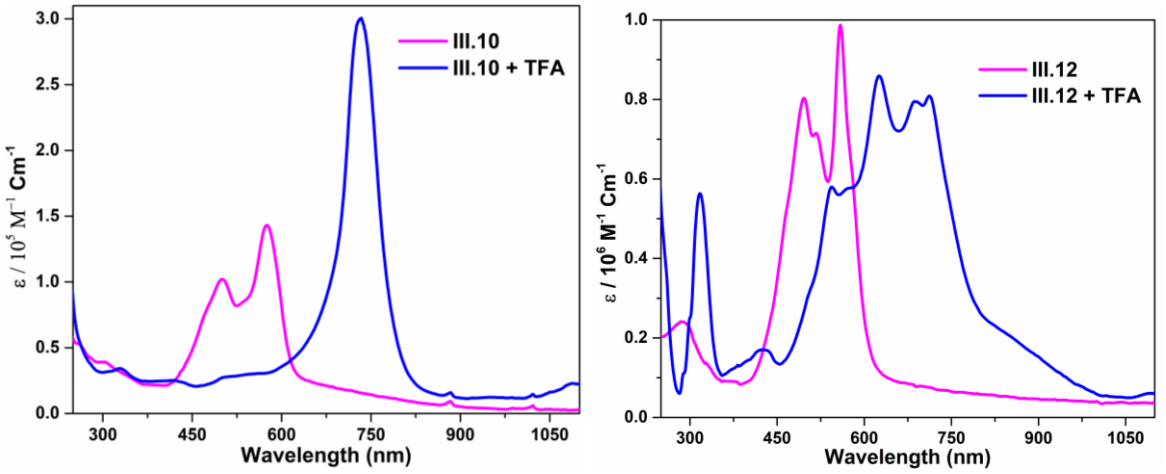

Figure III.12: UV/vis absorption spectrum of 10^{-6} M solution of **III.10** & **III.10**$^{2+}$ (left) and macrocycles **III.12** & **III.12**$^{2+}$ (right) recorded in $CHCl_3$.

The oxidations of aromatic systems were known to yield a radical cation, whereas antiaromatic macrocycles be expected to undergo two-electron oxidation to form corresponding dication species. The electrochemical studies, provides an insight to explore the ring oxidation of 4nπ macrocycle to its corresponding cations. One-electron oxidizing agents such as Meerwein salt $[Et_3O]^+[SbCl_6]^-$ or trifluoroacetic acid were known for their efficient oxidation of π conjugated molecules.[26] Addition of trifluoroacetic acid to a solution of **III.10,** in dry dichloromethane resulted in an immediate colour change from a pink to blue, suggestive of the expected ring oxidation. The drastic change in colour induced large red shifted absorptions at 732 nm. A bathochromic shift by more than 150 nm and with a two fold increase in the absorption coefficient (ε= 301200) of its intense absorption band showed a remarkable change in the electronic character of the macrocycle. Similar oxidation and colour change was observed for **III.12**, macrocycle (fig. **III.12**) with similar redox reagents. But, addition of zinc or base such as triethylamine didn't reduce these oxidised species back to neutral form. The high-resolution mass spectrum of the **III.12**$^{2+}$, displayed an *m/z* value corresponding to the dication formation of the macrocycle (fig. **III.13**). The isolated oxidized

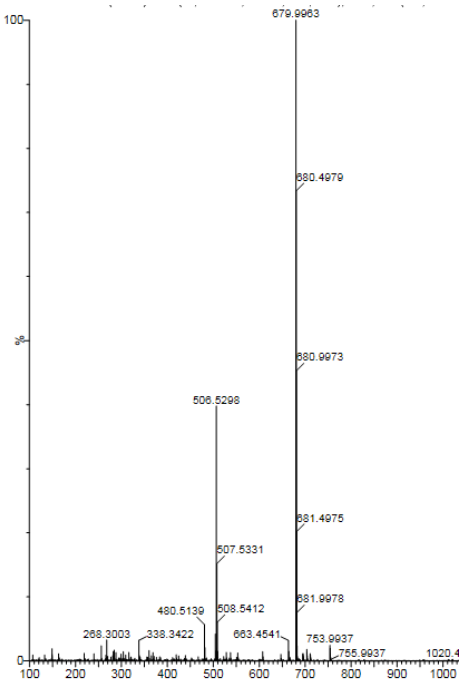

Figure III.13: HRMS spectrum of **III.12** dication.

product was subjected to ^{1}H NMR analysis. Surprisingly, only a broad signal was observed in its ^{1}H NMR spectrum even at low temperature, suggesting the possibility of a radical behaviour of oxidised product. The probable reason could be the presence of open-shell singlet diradical as a ground electronic state for the dicationic macrocycles. The electron paramagnetic resonance (EPR) spectrum of these products displayed a featureless broad signal at room temperature with a *g* value of 2.003 akin to an organic radical. The VT-ESR measurements in solid state for the dicationic macrocycles **III.10**$^{2+}$ and **III.12**$^{2+}$ revealed the

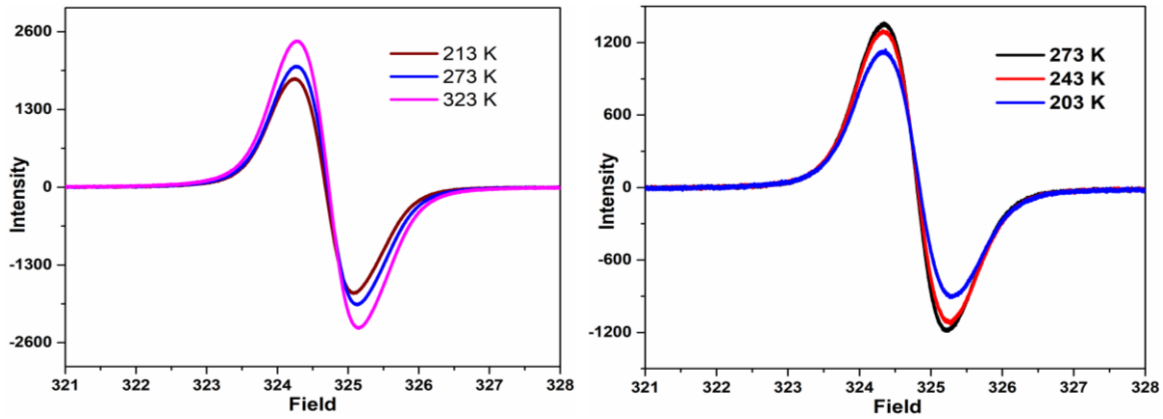

Figure III.14: VT EPR spectrum for **III.10**$^{2+}$ (left) and **III.12**$^{2+}$ (right).

significant temperature dependency of the signal intensities (figure **III.14**). The intensity of the EPR signal decreased with decreasing temperature suggesting the singlet diradical ground state, which is in equilibrium with a higher energy triplet diradical state for both the molecules.

III.8. Quantum mechanical calculation

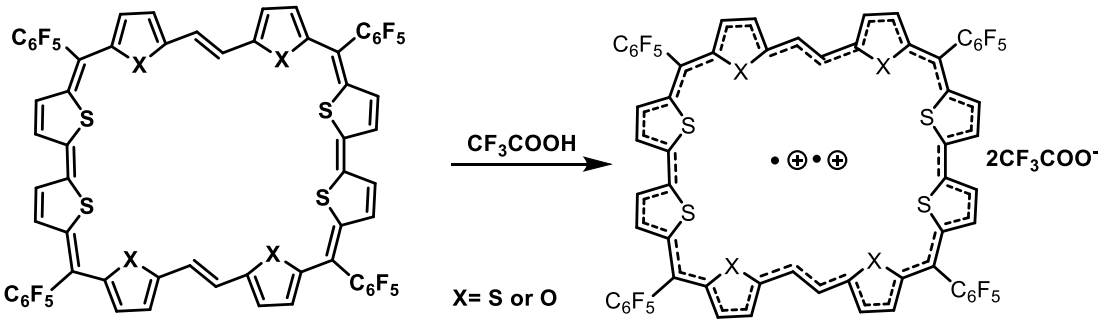

Scheme III.6: Two-electron oxidation of 40π isophlorins with trifluoroacetic acid.

The 40π expanded isophlorins antiaromatic character was further established by Nucleus Independent Chemical Shift (NICS) calculations at global ring centres.[27] The estimated NICS value of δ +4.51 and +3.62 ppm for **III.10** and **III.12** respectively was indicative of weak antiaromatic character. In contrast the computed NICS values were found to have moderately negative values of -6.6 and -5.1**,** for **III.10**$^{2+}$ and **III.12**$^{2+}$ suggesting their aromatic character.

The diradical character for both the oxidised macrocycles were further calculated by using unrestricted spin DFT calculations (UCAM B3LYP/631G (d)) on energy optimized geometry. It showed singlet to triplet energy gap (ΔE_{S-T}) of -8.21 kcal mol^{-1} for **III.10**$^{2+}$ and -1.62 kcal mol^{-1} for **III.12**$^{2+}$ (table **III.1**). The spatial diradical distribution in the singlet diradical structures shows delocalization of electron density throughout the macrocycle.

Table III.1: Energy difference between singlet and triplet energy states and diradical character calculations.

Molecule (Dication)	$E_{\text{Triplet-Singlet}}$ (Kcal/mol)	Diradical character Y_0
[**III.10**]$^{2+}$	-8.219	0.265
[**III.12**]$^{2+}$	-1.625	0.182

Accordingly, the diradical character (defined as the occupation number of the LUMO) estimated by NOON (natural orbital occupation number)[28-29] using CASSCF (complete active space self-consistent field) of the dicationic species was found to be 26% and 18% for **III.10**$^{2+}$ and **III.12**$^{2+}$ respectively.

To simulate the steady-state absorption spectra, time-dependent TD-DFT calculations were employed on the optimized structures. Simulated absorption spectra for both the molecules **III.10** and **III.12** and all the oxidised species of **III.10**$^{2+}$ and **III.12**$^{2+}$ matched the experimental results (figure **III.15** and **III.16**).

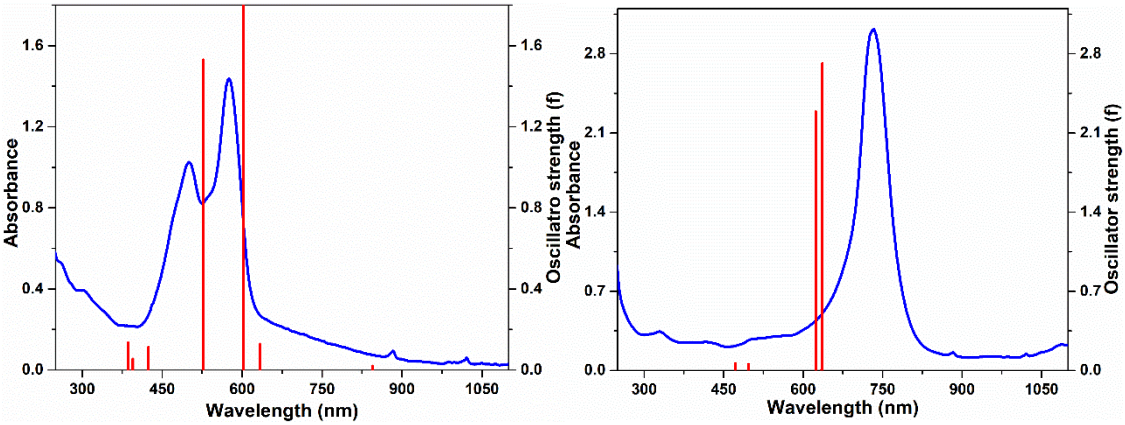

Figure III.15: The steady state absorption spectra (blue line) of **III.10** (left) and **III.10**$^{2+}$ (right) along with the theoretical vertical excitation energies (red bar) obtained from TD-DFT calculations carried out at the B3LYP/6-31G(d,p) level.

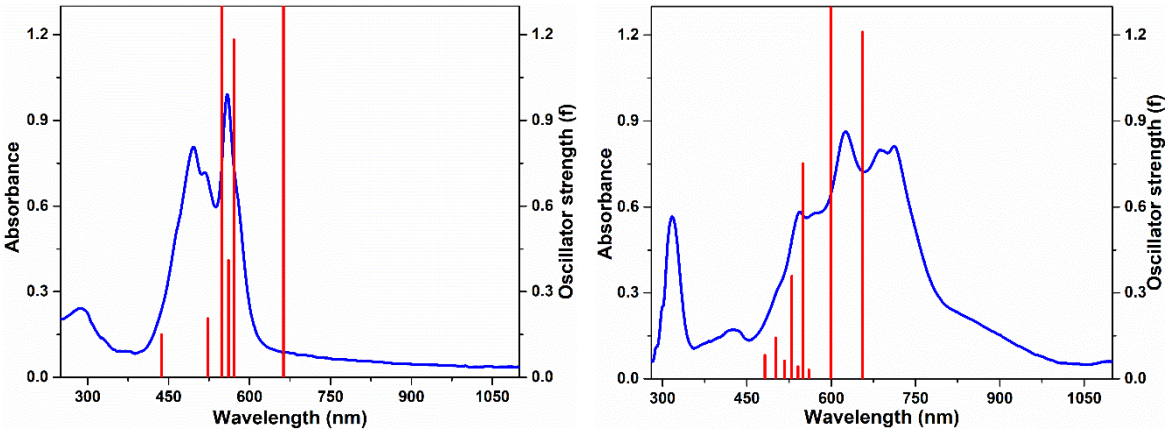

Figure III.16: The steady state absorption spectra (blue line) of **III.12** (left) and **III.12**$^{2+}$ (right) along with the theoretical vertical excitation energies (red bar) obtained from TD-DFT calculations carried out at the B3LYP/6-31G(d,p) level.

III.9. Synthesis of S-confused expanded isophlorin

By flipping one of the pyrrole units, core modified porphyrins like N-confused porphyrin[30] derivatives were synthesised as a novel ligand for organometallic complexes.[31] Similar chemistry has not been scarcely explored in anti-aromatic isophlorin molecules. In fact, there is only one report on S-confused isophlorin with unique redox property.[32] Flipping of the thiophene units of ethylene bridged monomer should result in the formation S-confused expanded isophlorin, **III.14**. To synthesise this structural isomer **III.14**, precursor, **III.9** was modified by bridging thiophene β-positions with ethylene and condensed with the bithiophene diol, **III.8** under similar reaction conditions as described in scheme **III.4**. Unfortunately, the MALDI-TOF/TOF mass spectrum of this reaction mixture did not reveal any *m*/*z* values corresponding to expected S-confused expanded isophlorin, **III.14** or any other macrocyclic products.

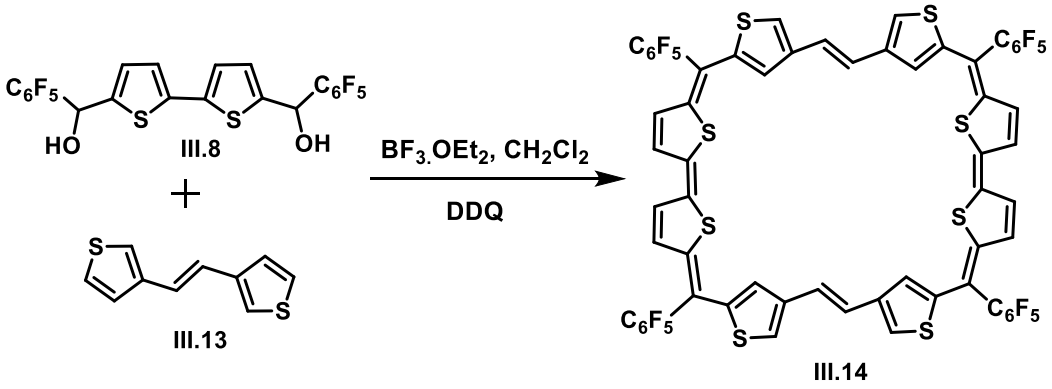

Scheme III.7: Synthesis of S-confused expanded isophlorin **III.14**.

III.10. Conclusion

Using simple synthetic variations, ethylene bridged 40π expanded isophlorins with core modifications were synthesized and characterized in solution and solid states. These macrocycles displayed fluxional characteristics in solution state. The single crystal X-ray diffraction study confirmed the formation of supramolecular complexes of 40π anti-aromatic isophlorin with fullerene. The solid state structure displayed the formation of 1:2 complex and also supports the non-covalent interaction between the 40π anti-aromatic macrocycle and the curved π surface of C60. The distance between the C_{60} and isophlorin is much shorter than the reported porphyrin- C_{60} complexes. This result reveals the anti-aromatic π surface is also as good as aromatic π surfaces for binding fullerenes. Although these molecules had diverse structural features, they displayed redox properties expected of antiaromatic

macrocycles. Both the 40π macrocycles were found to undergo two-electron oxidation to form the corresponding 38π aromatic dication diradical. These systems exhibited significant change in the colour with a variety of oxidizing agents such as TFA and Meerwein's salt $[Et_3O]^+[SbCl_6]^-$. Their oxidation reactions produced the same oxidized product irrespective of the oxidising agent used, as revealed by the similar electronic absorption spectrum. Interestingly, these dicationic macrocycles shows open shell singlet diradical ground state with moderate diradical character because of a small singlet-triplet energy gaps. The diradical property of these dication systems were confirmed by EPR and computational studies. To conclude, insertion of ethylene bridge into the macrocyclic conjugation pathway appears to be good strategy for the synthesis of variety of expanded antiaromatic macrocycles. It was observed that the oxidation products for these expanded antiaromatic molecules vary significantly in contrast to 20π or 32π antiaromatic macrocycles.

III.11. Experimental section

Synthesis and characterisation of macrocycle III.10:

A mixture of bisthienylethylene, **III.9**, (192 mg, 1 mmol) and bithiophene diol, **III.8** (557 mg, 1 mmol) were stirred in 100 mL of dry dichloromethane. The solution was purged with argon for 10 min. and shielded from light. $BF_3.OEt_2$ (122μL, 1 mmol) was added and stirring continued for 2h. Then, DDQ (567 mg, 2.5 mmol) was added and the mixture was stirred for an additional two hours. Finally solution was passed through short pad of basic alumina column. This mixture was concentrated and further purified by silica gel column chromatography using CH_2Cl_2/Hexane as eluent.

Characterisation of macrocycle III.10:
Yield- 7%
HR-MS (ESI-TOF): *m*/*z* = 1423.8971 (found), 1423.9011 (calcd. For $C_{64}H_{20}F_{20}S_8$).
UV-Vis ($CHCl_3$): λ_{max} nm (ε) L mol^{-1} cm^{-1} = 499 (124400), 575 (143400).

NMR Data: ^{1}H NMR (400 MHz, $CDCl_3$, 298K) δ 7.94 (s, 4H), 6.83 (d, *J* = 4.8 Hz, 4H), 6.64 (d, *J* = 4.8 Hz, 4H), 6.34 (d, *J* = 4.8 Hz, 8H)

Crystal data of III.10:C_{60} co crystal: $C_{67}H_{20}F_{20}S_8$, 2(C60), 4(C_7H_8) (*M*r 3235.02), triclinic, space group *P-1*, a = 13.43(3), b = 15.46(6), c = 16.62(7) Å, α= 95, β= 100.66(3), γ= 99.83, V = 3317(40) $Å^3$, Z = 1, T = 100(2) K, D_{calcd} = 1.619 cm^{-3}, R_1 = 0.0688 (11707), R_w (all data) = 0.2246 (16335), GOF = 1.239.

Synthesis and characterisation of macrocycle III.12:

Bisfuran, **III.11** (160 mg, 1 mmol) and bithiophene diol, **III.8** (557 mg, 1 mmol) were reacted as described above to yield **III.12** in 6% yields.

HR-MS (ESI-TOF): *m*/*z* = 1359.9943 (found), 1359.9925 (calcd. For $C_{64}H_{20}F_{20}S_4O_4$).

UV-Vis ($CHCl_3$): λ_{max} nm (ε) L mol^{-1} cm^{-1} = 495 (879200), 558 (991200).

NMR Data: ^{1}H NMR (400 MHz, $CDCl_3$, 298K) δ 10.17 (d, *J* = 5.6 Hz, 2H), 9.80 (d, *J* = 13.2 Hz, 2H), 9.60 (d, *J* = 5.2 Hz, 2H), 6.26 (d, *J* = 4.4 Hz, 4H), 5.98 (d, *J* = 5.6 Hz, 2H), 5.71 (d, *J* = 4.4 Hz, 4H), 5.59 (d, *J* = 5.2 Hz, 4H).

Synthesis and characterisation of ethylene bridged monomers:

(E)-1,2-di(thiophen-2-yl)ethene (III.9):

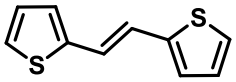

To a stirred solution of thiophene-2-carbaldehyde (11.2 g, 0.1 mol) in THF (200 ml) titanium(IV) chloride (13 ml, 0.12 mol) was added over a period of 0.5 h at -18 °C. After stirring at this temperature for 0.5 h, zinc powder (15.7 g, 0.24 mol) was added in small portions over a period of 0.5 h. The mixture was stirred at -18 °C for 0.5 h, warmed to room temperature, and refluxed for 3.5 h. The reaction was quenched by addition of ice-water (150 ml) and the resulting solid was collected by filtration and dried. The solid was dissolved in methylene chloride (150 ml) and the insoluble inorganic material was removed by filtration. The filtrate was evaporated and purified by recrystallization to yield compound in 85% yield. The spectroscopic data matches with the data already reported in literature.[33]

NMR Data: ^{1}H NMR (400 MHz, $CDCl_3$, 298K) δ 7.18 (d, *J* = 8 Hz, 2H), 7.05 (s, 2H), 7.03 (d, *J* = 4 Hz, 2H), 6.99 (dd, *J* = 8 Hz, 4 Hz, 2H).

E-1,2-di(furan-2-yl)ethene (III.11):

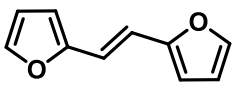

Furan-2-carbaldehyde (1.2 g, 12.5 mmol), titanium(IV) chloride (1.64 ml, 15 mmol) and zinc powder (2 g, 30 mmol) were reacted as described in the synthesis of **III.9** to give **III.11** in 55% yields. The spectroscopic data matches with the data already reported in literature.[34]

NMR Data: ^{1}H NMR (400 MHz, $CDCl_3$, 298K) δ 7.41 (d, *J* = 1.8 Hz, 2H), 6.84 (s, 2H), 6.43 (dd, *J* = 3.6 Hz, 1.8 Hz, 2H), 6.35 (d, *J* = 3.6 Hz, 2H).

(E)-1,2-di(thiophen-3-yl)ethene (III.13):

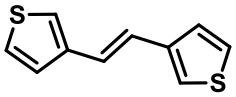

Thiophene-3-carbaldehyde (2 g, 17.8 mmol), titanium(IV) chloride (2.35 ml, 21.42 mmol) and zinc powder (2.78 g, 42.84 mmol) were reacted as described in the synthesis of **III.9** to give **III.13** in 67% yields. The spectroscopic data matches with the data already reported in literature.[35]

NMR Data: ^{1}H NMR (400 MHz, $CDCl_3$, 298K) δ 7.38 (dd, *J* = 2.8 Hz, 5.2 Hz, 2H), 7.32 (dd, *J* = 5.2 Hz, 1.2 Hz, 2H), 7.28 (dd, *J* = 2.8 Hz, 1.2 Hz, 2H), 7.04 (s, 2H).

III.12. References

1. Reddy, B. K.; Basavarajappa, A.; Ambhore, M. D.; Anand, V. G., *Chem. Rev.* **2017,** *117,* 3420-3443.
2. Vogel, E.; Bröring, M.; Fink, J.; Rosen, D.; Schmickler, H.; Lex, J.; Chan, K. W. K.; Wu, Y.-D.; Plattner, D. A.; Nendel, M.; Houk, K. N., *Angew. Chem., Int. Ed.* **1995,** *34,* 2511-2514.
3. Setsune, J.-i.; Katakami, Y.; Iizuna, N., *J. Am. Chem. Soc.* **1999,** *121,* 8957-8958.
4. Lash, T. D., *Angew. Chem., Int. Ed.* **2000,** *39,* 1763-1767.
5. Cha, W.-Y.; Soya, T.; Tanaka, T.; Mori, H.; Hong, Y.; Lee, S.; Park, K. H.; Osuka, A.; Kim, D., *Chem. Comm.* **2016,** *52,* 6076-6078.
6. Gopalakrishna, T. Y.; Reddy, J. S.; Anand, V. G., *Angew. Chem., Int. Ed.* **2013,** *52,* 1763-7.
7. Liu, C.; Shen, D.-M.; Chen, Q.-Y., *J. Am. Chem. Soc.* **2007,** *129,* 5814-5815.
8. Cissell, J. A.; Vaid, T. P.; Yap, G. P., *J. Am. Chem. Soc.* **2007,** *129,* 7841-7.
9. Haas, W.; Knipp, B.; Sicken, M.; Lex, J.; Vogel, E., *Angew. Chem., Int. Ed.* **1988,** *27,* 409-411.
10. Reddy, J. S.; Anand, V. G., *J. Am. Chem. Soc.* **2009,** *131,* 15433-15439.
11. Hu, Z. Y.; Atwood, J. L.; Cava, M. P., *J. Org. Chem.* **1994,** *59,* 8071-8075.
12. Williams-Harry, M.; Bhaskar, A.; Ramakrishna, G.; Goodson, T., 3rd; Imamura, M.; Mawatari, A.; Nakao, K.; Enozawa, H.; Nishinaga, T.; Iyoda, M., *J. Am. Chem. Soc.* **2008,** *130,* 3252-3.
13. Zhang, F.; Gotz, G.; Winkler, H. D.; Schalley, C. A.; Bauerle, P., *Angew. Chem., Int. Ed.* **2009,** *48,* 6632-5.
14. Reddy, J. S.; Mandal, S.; Anand, V. G., *Org. Lett.* **2006,** *8,* 5541-5543.

15. Anand, V. G.; Pushpan, S. K.; Venkatraman, S.; Dey, A.; Chandrashekar, T. K.; Joshi, B. S.; Roy, R.; Teng, W.; Senge, K. R., *J. Am. Chem. Soc.* **2001,** *123,* 8620-8621.

16. Gupta, P.; Panchal, S. P.; Anand, V. G., *J. Chem. Sci.* **2016,** *128,* 1703-1707.

17. Ambhore, M. D.; Basavarajappa, A.; Anand, V. G., *Chem. Comm.* **2019,** *55,* 6763-6766.

18. Seidel, D.; Lynch, V.; Sessler, J. L., *Angew. Chem., Int. Ed.* **2002,** *41,* 1422-1425.

19. Vogel, E.; Sicken, M.; Röhrig, P.; Schmickler, H.; Lex, J.; Ermer, O., *Angew. Chem., Int. Ed.* **1988,** *27,* 411-414.

20. Gopalakrishna, T. Y.; Anand, V. G., *Angew. Chem., Int. Ed.* **2014,** *53,* 6678-6682.

21. Sygula, A.; Fronczek, F. R.; Sygula, R.; Rabideau, P. W.; Olmstead, M. M., *J. Am. Chem. Soc.* **2007,** *129,* 3842-3843.

22. Mizyed, S.; Georghiou, P. E.; Bancu, M.; Cuadra, B.; Rai, A. K.; Cheng, P.; Scott, L. T., *J. Am. Chem. Soc.* **2001,** *123,* 12770-12774.

23. Sun, D.; Tham, F. S.; Reed, C. A.; Chaker, L.; Burgess, M.; Boyd, P. D. W., *J. Am. Chem. Soc.* **2000,** *122,* 10704-10705.

24. Hosseini, A.; Taylor, S.; Accorsi, G.; Armaroli, N.; Reed, C. A.; Boyd, P. D. W., *J. Am. Chem. Soc.* **2006,** *128,* 15903-15913.

25. Reddy, B. K.; Gadekar, S. C.; Anand, V. G., *Chem. Comm.* **2015,** *51,* 8276-8279.

26. Rathore, R.; Kumar, A. S.; Lindeman, S. V.; Kochi, J. K., *J. Org. Chem.* **1998,** *63,* 5847-5856.

27. Schleyer, P. v. R.; Maerker, C.; Dransfeld, A.; Jiao, H.; van Eikema Hommes, N. J. R., *J. Am. Chem. Soc.* **1996,** *118,* 6317-6318.

28. Kamada, K.; Ohta, K.; Shimizu, A.; Kubo, T.; Kishi, R.; Takahashi, H.; Botek, E.; Champagne, B.; Nakano, M., *J. Phy. Chem. Lett.* **2010,** *1,* 937-940.

29. Yamanaka, S.; Okumura, M.; Nakano, M.; Yamaguchi, K., *J. Mol. Struct. : THEOCHEM* **1994,** *310,* 205-218.

30. Furuta, H.; Asano, T.; Ogawa, T., *J. Am. Chem. Soc.* **1994,** *116,* 767-768.

31. Lash, T. D., *Angew. Chem., Int. Ed.* **2014,** *9,* 682-705.

32. Panchal, S. P.; Anand, V. G., *Org. Lett.* **2017,** *19,* 4854-4857.

33. Kim, R.; Amegadze, P. S. K.; Kang, I.; Yun, H.-J.; Noh, Y.-Y.; Kwon, S.-K.; Kim, Y.-H., *Adv. Funct. Mater.* **2013,** *23,* 5719-5727.

34. Viglianti, L.; Villafiorita-Monteleone, F.; Botta, C.; Mussini, P. R.; Ortoleva, E.; Cauteruccio, S.; Licandro, E.; Baldoli, C., *ChemistrySelect.* **2017,** *2,* 2763-2773.

35. Ngwendson, J. N.; Atemnkeng, W. N.; Schultze, C. M.; Banerjee, A., *Org. Lett.* **2006,** *8*, 4085-4088.

CHAPTER IV

Synthesis of 3D π-Conjugated Molecular Cages

IV.1. Introduction

Unlike aromatic porphyrinoids, its counterpart antiaromatic expanded isophlorinoids are not much celebrated molecules due to lack of straightforward synthetic strategies.[1] A handful of methods were known to extend the π-delocalization pathway of porphyrins. One among them is to either insert additional heterocyclic units or to increase the number of *meso* carbon bridges, resulting in the formation of expanded porphyrins.[2] An alternate way to synthesize the extended π-conjugated framework is by covalently connecting individual porphyrin units to one another leading to discrete oligomeric arrays.[3-4] Such dimerization of anti-aromatic molecules is not known till date. A reaction mechanism similar to oxidative coupling of aromatic units[5] is unknown even for the simple anti-aromatic systems such as cyclobutene or cyclooctatetraene.

A recent study revealed that the direct syntheses of a 20π *meso–meso* linked isophlorin[6] dimer from oxidative coupling of *meso*-free isophlorin cannot be achieved in a process similar to that of metallated porphyrins.[3] The synthesis of tetroxaisophlorin dimer having bridging double bond predicted the formation of unstable biradical, **IV.2**' (scheme **IV.1**). as an intermediate species. Antiaromatic isophlorin dimers have the potential to form diradicaloids, but still evade synthetic chemists. An attempt to synthesize such a radical dimer by condensing dicarbinols with tetraheteroethylenes yielded only the closed shell dimer (scheme **IV.2**).[7] This kind of structure-dependent spin states for dimers of expanded isophlorinoids have not been foreseen till date.

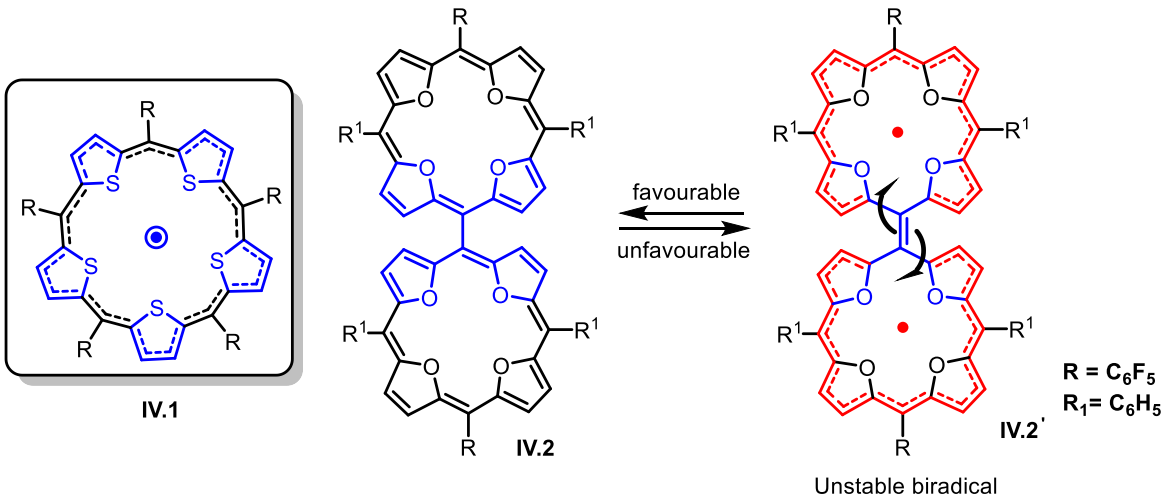

Scheme IV.1: Structures of cyclic pentathiophene radical and anti-aromatic dimer of tetraoxaisophlorin.

Cyclic π-conjugated systems with odd number of atoms in their conjugation pathway tend to form a radical species which can be stabilized by the delocalized π-bonds. An expanded isophlorin macrocycle, **IV.1,** with 25π electrons consisting of five thiophene units was isolated and characterized as an air- and water-stable neutral radical (scheme **IV.1**).[8] In a modified synthetic strategy, an attempt was made to synthesize a potential isophlorinoid dimer diradicaloid, **IV.11**, by condensing appropriate precursors derived from thiophene subunits. Dimerizing through one of the *meso* carbons can form either a biradical or a closed-shell double bond bridge involving the covalently linked individual macrocyclic units (scheme **IV.3**).

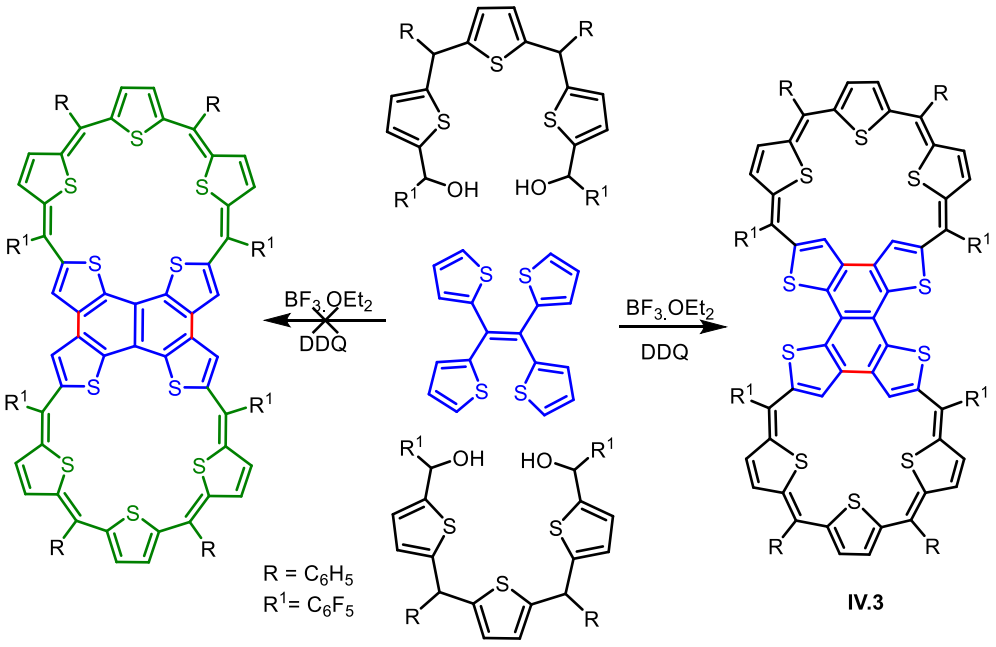

Scheme IV.2: Synthesis of fused pentaphyrin dimer.

IV.2. Synthesis and Characterization

As described above (scheme **IV.2**) the synthesis was attempted by employing MacDonald type condensation of bithiophene diol,[9] **IV.4** with tetrathienylethene,[10] **IV.5** in dichloromethane in the presence of boron trifluoride etherate, followed by oxidation with DDQ (scheme **IV.3**). In principle, more than one product can be hypothesized under this reaction condition. Based on previous report of pentaphyrin dimer (scheme **IV.2**),[7] it was expected that a potential competition exists between the radical dimer, **IV.11**, and the bicyclic fused system, **IV.10** depending on the orientation of the tetrathienylethane **IV.5** towards bithiophene diol **IV.4**.

In contrast to these expectations, the MALDI–TOF/TOF mass spectrum of the reaction mixture exhibited predominantly three *m/z* values (fig. **IV.1**). They could be identified as 2:1 (**IV.6**), 1:1 (**IV.7**) and 3:2 (**IV.8**) stoichiometric ratios, respectively, formed by the condensation of bithiophene units, **IV.4**, with two units of tetrathienylethene, **IV.5**, in a stepwise fashion. Changing the stoichiometric ratio of the precursors as 1:2.2, 1:1.2 and 1:1.6 (tetrathienylethene : bithiophene diol) under identical reaction conditions provided substantial control over the yield of these products. It was observed that a maximum yield of 4% for **6** was obtained when the precursors were condensed in a 1:2.2 ratio. These yields further decreased to less than 2% and 1% when the ratios were 1:1.6 and 1:1.2, respectively. The yields of **IV.8** were also found to slightly decrease for the same ratios. However, the yield of **IV.7** was found to be a maximum of 8% with the ratio of 1:1.2 of the precursors (table **IV.1**). The formed products were isolated by repeated silica gel column chromatography followed by size-exclusion chromatography with toluene.

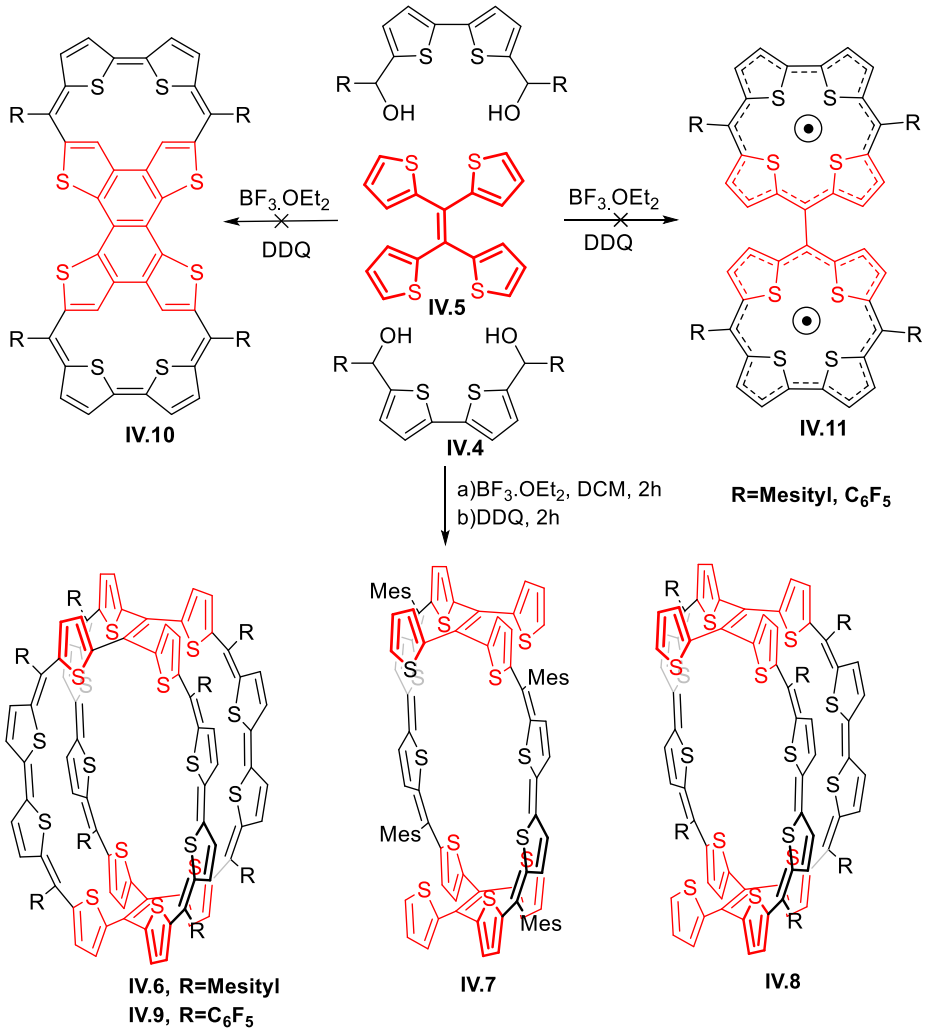

Scheme IV.3: Acid catalysed synthesis of 3D molecular cages.

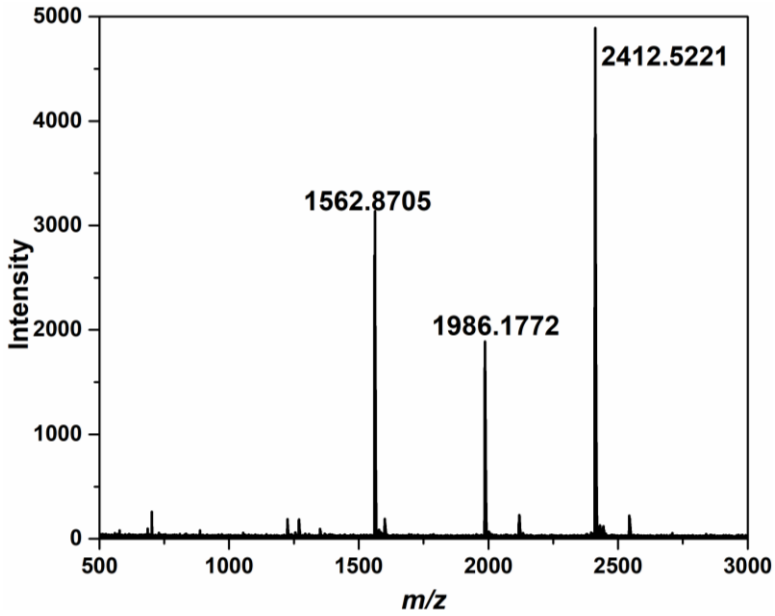

Figure IV.1: MALDI-TOF/TOF mass spectrum of the reaction mixture.

Table IV.1: Yields of cage molecules isolated when different stoichiometric ratio of the precursors used.

Stoichiometric ratio of the precursors (**IV.4** : **IV.5**)	Yields		
	IV.6	**IV.7**	**IV.8**
1:1.2	Trace	Major (8%)	Minor
1:1.6	Minor	Minor	Minor
1:2.2	Major (4%)	Minor	Minor

IV.2.1. Single Crystal X-ray Diffraction Studies

A pink coloured band isolated from column chromatographic separation displayed a *m*/*z* value of 2411.1292 in its HR-MS spectrum and was identified as **IV.6**. It yielded a metallic solid upon evaporation of the solvent. Single crystal X-ray diffraction analysis revealed a three dimensional molecular cage for **IV.6**, in which four bithiophene units (**IV.4**) had condensed with two tetrathienylethene (**IV.5**) units (fig. **IV.2**). The bithiophene units, **IV.4**, represent the bridging unit whilst tetrathienylethene unit, **IV.5**, is a bridge head unit. A disordered hexane, as a solvent of crystallization, was found trapped in the void of this cage. Efforts to crystallize **IV.6** in other common solvents went futile. The cage adopts C_4

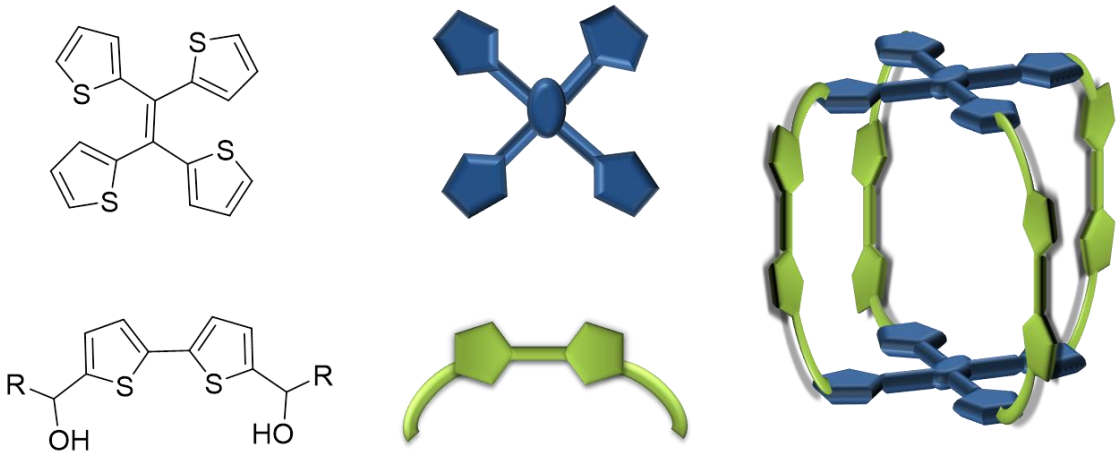

Figure IV.2. Schematic representation of cage molecule **IV.6**.

symmetry and all sulphur atoms were oriented towards the centre of the cage. As in the case of many porphyrinoids, the *meso* mesityl substituents were found near orthogonal in orientation to the cage architecture (fig. **IV.3**). It was observed that the distance between the centre of two tetrathienylethene bridgeheads was 9.21 Å, while the distance between the diagonally opposite *meso* carbon atoms was found to be 13.11 Å. As described above, this strategy was designed to synthesize a diradical dimer, **IV.11**. However, in hindsight it appears that the bulky thiophene units induce steric hindrance for the proposed tetrathiophene macrocyclic radical, **IV.11**. This proposition is further supported by the fact (during the course of this work) that a pyrrole analogue of a structurally similar dimer, **IV.12** was successfully synthesized from an alternate strategy (scheme **IV.4**). The 3D expanded carbaporphyrin, **IV.12** was isolated during the synthesis of bis-dicarbacorrole, **IV.13** from the condensation of tetrapyrrole precursor and pentafluorobenzaldehyde.[11]

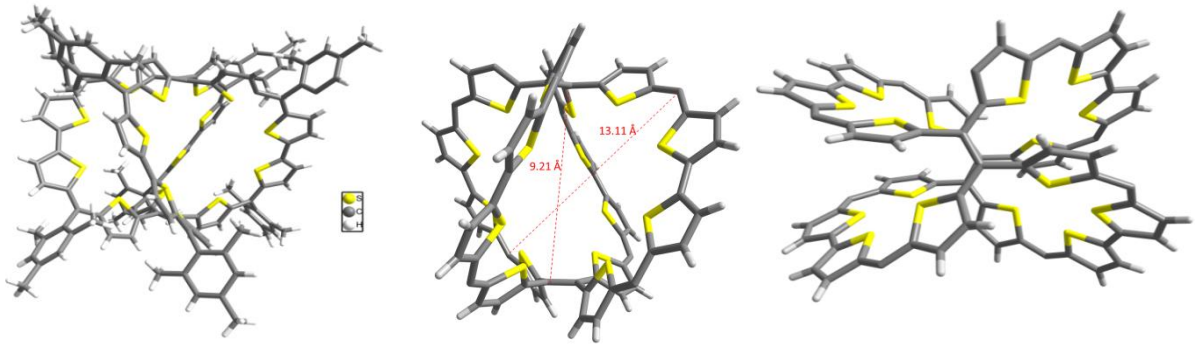

Figure IV.3: Molecular structure of cage **IV.6**, top view with *meso* mesityl substituents (left) and top view (middle) and side view (right); *meso* mesityl substituents have been omitted for clarity.

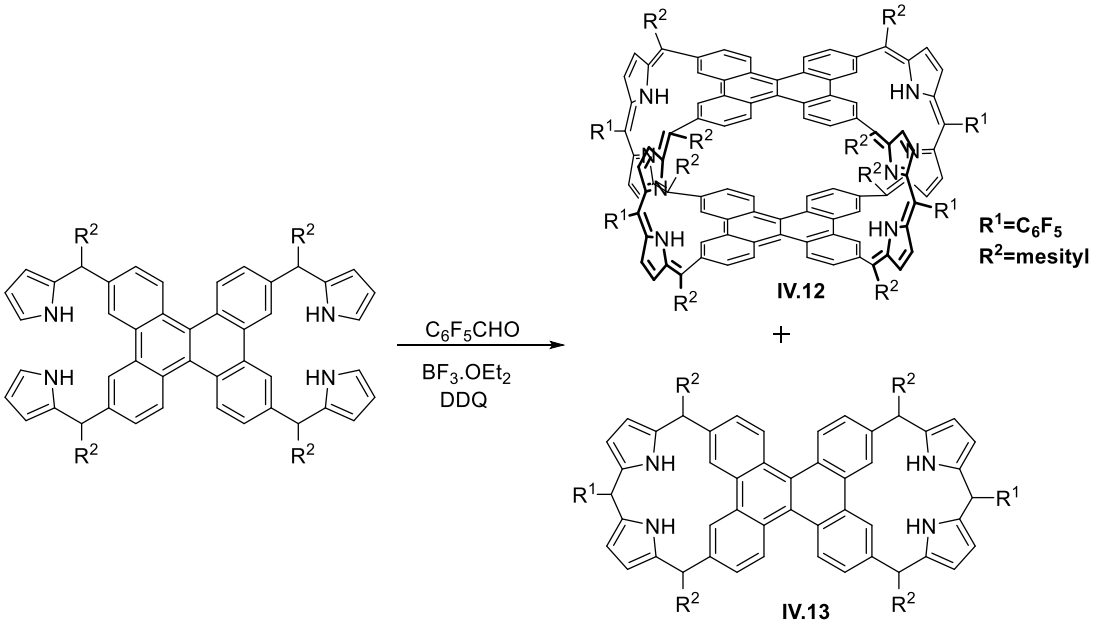

Scheme IV.4: Synthesis of carbaporphyrin cage, **IV.12**.

IV.2.2. ^{1}H NMR Studies

^{1}H NMR spectrum of **IV.6** recorded in THF-d_8 displayed only broad signals at room temperature suggestive of fluxional behaviour as anticipated in large sized molecules. Therefore, variable temperature ^{1}H NMR (fig. **IV.4**) was recorded to arrest the probable dynamic behaviour of the cage in solution state. This was confirmed upon lowering the temperature to 198 K yielded a relatively well resolved spectrum (fig. **IV.5**). Based on the structure obtained from the single crystal X-ray diffraction analysis, this molecule adopts a C_4 symmetry. In support of this symmetry, only four signals were observed in its ^{1}H NMR spectrum corresponding to an equal number of protons in the region δ 6.14–7.40 ppm. A set of these doublets correspond to the β protons of bithiophene units, while the other set is attributed to the β protons of the two tetrathienylethene units. Further support for this analysis was obtained from the ^{1}H–^{1}H COSY spectrum (fig. **IV.6**), which displayed four sets of correlations accounting for the thirty-two protons from sixteen thiophene rings. In addition to these resonances, methyl protons of *meso* mesityl rings resonated as three different signals at δ 1.91, 2.04 and 2.28 ppm. Alternatively, this cage molecule can also be identified as a fusion of two 40π octathiophene macrocycles. However, the steric strain induced by the formation of a three dimensional structure leads to a non-planar geometry diminishing the ring current effects of the 4nπ antiaromaticity.

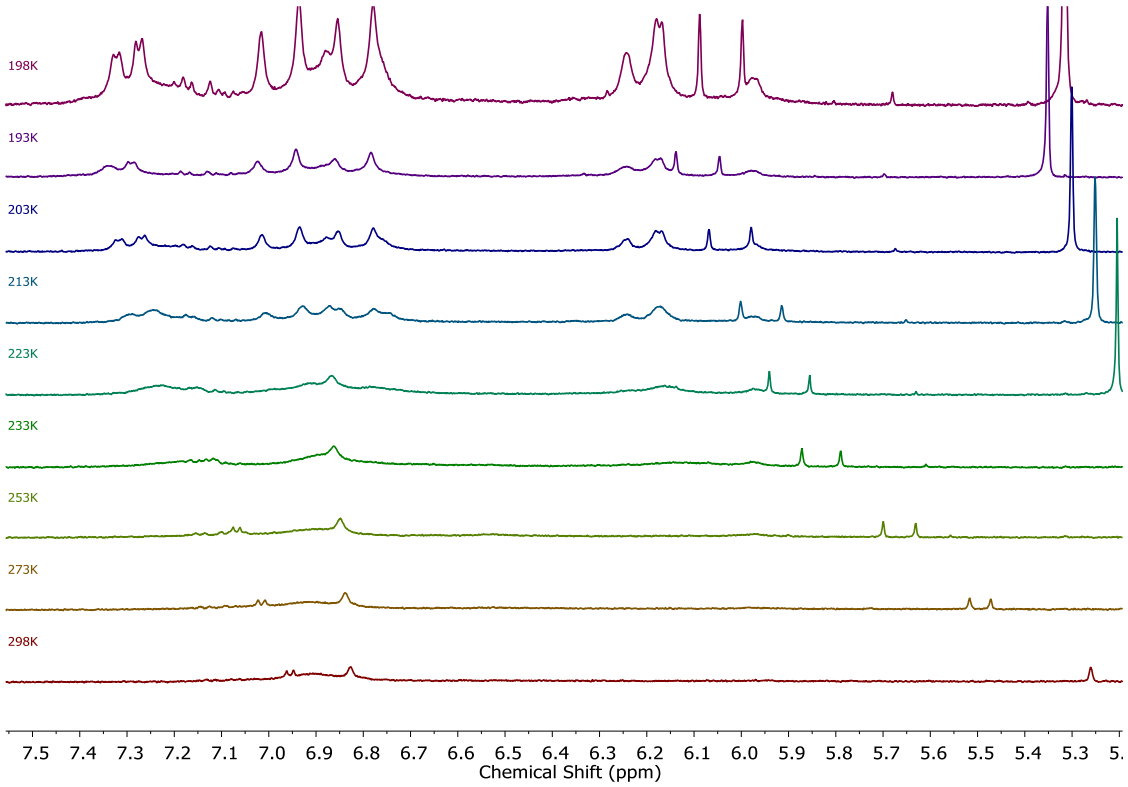

Figure IV.4: Variable temperature ^{1}H NMR spectrum of **IV.6** in THF-d_8

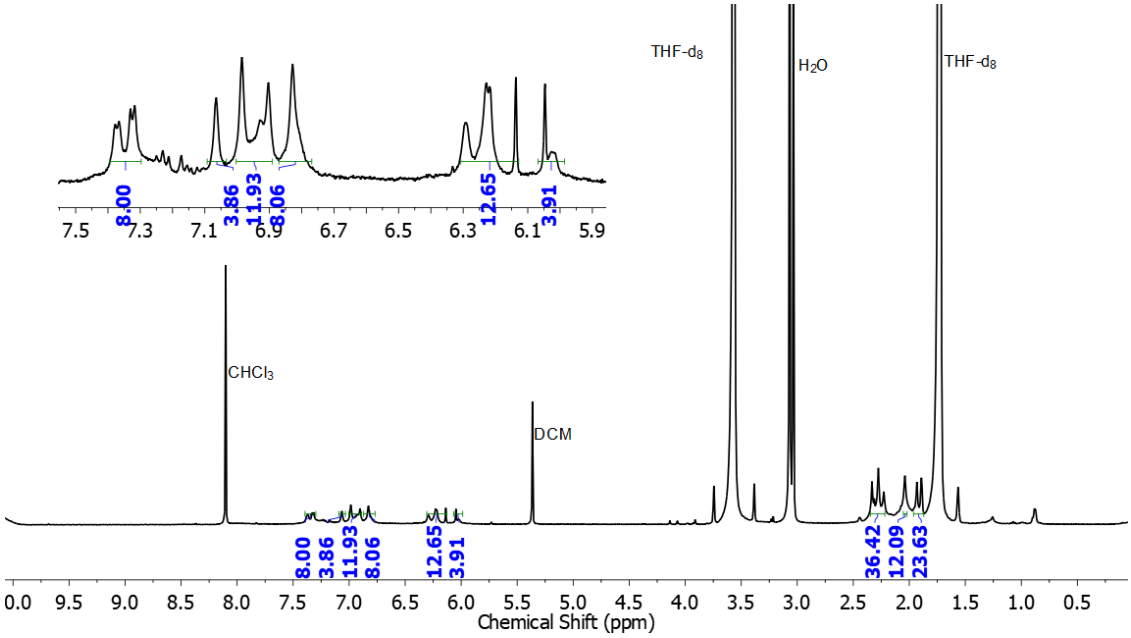

Figure IV.5: ^{1}H NMR spectrum of **IV.6** in THF-d_8 at 198K

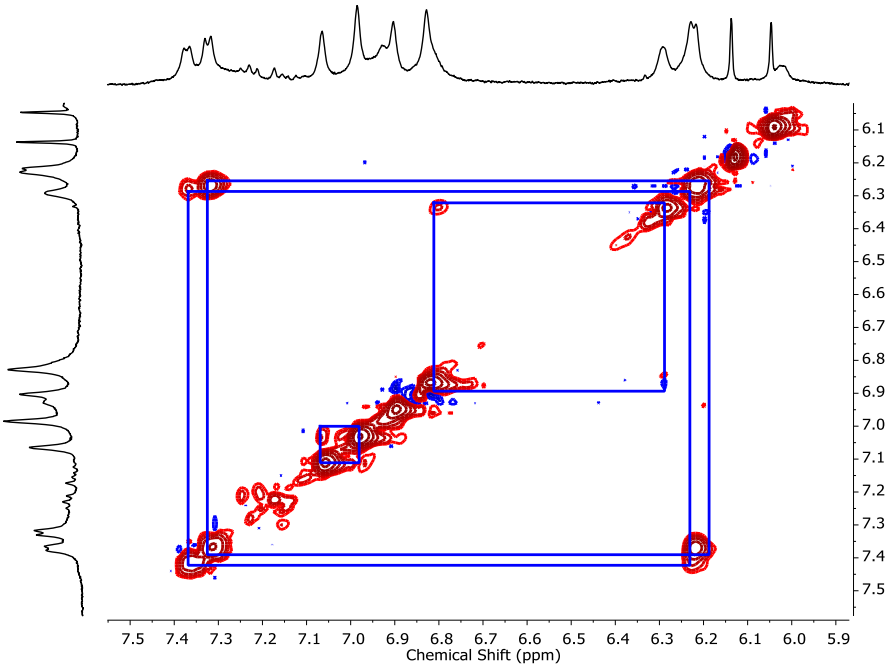

Figure IV.6: ^{1}H -^{1}H COSY spectrum of **IV.6** in THF-d_8 at 198K

IV.2.3. Electronic Absorption Studies

Despite bearing sixteen thiophene units, **IV.6** was found to be highly soluble in most of the common organic solvents. Due to its conjugated network, **IV.6** displayed an absorption maximum at 532 nm (ε = 258 000) (fig. **IV.7**). Thiophene only macrocycles or cages bear close resemblance to 4nπ isophlorinoids and hence expected to undergo reversible two-electron ring oxidation to yield the corresponding dicationic species. Both, protic acids and

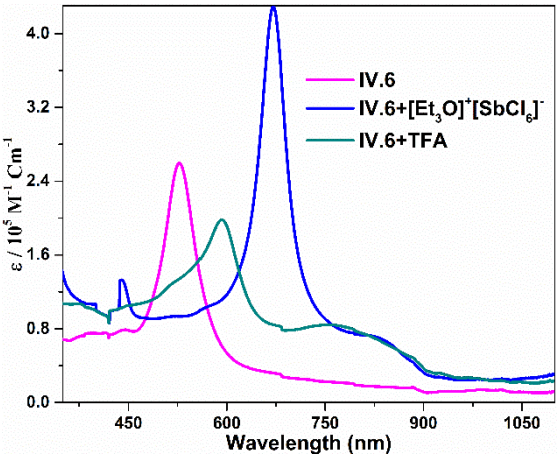

Figure IV.7: UV/Vis absorption spectrum of 10^{-6} M solution of **IV.6** and its oxidised species recorded in $CHCl_3$.

one electron oxidizing agents such as Meerwein's salts are known to oxidize modified isophlorins to their corresponding dicationic species.[1, 12] Upon oxidation with $[Et_3O]^+[SbCl_6]^-$ a significantly red shifted absorption maximum was observed at 675 nm (429 000). In contrast, the addition of TFA led to a relatively low intensity absorption at 598 nm (198 000). Surprisingly, reduction neither by zinc dust nor by a base such as triethylamine or pyridine yielded the expected freebase. Such an irreversible redox did not support the framework of antiaromatic isophlorinoids.

IV.2.4. Cyclic voltammetric (CV) and Spectroelectrochemical Studies

In support of the above observations, CV studies revealed two irreversible oxidations at +0.36 V and +0.90 V, respectively, along with a reduction wave at -1.21 V. All these potentials were further confirmed by differential pulse voltammetry (fig. **IV.8**). Further to examine the two distinct oxidised species observed in the absorption spectrum, spectroelectrochemical measurements were recorded in dichloromethane.

Changes in the absorption were monitored through electrochemical oxidation of cage at two different oxidation potentials as observed in the cyclic voltammogram. The spectroelectrochemical measurements at a lower oxidation potential of +0.4 V was suggestive of one-electron oxidation and at this potential it displayed an absorption maximum at 598 nm. Upon increasing potential to +1.1 V the absorption was further red shifted to 660 nm (fig. **IV.9**). Based on these observations, it could be explained that TFA yields the one-electron oxidized radical cation species, and the Meerwein's salt oxidized the cage to a dicationic species of the cage, **IV.6**. However, the unexpected irreversibility of chemical and electrochemical redox reflects a highly unstable nature of the oxidized products.

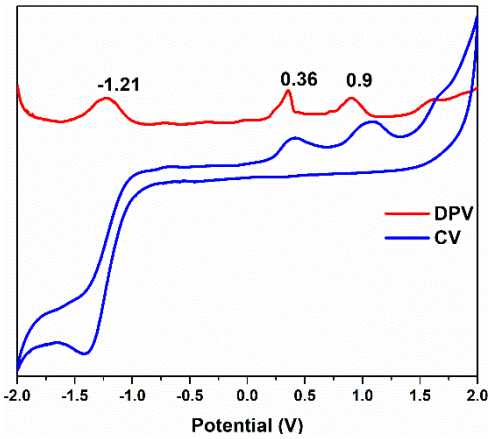

Figure IV.8: Cyclic voltammogram (CV, blue) and differential pulse voltammogram (DPV, red) of **IV.6** in CH_2Cl_2 (with 0.1 M Bu_4NPF_6 as the supporting electrolyte).

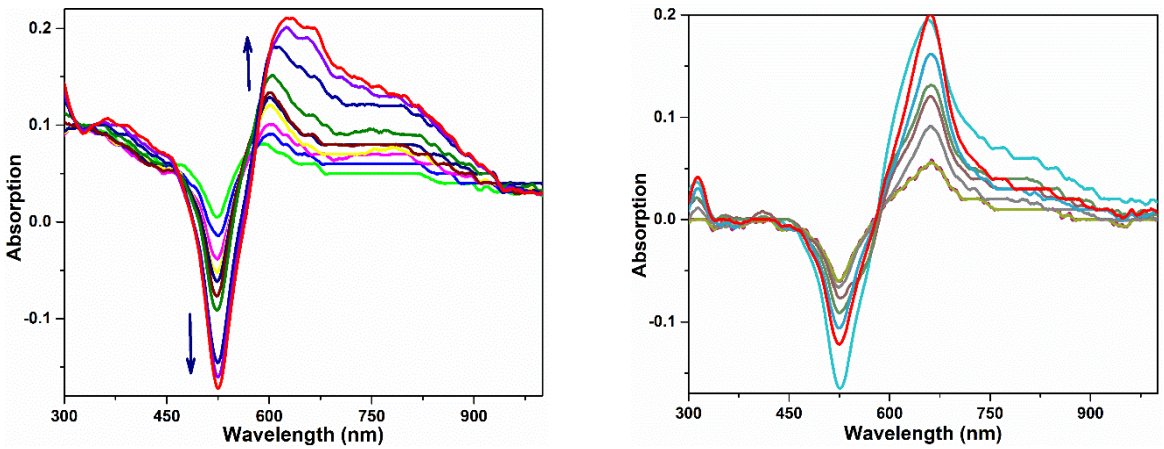

Figure IV.9: Change in absorption spectra of **IV.6** after applying a potential of +0.4 V (left) and +1.1 V (right), respectively.

IV.3. Synthesis and characterization of (IV.9)

Most of the stable antiaromatic isophlorinoids synthesized till date are known to be stabilized due to electron withdrawing substituents.[1] In tune with the established protocol, the cage **9** was synthesised with *meso* pentafluorophenyl substituents instead of mesityl groups. A pink coloured fraction that eluted with dichloromethane/petroleum ether using column chromatography was identified as **IV.9** and isolated with 5% yields. In its high resolution mass spectrum, the molecule displayed an *m/2* value of 1395.8707 (calcd. For $[C_{124}H_{32}F_{40}S_{16}]^{2+}$ 1395.8698) with a separation of 0.5 amu, corresponding to half of the molecular mass of the cage molecule suggesting the oxidation of **IV.9** into its dication. Cage **IV.9**, displayed intense pink coloured solution in common organic solvents and exhibited a single, relatively

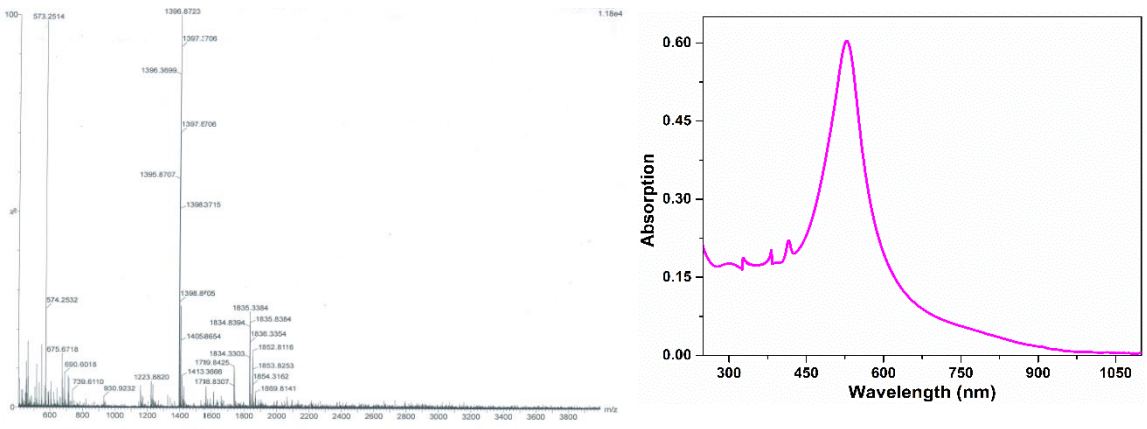

Figure IV.10: High resolution mass spectrum (HRMS) of **IV.9** spectrum (left) and Uv-visible absorption spectrum of 10^{-6} M solution of **IV.9** in CH_2Cl_2 (right).

broad absorption (fig. **IV.10**) at 528 nm (ε = 335 000). This red shifted absorption can be attributed to the increased length of the extended π-conjugation in cage molecule. In contrast to **IV.6**, a well resolved ^{1}H NMR spectrum of **IV.9** with a similar pattern was observed at room temperature (fig. **IV.11**). Three signals corresponding to thirty-two protons were observed in the region δ 6.25 – 6.96 ppm. Two doublets at δ 6.28 and 6.81 ppm corresponding to eight protons each and a doublet at δ 6.96 ppm corresponding to sixteen protons were observed in the room temperature ^{1}H NMR spectrum. However, all efforts to crystallize **IV.9** in a variety of solvents did not yield single crystals good enough for X-ray diffraction.

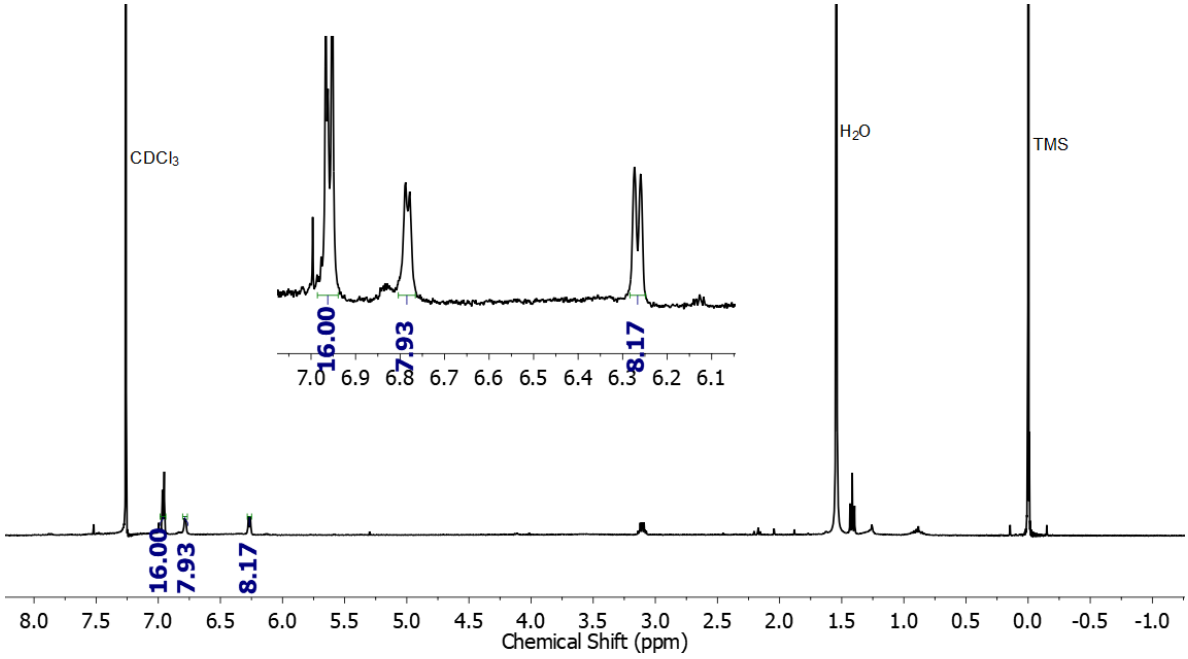

Figure IV.11: ^{1}H NMR spectrum of **IV.9** in $CDCl_3$ at 298K

IV.4. Synthesis and Characterization of (IV.7)

Another product, **IV.7**, isolated from this reaction in 8% yields displayed an *m/z* value of 1560.2346 (fig. **IV.12**) in its high-resolution mass spectrum, did not correspond to either of the anticipated competitive products, i.e. dimer **IV.11** or the fused π-system, **IV.10** (Scheme **IV.3**).

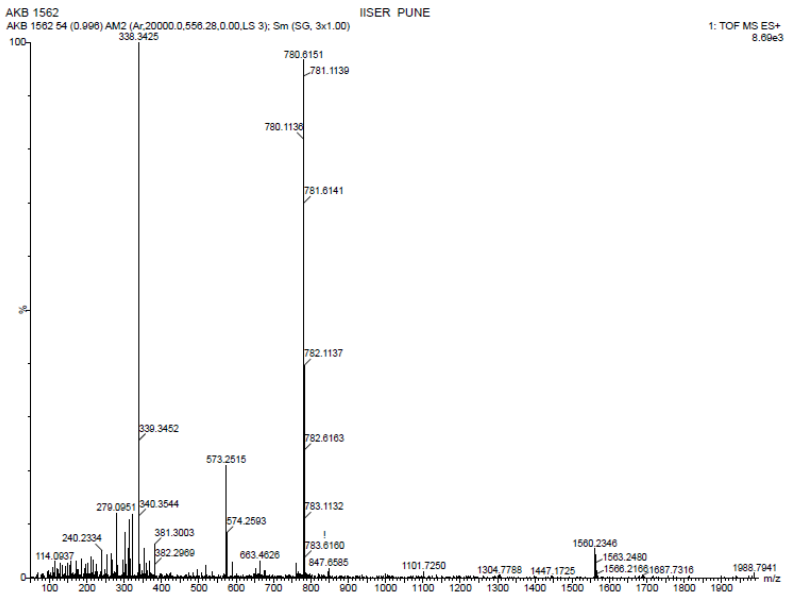

Figure IV.12: High resolution mass spectrum (HRMS) of **IV.7.**

IV.4.1. Single Crystal X-ray Diffraction Studies

The molecular structure of this macrocycle, **IV.7,** was unambiguously determined from single crystal X-ray diffraction studies (fig. **IV.13**). Single crystals of **IV.7** suitable for X-ray diffraction were obtained by vapour diffusion of n-hexane into their solution in chloroform. Its structure elucidated from the X-ray crystallographic analysis revealed a non-planar structure in which two tetrathienylethene units were connected by two bithiophene linkers. Since only two thiophene units of **IV.5** are involved in the covalent macrocyclic structure, its two other thiophenes were found tethered in a trans-like conformation and facing away from each other. Hence, one thiophene unit of **IV.5** is oriented towards the core of the macrocycle and the other away from the core of the macrocycle.

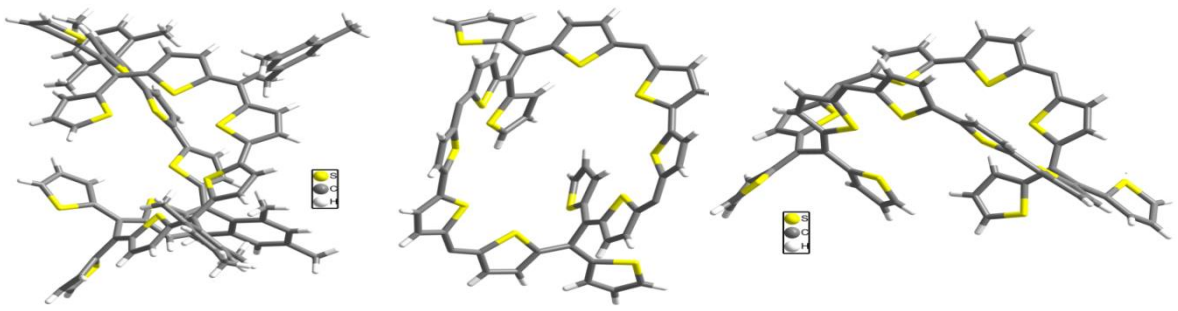

Figure IV.13: Molecular structure of macrocycle **IV.7**, top view with *meso* substituents (left) and top view (middle) and side view (right); *meso* mesityl substituents have been omitted for clarity.

IV.4.2. ^{1}H NMR Studies

^{1}H NMR spectrum of **IV.7** did not display a well-resolved spectrum at room temperature, suggestive of fluxional behaviour in the solution state. An attempt was made to arrest the fluxionality by recording its ^{1}H NMR spectrum at lower temperatures (fig. **IV.14**). Relatively, a well resolved spectrum was observed at 223 K (fig. **IV.15**). All the thiophene protons and the *meso* mesityl aryl protons were found to resonate in the region between δ 6.0 and 7.5 δ ppm and two signals were observed for meso mesityl methyl groups at δ 2.0 and 2.27 ppm, respectively. The ^{1}H –^{1}H COSY spectrum (fig. **IV.16**) recorded at 223 K exhibited five correlations to confirm the highly symmetrical nature of this molecule in the solution state. Even though **IV.7** is relatively a two dimensional structure, it did not reveal any characteristics of paratropic ring current effect expected from 40π anti-aromatic macrocycle. Perhaps, this can be attributed to the poor overlap of the π-orbitals at the ethylene junction of **5**, which might obstruct the access to global antiaromaticity for the macrocyclic structure. Structure of macrocycle **IV.7** in solution and solid-state are found to be different. ^{1}H NMR shows less number of signals, indicating that the molecule is highly symmetrical and possibly has a planar structure in the solution state. However, the molecular structure elucidated from single crystal analysis displayed relatively non-planar structure.

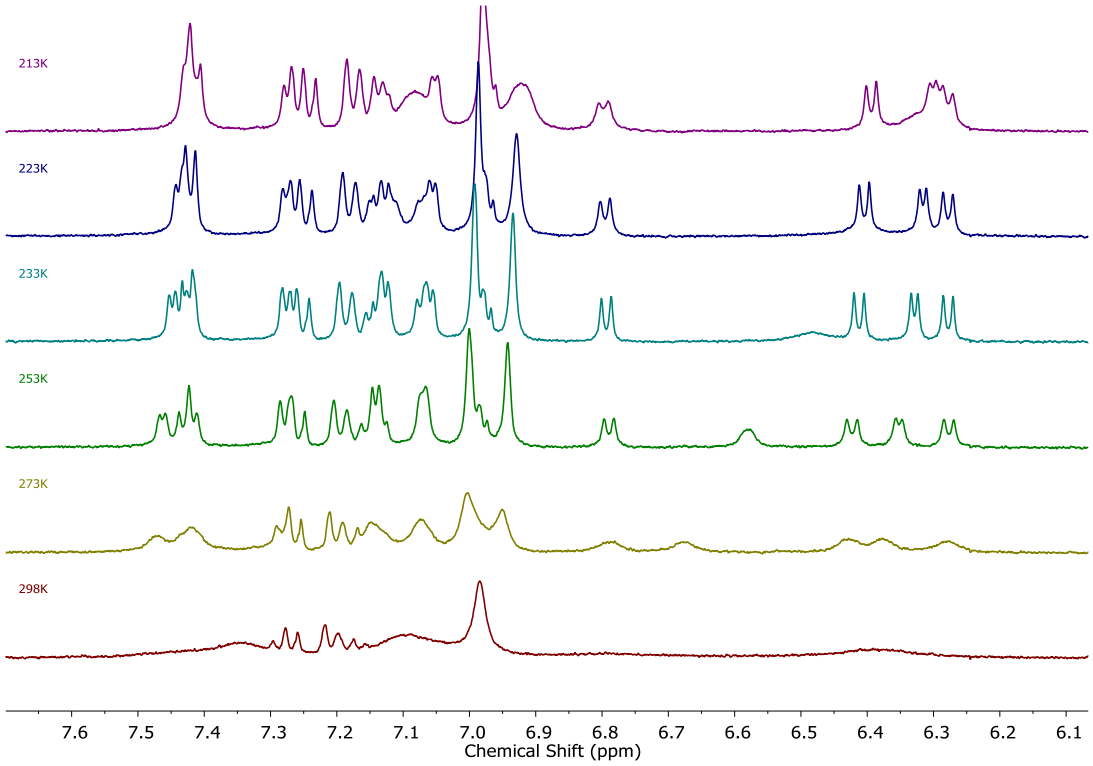

Figure IV.14: Variable temperature ^{1}H NMR spectrum of **IV.7** in dichloromethane-d_2

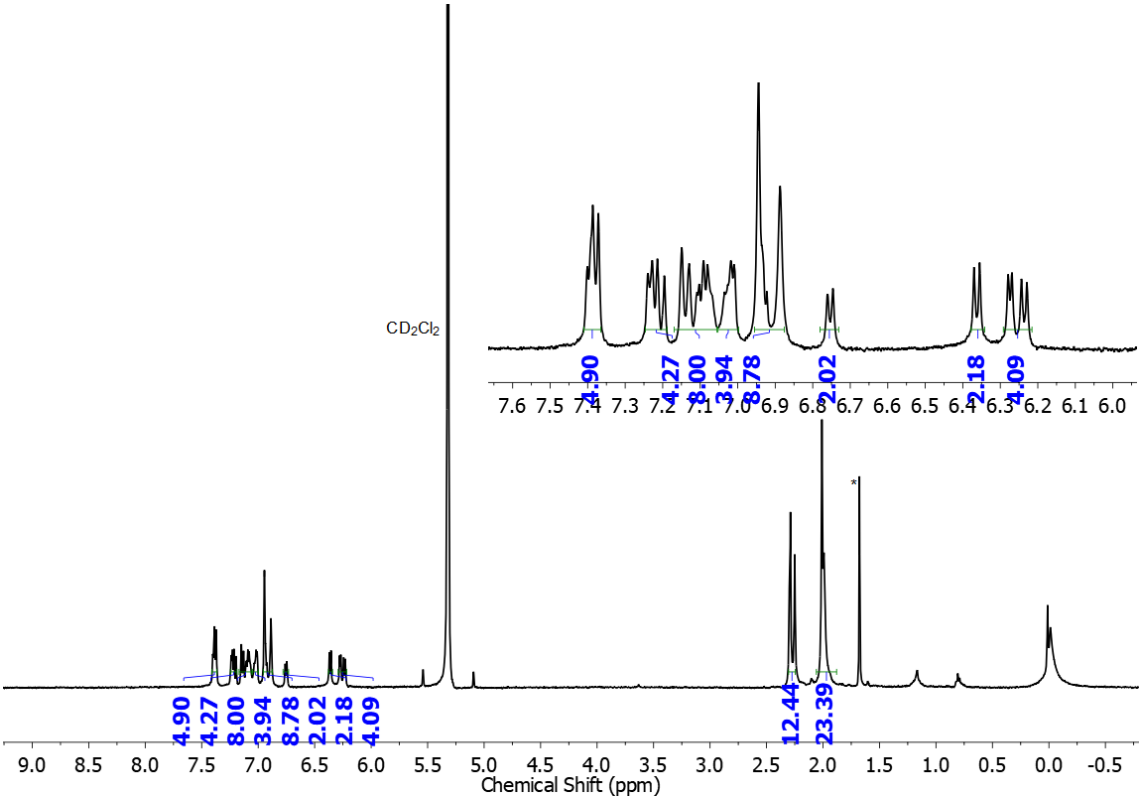

Figure IV.15: ^{1}H NMR spectrum of **IV.7** in Dichloromethane-d_2 at 223K

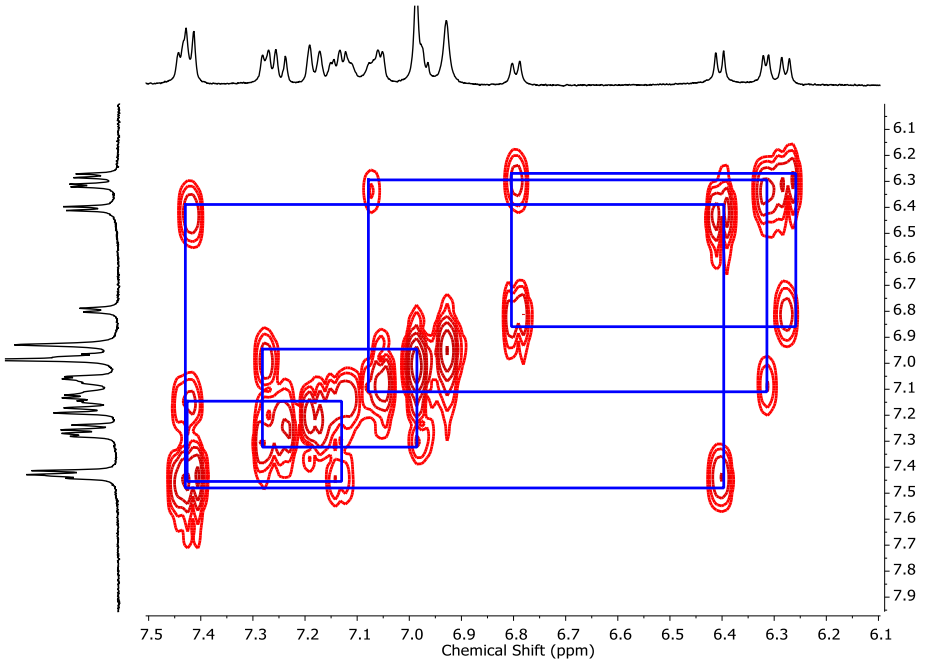

Figure IV.16: ^{1}H -^{1}H COSY spectrum of **IV.7** in Dichloromethane-d_2 at 223K

IV.4.3. Electronic Absorption Studies

Due to the extended conjugation, the brownish coloured macrocycle, **IV.7**, absorbs in the visible region of the electromagnetic spectrum. Multiple absorptions with high extinction co-efficient were observed (fig. **IV.17**) at 443 nm (95,800), 470 nm (89,900) and 575 nm (80,400). Being a 40π system, **IV.7** can be expected to undergo reversible two-electron ring oxidation similar to antiaromatic porphyrinoids. Accordingly, the addition of oxidizing agents like the Meerwein's salt induced a subtle change from brownish to blue colour in dichloromethane. Consequently, it displayed a red shift by more than 300 nm for the intense absorption band observed at 825 nm (209000). A bathochromic shift by more than 300 nm with a significant increase in the absorption coefficient of its intense absorption band suggested the formation of the ring oxidised dicationic species.

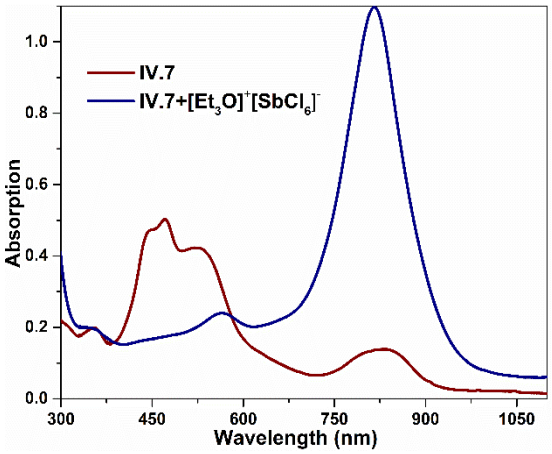

Figure IV.17: UV/Vis absorption spectrum of 10^{-6} M solution of **IV.7** and its oxidised species recorded in $CHCl_3$.

IV.4.4. Cyclic voltammetric and Spectroelectrochemical Studies

Based on the chemical oxidation studies described above, CV studies were employed to estimate the oxidation potential for the ring oxidation of **IV.7**. Accordingly, this 40π macrocycle displayed two irreversible oxidation waves at +0.014 V and +0.2 V and one reduction wave at -1.2 V (fig. **IV.18**). All these potentials were further confirmed by differential pulse voltammetry. To justify the observed colour change upon oxidation, spectroelectrochemical studies (fig. **IV.18**) were employed to analyse the formed oxidised species. The absorption maxima of the parent neutral species progressively vanished upon applying a potential of +0.35 V (second oxidation potential) and a new intense sharp peak

was observed at a longer wavelength (825 nm). A new peak that was observed in the absorption spectra upon electro-oxidation was similar to that obtained from chemical oxidation of the macrocycle by Meerwein's salt. Hence it confirmed the formation of dicationic species in both chemical and electrochemical processes. However, these dicationic species were not found to be stable for a long period of time, perhaps due to their unstable radical-like species.

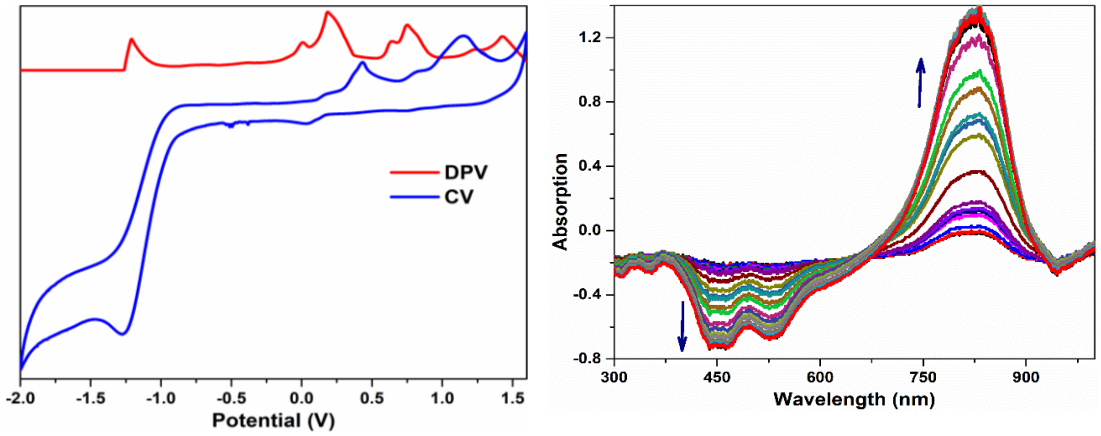

Figure IV.18: Cyclic voltammogram (CV, blue) and differential pulse voltammogram (DPV, red) of **IV.7** in CH_2Cl_2 (with 0.1 M Bu_4NPF_6 as the supporting electrolyte) (left). Change in absorption spectra of **IV.7** after applying a potential of 0.35 V (right).

IV.5. Synthesis and characterization of (IV.8)

From the mass spectrometric studies, we could also identify the formation of a 3:2 condensed product, **IV.8**. The MALDI TOF/TOF mass spectrometric analysis of **IV.8** displayed m/z at 1986.0893 (fig. **IV.19**) and due to an intense colour, it was found to absorb in the visible part

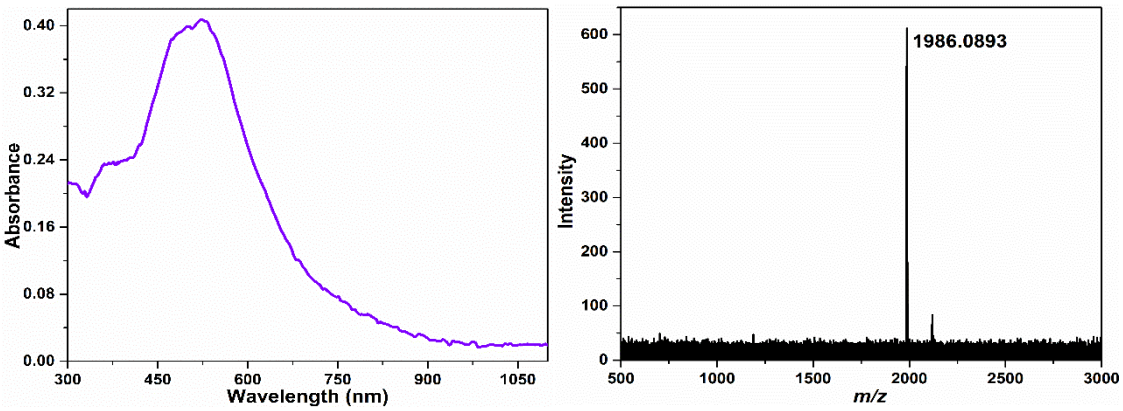

Figure IV.19: Uv-visible absorption spectrum of 10^{-6} M solution of **IV.8** in CH_2Cl_2 (left) and MALDI TOF/TOF mass spectrum of **IV.8** spectrum (right).

of the electromagnetic spectrum with an absorption maxima at 522 nm (fig. **IV.19**). It is expected to adopt a vesicle like structure, but could not be completely characterized due to its poor yields despite varying the reaction conditions.

IV.6. Quantum mechanical calculations

The global ring centers for the NICS (0) values were designated at the non-weighted mean centers of the molecules.[13] The estimated nucleus independent chemical shift (NICS) value for **IV.6** was found to be d +4.2 ppm. Such a low value clearly suggested the weak delocalization of π-electrons in the 3D structure and a feeble antiaromatic character of **IV.6**. Whereas the estimated NICS (0) of +0.8 ppm for **IV.7** emphasized the weak delocalization of π-electrons and hence non-antiaromatic nature.To simulate the steady-state absorption spectra, time-dependent TD-DFT calculations were employed on the optimized structures. Simulated absorption spectra for both the molecules **IV.6** and **IV.7** (fig. **IV.20**) and all the oxidised species of **IV.6** and **IV.7** (fig. **IV.21**) matched with the experimental results.

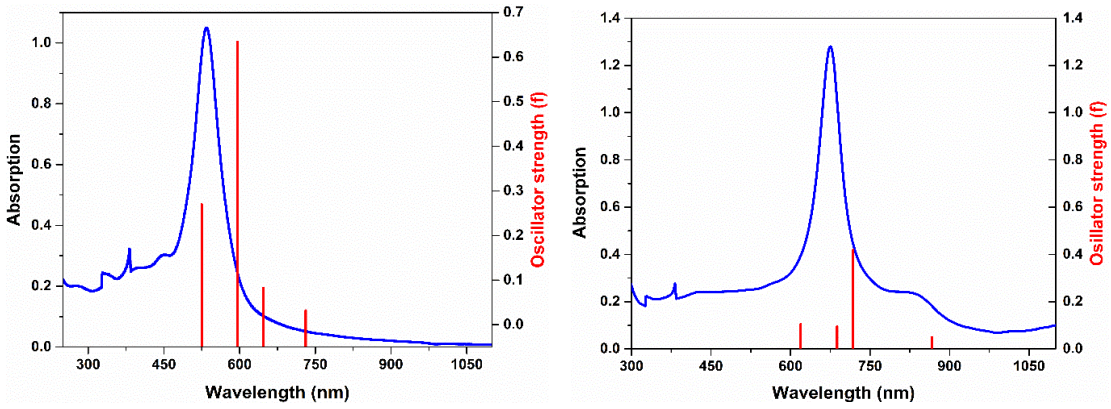

Figure IV.20: The steady state absorption spectra (blue line) of **IV.6** (left) and its dication (right) recorded in $CHCl_3$ along with the theoretical vertical excitation energies (red bar) obtained from TD-DFT calculations carried out at the B3LYP/6-31G(d,p) level.

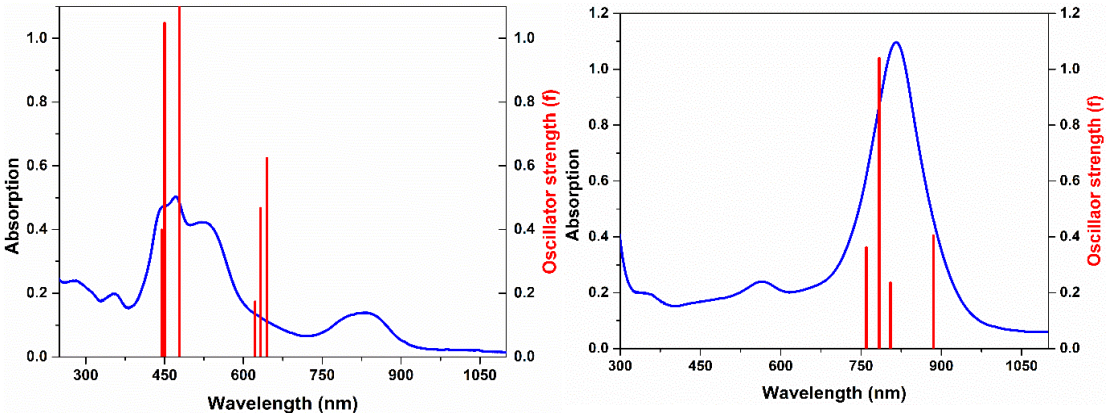

Figure IV.21: The steady state absorption spectra (blue line) of **IV.7** (left) and its dication (right) recorded in $CHCl_3$ along with the theoretical vertical excitation energies (red bar) obtained from TD-DFT calculations carried out at the B3LYP/6-31G(d,p) level.

IV.7. Synthesis of contracted and expanded molecular cages

Shape persistent 3D molecular cages with a well confined cavity have recently received considerable attention not only for their structural appeal but also for their fundamental and application perspectives.[14-15] Therefore, molecular cages bearing Csp^2 – Csp^2 and/or sp hybridised carbons were explored due to the enhanced stability derived from a rigid framework.[16] However, the synthesis of three dimensional molecular cages is a challenging task because of the multistep syntheses, preorganization of monomer units, non-availability of general methods and overall poor yields.[17] Therefore, the development of a new approach and general procedure to synthesize π-conjugated cages is not only a major challenge but also a fundamental contribution to the field of shape persistent 3D molecular cages. Comparing with the reported π-conjugated molecular cages, the isolated molecular cage, **IV.6** was having 3D global π-conjugation and synthesis involves simple acid catalysed condensed reaction followed by oxidation without the need of any preorganization of precursors. Therefore, the synthetic protocol developed during the synthesis of cage **IV.6** is having many advantages compare to the literature reported procedures. So, attempts were made to utilise this novel synthetic protocol for the synthesis of π-conjugated molecular cages.

Firstly, using synthetic procedure reported for **IV.6**, the contracted cage, **IV.15** was synthesised from the condensation of thiophene diol, **IV.14** and tetrathienylethene, **IV.5** under acidic condition followed by oxidation (scheme **IV.5**). The product, **IV.15,** in its MALDI-TOF/TOF mass spectrum displayed an m/z value of 2468.7425 and shows brown

coloured solutions when dissolved in common organic solvents. The solution colour is due to the extensive conjugation and was found to absorb in the visible region at 498 nm (fig. **IV.22**).

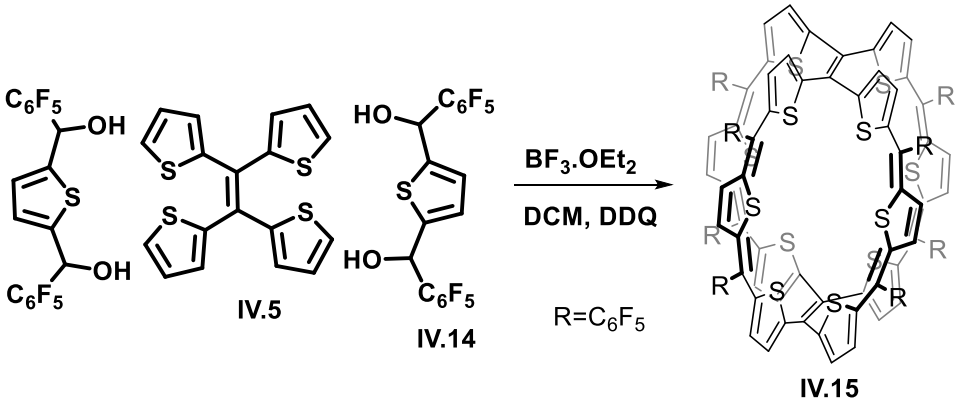

Scheme IV.5: Acid catalysed synthesis of contracted 3D molecular cage **IV.15**.

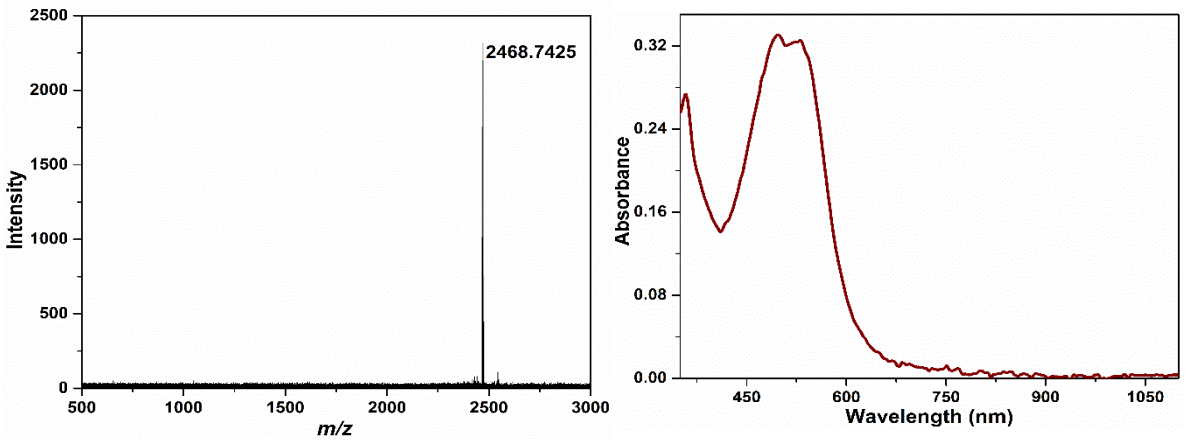

Figure IV.22: MALDI TOF/TOF mass spectrum of **IV.15** (left) and Uv-visible absorption spectrum of 10^{-6} M solution of **IV.15** in CH_2Cl_2 (right).

Further, the length of bridging unit was increased from bithiophene diol, **IV.1** to terthiophene diol, **IV.16** and condensed with tetrathienylethene, **IV.5** under similar reaction condition as described in scheme **IV.3** to obtain expanded cage **IV.17** (scheme **IV.6**). Formation of the expanded molecular cage **IV.17** was identified from the MALDI-TOF/TOF mass spectrum. Due to an extended π conjugation, the bluish coloured molecular cage shows an absorption maximum at 633 nm in the visible region of the electromagnetic spectrum (fig. **IV.23**).

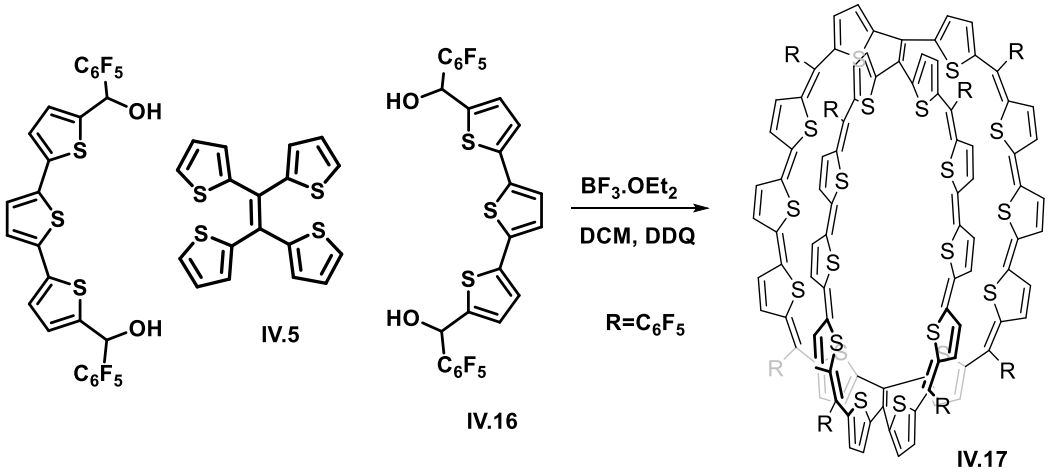

Scheme IV.6: Acid catalysed synthesis of expanded 3D molecular cage **IV.17**.

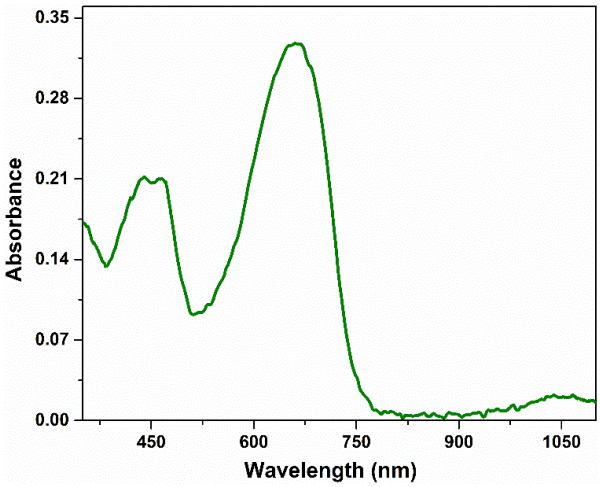

Figure IV.23: Uv-visible absorption spectrum of 10^{-6} M solution of **IV.17** in CH_2Cl_2.

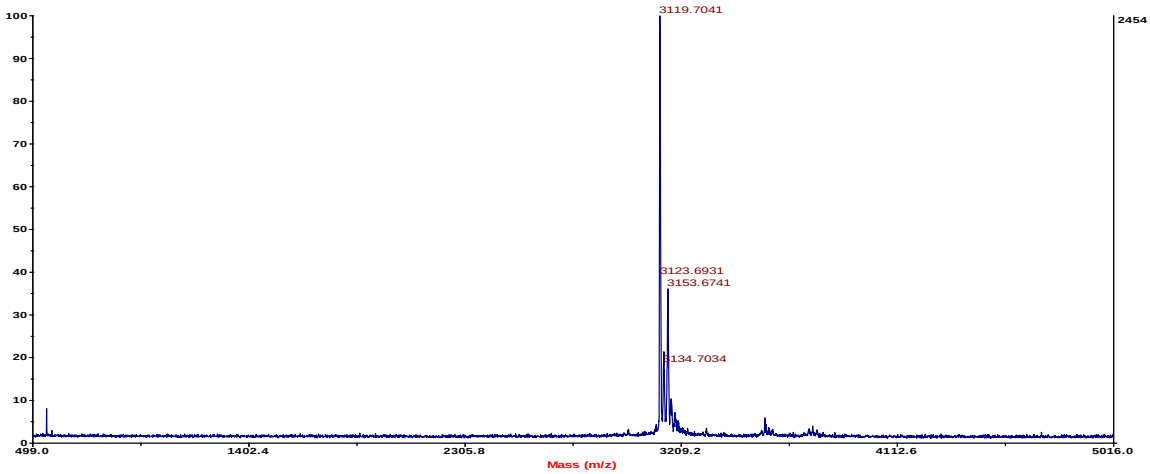

Figure IV.24: MALDI TOF/TOF mass spectrum of **IV.17**.

IV.8. Conclusions

A novel protocol was developed for the synthesis of three dimensional π-conjugated cage and semi-cage like molecules by employing appropriate thiophene based precursors using a simple acid catalysed reaction. Steric hindrance induced by heterocyclic units such as thiophene can yield cage-like π-conjugated systems at the expense of macrocycles. Variable temperature ^{1}H NMR studies and single crystal X-ray diffraction studies revealed the structural elucidation of tetrapodal 3D fully π-conjugated molecular cage and quasi-cage like molecules. Despite bearing a close resemblance to isophlorin like π-conjugation, they are devoid of ring current effects due to significant deviation from the planar geometry. The one and two-electron oxidation of the cage and semi cage molecules has been uniquely proven and these observations were studied through experiments including UV-Vis, Cyclic voltammetry and Spectroelectrochemistry. Even though they appear to be redox active, they tend to yield reactive radical intermediates as determined from cyclic voltammetric studies. Generally, syntheses of 3D π-conjugated molecular cages are highly challenging tasks in structural organic chemistry. Therefore, this developed novel synthetic approach was used to synthesise contracted as well as expanded molecular cages by varying the bridging unit length. However, many more molecular cages with different kind of bridging and capping units should be synthesised to generalise this novel synthetic procedure. Also, they have the potential to be developed as π-hosts if the cage can be modified to yield better access for the guest molecules.

IV.9. Experimental section

Synthesis and characterisation of IV.5:

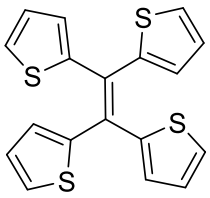

Titanium tetrachloride (2.26 mL, 20.5 mmol) was added into dry THF (80 mL) at 0 °C. After keeping at 0 °C for 30 min, zinc dust (2.68 g, 41 mmol) was added. The mixture was refluxed at 85 °C for 2 h. Then, pyridine (1.65 mL, 20.5 mmol) was added and the mixture was refluxed for 1 h. After cooling to ambient temperature, a solution of dithienyl ketone (2 g, 10 mmol) in dry THF (25 mL) was added into the reaction mixture. The reaction mixture was

refluxed at 85 °C for overnight. The reaction was quenched with water at 0 °C, then extracted with dichloromethane and washed with saturated sodium bicarbonate and water, and then dried over anhydrous sodium sulphate. After removing the solvent in vacuum, the crude product was purified by column chromatography on silica gel with petroleum ether as eluent to yield compound in 45% yields. The spectroscopic data matches with the data already reported in literature.[18]

NMR Data: ^{1}H NMR (400 MHz, $CDCl_3$, 298K) δ 7.34 (dd, *J* = 5.2, 1.2 Hz, 4H), 6.96 (dd, *J* = 5.2, 3.6 Hz, 4H), 6.9 (dd, *J* = 3.6, 1.2 Hz, 4H).

Synthesis of cage II.6:

A mixture of tetrathienylethene, **IV.5**, (178 mg, 0.5 mmol) and bithiophene diol, **IV.4** (470 mg, 3 mmol) were stirred in 100 mL of dry dichloromethane. The solution was purged with argon for 10 min. and shielded from light. $BF_3.OEt_2$ (60μL, 0.5 mmol) was added and stirring continued for 2h. Then, DDQ (283 mg, 2.5 mmol) was added and the mixture was stirred for an additional two hours. Finally solution was passed through short pad of basic alumina column. This mixture was concentrated and further purified by silica gel column chromatography using CH_2Cl_2/Hexane as eluent. Finally the products were isolated through size exclusion chromatography.

Characterisation of cage IV.6:

Yield- 4%

MS (MALDI TOF/TOF): *m*/*z* = 2411.1292 (found), 2411.5480 (calcd. For $C_{148}H_{120}S_{16}$).

UV-Vis ($CHCl_3$): λ_{max} (ε) L mol^{-1} cm^{-1} = 532nm (253000)

NMR Data: ^{1}H NMR (400 MHz, THF-d_8, 198K) δ 7.34 (m, 8H), 7.06 (s, 4H), 6.94 (m, 12H), 6.82 (s, 8H), 6.22 (m, 12H), 6.04 (d, *J* = 10.4 Hz, 4H), 2.28 (m, 36H), 2.04 (s, 12H), 1.91 (d, *J* = 16.8 Hz, 24H).

Crystal data: C_{148} H_{120} S_{16}, (+ Solvent) (*M*r 2411.40), tetragonal, space group *P -4 n 2*, a = 26.025(8), b = 26.025(8), c = 12.283(5) Å, α= 90, β= 90, γ= 90, V = 8319.28(6) Å^3, Z = 2, T = 100(2) K, D_{calcd} = 0.963 cm^{-3}, R_1 = 0.095 (5517), R_w (all data) = 0.2857(7428), GOF = 1.038.

Characterisation of macrocycle IV.7:

Yield- 2%

HR-MS (ESI-TOF): *m/z* = 1560.2346 (found), 1560.2283 (calcd. For $C_{92}H_{72}S_{12}$).

UV-Vis ($CHCl_3$): λ_{max} nm (ε) L mol^{-1} cm^{-1} = 443 (95240), 470 (89900), 575 (80000).

NMR Data: ^{1}H NMR (400 MHz, CD_2Cl_2, 223K) δ 7.39 (m, 4H), 7.21 (m, 4H), 7.11 (m, 8H), 7.01 (m, 4H), 6.9 (m, 8H), 6.75 (d, *J* = 6 Hz, 2H), 6.35 (d, *J* = 4 Hz, 2H), 6.25 (m, 4H), 2.27 (d, *J* = 15.2 Hz, 12H), 2.01 (s, 24H).

Crystal data: C_{92} H_{72} S_{12}, (*M*r 1562.12), monoclinic, space group *P* $2_1/c$, a = 13.11(3), b = 25.03(6), c = 28.95(7) Å, α= 90, β= 90.27(3), γ= 90, V = 9495(40) $Å^3$, Z = 4, T = 100(2) K, D_{calcd} = 1.093 cm^{-3}, R_1 = 0.1378 (9215), R_w (all data) = 0.3744(16829), GOF = 1.053.

Synthesis and characterisation of cage IV.9:

Tetrathienylethene, **IV.5** (178 mg, 0.5 mmol) and bithiophene diol, **IV.4** (612 mg, 2.2 mmol) were reacted as described above to yield **IV.9** in 5% yields.

HR-MS (ESI-TOF): *m/2* = 1395.8707 (found), 2791.7397 (calcd. For $C_{124}H_{32}F_{40}$ S_{16}).

NMR Data: ^{1}H NMR (400 MHz, $CDCl_3$, 298K) δ 6.96 (m, 16H), 6.78 (d, *J* = 8 Hz, 8H), 6.27 (d, *J* = 8 Hz, 8H).

IV.10. References

1. Reddy, B. K.; Basavarajappa, A.; Ambhore, M. D.; Anand, V. G., *Chem. Rev.* **2017,** *117,* 3420-3443.
2. Tanaka, T.; Osuka, A., *Chem. Rev.* **2017,** *117,* 2584-2640.
3. Osuka, A.; Shimidzu, H., *Angew. Chem., Int. Ed.* **1997,** *36,* 135-137.
4. Tsuda, A.; Osuka, A., *Science.* **2001,** *293,* 79-82.
5. Grzybowski, M.; Sadowski, B.; Butenschön, H.; Gryko, D. T., *Angew. Chem., Int. Ed.* **2020,** *59,* 2998-3027.
6. Reddy, B. K.; Gadekar, S. C.; Anand, V. G., *Chem. Comm.* **2016,** *52,* 3007-3009.
7. Reddy, B. K.; Rawson, J.; Gadekar, S. C.; Kögerler, P.; Anand, V. G., *Chem. Comm.* **2017,** *53,* 8211-8214.
8. Gopalakrishna, T. Y.; Reddy, J. S.; Anand, V. G., *Angew. Chem., Int. Ed.* **2014,** *53,* 10984-10987.
9. Anand, V. G.; Pushpan, S. K.; Venkatraman, S.; Dey, A.; Chandrashekar, T. K.; Joshi, B. S.; Roy, R.; Teng, W.; Senge, K. R., *J. Am. Chem. Soc.* **2001,** *123,* 8620-8621.

10. Suzuki, T.; Shiohara, H.; Monobe, M.; Sakimura, T.; Tanaka, S.; Yamashita, Y.; Miyashi, T., *Angew. Chem., Int. Ed.* **1992,** *31,* 455-458.

11. Ke, X.-S.; Kim, T.; He, Q.; Lynch, V. M.; Kim, D.; Sessler, J. L., *J. Am. Chem. Soc.* **2018,** *140,* 16455-16459.

12. Rathore, R.; Kumar, A. S.; Lindeman, S. V.; Kochi, J. K., *J. Org. Chem.* **1998,** *63,* 5847-5856.

13. Schleyer, P. v. R.; Maerker, C.; Dransfeld, A.; Jiao, H.; van Eikema Hommes, N. J. R., *J. Am. Chem. Soc.* **1996,** *118,* 6317-6318.

14. Hasell, T.; Cooper, A. I., *Nat. Rev. Mat.* **2016,** *1,* 16053.

15. Zhang, G.; Mastalerz, M., *Chem. Soc. Rev.* **2014,** *43,* 1934-1947.

16. Matsui, K.; Segawa, Y.; Itami, K., *J. Am. Chem. Soc.* **2014,** *136,* 16452-16458.

17. Kayahara, E.; Iwamoto, T.; Takaya, H.; Suzuki, T.; Fujitsuka, M.; Majima, T.; Yasuda, N.; Matsuyama, N.; Seki, S.; Yamago, S., *Nat. Comm.* **2013,** *4,* 2694.

18. Yamamoto, A.; Matsui, Y.; Asada, T.; Kumeda, M.; Takagi, K.; Suenaga, Y.; Nagae, K.; Ohta, E.; Sato, H.; Koseki, S.; Naito, H.; Ikeda, H., *J. Org. Chem.* **2016,** *81,* 3168-3176.

Summary

This thesis demonstrates the synthetic aspects and redox properties of 2D and 3D expanded isophlorinoids mainly derived from thiophene units. From the synthetic point of view, easy and efficient synthetic routes were developed to obtain 2D expanded isophlorinoids and 3D π conjugated molecular cages in reasonable yields, from easily available precursors. Detailed analyses and combination of various spectroscopic techniques were used for the characterization of isophlorinoid macrocycles. Especially spectroelectrochemistry studies were used extensively to analyse the redox species formed during various oxidation and reduction reactions. During the attempted synthesis of acetylene bridged isophlorins, a rare organic radical was discovered. Once again the thiophene's handy electronic and structural feature helps to form a (4n+1)π neutral radical. This stable organic radical with multiple oxidation states expected to behave like metal have the potential to become a catalyst.

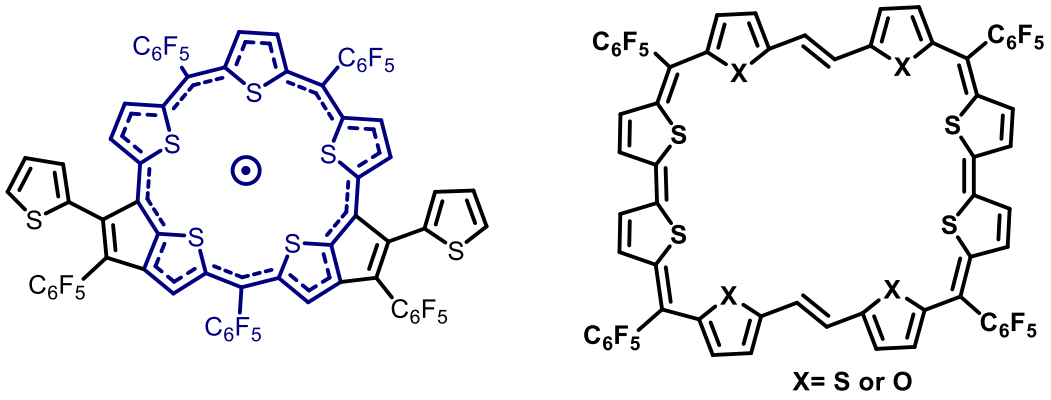

The 40π expanded isophlorins described in this thesis showed altered topologies with different heterocycles. The close contact between fullerenes and isophlorin in the supramolecular complex shows that the anti-aromatic macrocycles are also good receptor for fullerenes like aromatic porphyrins. The oxidised species of these 40π isophlorins existed as open shell singlet diradical, as their electronic ground state. The highlight of this thesis is the development of novel synthetic procedure to synthesise π conjugated molecular cages and quasi-cage like molecules using a simple acid catalysed reaction. Steric hindrance induced by thiophene units in predesigned precursors favours the exclusive formation 3D cages over macrocyclic dimers. One important feature of this novel method is control over the products by varying the stoichiometric ratio of precursors. The cage molecules formed appeared to be redox active, but yielded reactive radical intermediates as determined from spectroscopic studies. As there are no general methods available for the synthesis of π conjugated cages, the

novel and simple synthetic approach described in this thesis is good contribution to the field of shape persistent 3D molecular cages.

To conclude, thiophene seems to be suitable building block in the synthesis of variety of topological anti-aromatic molecules. If the yields of these reactions were increased, the many unexplored factors of antiaromatic isophlorinoids can be explored easily in parallel to aromatic porphyrinoids. Nevertheless, these anti-aromatic macrocycles possess superior redox properties compared to aromatic molecules have a great potential in the field of functional organic materials. The interesting molecules of this thesis 3D π conjugated molecules have an enormous potential to be developed as supramolecular hosts for binding a variety of guests.